AD-A195 396   A SIMPLE ONE-DIMENSIONAL ONE-FLUID DIVERTOR MODEL(U)   1/4
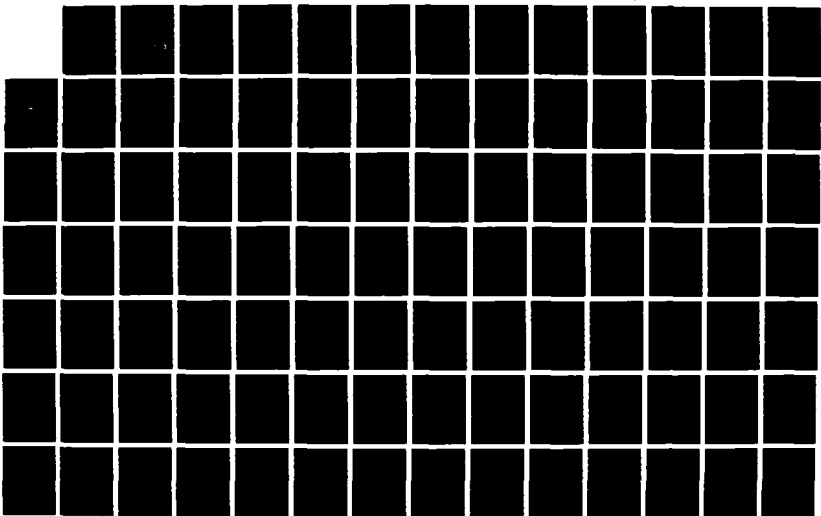ARMY MILITARY PERSONNEL CENTER ALEXANDRIA VA
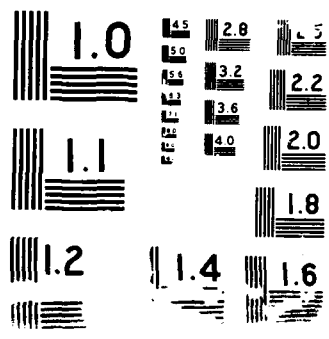M D BAEHRE 20 MAY 88

UNCLASSIFIED   F/G 18/1   NL

①

AD-A195 396

A SIMPLE ONE-DIMENSIONAL, ONE-FLUID DIVERTOR MODEL

Michael D. Baehre, O3
HQDA, MILPERCEN (DAPC-OPA-E
200 Stovall Street
Alexandria, VA 22332

FINAL REPORT: 20 May 1988

DISTRIBUTION: A

A Thesis Submitted to Rensselaer Polytechnic Institute,
Troy, New York, in Partial Fulfillment of the Requirements
for the Degree of Master of Science of Nuclear Engineering

131

REPORT DOCUMENTATION PAGE

1a. REPORT SECURITY CLASSIFICATION	1b. RESTRICTIVE MARKINGS
Unclassified	NA

2a. SECURITY CLASSIFICATION AUTHORITY	3. DISTRIBUTION / AVAILABILITY OF REPORT
NA	
2b. DECLASSIFICATION / DOWNGRADING SCHEDULE	Distribution: A , Unlimited
NA	

4. PERFORMING ORGANIZATION REPORT NUMBER(S)	5. MONITORING ORGANIZATION REPORT NUMBER(S)
Student HQDA, MILPERCEN	

6a. NAME OF PERFORMING ORGANIZATION	6b. OFFICE SYMBOL (If applicable)	7a. NAME OF MONITORING ORGANIZATION
Student HQDA, MILPERCEN	DAPC-OPA-E	

6c. ADDRESS (City, State, and ZIP Code)	7b. ADDRESS (City, State, and ZIP Code)
200 Stovall Street Alexandria, VA 22332	

8a. NAME OF FUNDING / SPONSORING ORGANIZATION	8b. OFFICE SYMBOL (If applicable)	9. PROCUREMENT INSTRUMENT IDENTIFICATION NUMBER

8c. ADDRESS (City, State, and ZIP Code)	10. SOURCE OF FUNDING NUMBERS			
	PROGRAM ELEMENT NO.	PROJECT NO.	TASK NO.	WORK UNIT ACCESSION NO

11. TITLE (Include Security Classification)

A Simple, One-dimensional, One-fluid Divertor Model

12. PERSONAL AUTHOR(S) CPT Michael David Baehre

13a. TYPE OF REPORT	13b. TIME COVERED	14. DATE OF REPORT (Year, Month, Day)	15. PAGE COUNT
Final	FROM _____ TO _____	88/5/20	173

16. SUPPLEMENTARY NOTATION

Master's Thesis for Master of Science in Nuclear Engineering at Rensselaer Polytechnic Institute, Troy, New York

17.	COSATI CODES		18. SUBJECT TERMS (Continue on reverse if necessary and identify by block number)
FIELD	GROUP	SUB-GROUP	Fusion, Divertor, Plasma Modeling, Plasma-wall interaction

19. ABSTRACT (Continue on reverse if necessary and identify by block number)

This thesis presents the development of a simple and comprehensive model of the divertor region of a fusion reactor which can be implemented on a PC to make it highly "usable" and user friendly. The model includes the critical processes of; neutral recycling, impurity production and radiation, remote radiative cooling, neutral pumping, particle convection, ash effects, and the effects of divertor geometry and plate material. A set of fluid equations is solved for the plate temperature and density, and the throat temperature, using a fixed point iteration routine, and gauss-seidel updating. Neutral Particle modeling is accomplished with a simple model of a wedge-shaped section of plasma overlying the divertor plate and a simple slab attenuation model. The results of benchmarking the model developed in this thesis against four other divertor models was very successful and validates the approach taken.

20. DISTRIBUTION / AVAILABILITY OF ABSTRACT	21 ABSTRACT SECURITY CLASSIFICATION
☒ UNCLASSIFIED/UNLIMITED ☐ SAME AS RPT ☐ DTIC USERS	Unclassified
22a. NAME OF RESPONSIBLE INDIVIDUAL	22b TELEPHONE (Include Area Code) | 22c OFFICE SYMBOL
Michael L. Greene	

A SIMPLE ONE-DIMENSIONAL, ONE-FLUID DIVERTOR MODEL

by

Michael D. Baehre

A Thesis Submitted to the Graduate

Faculty of Rensselaer Polytechnic Institute

in Partial Fulfillment of the

Requirements for the Degree of

MASTER OF SCIENCE

Approved:

_____

Don Steiner
Thesis Advisor

Rensselaer Polytechnic Institute
Troy, New York

May 1988

CONTENTS

ii

LIST OF TABLES

LIST OF FIGURES

ACKNOWLEDGEMENT

I would like to express my gratitude to Dr. Don Steiner for his guidance, encouragement, and tireless patience as advisor for this research. Thanks should also go to Dr. Mark Embrechts for the discussions we had on divertor modeling. Acknowledgement must also be made of the support of the United States Army in financing my graduate studies. I would also like to extend my thanks to the members, past and present, of the fusion group at RPI for not only their help, but for their conviviality. Finally I wish to thank my parents and fiance for their interest in, and encouragement of what I've spent the last two years doing.

ABSTRACT

Plasma exhaust and impurity control represent significant problems for the viability of fusion as an energy source. The divertor concept is an attractive solution to these problems in which fuel particles and ash are exhausted into a separate chamber, away from the plasma, where they can be impacted on a target plate, neutralized, and pumped out of the reactor. The performance of conceptual divertor designs, though, can presently only be assessed with the use of plasma edge models. This thesis examines the necessary components of these models and develops a simple, comprehensive, and accurate divertor model.

Divertor modeling is a complex process because of the strong coupling between numerous reactor systems (core plasma, first wall, divertor, pumping,...) and the nonlinearity of the fluid equations used in modeling. Some models oversimplify both the equations and processes included to obtain analytic expressions for divertor parameters. While these approaches have identified useful dependencies, they do not yield quantitatively accurate results. More sophisticated models attempt to include all the physics and solve the fluid equations in two dimensions (axially and radially) resulting in computer codes which are highly numerical and complex.

The objective in this thesis has been to develop a simple and comprehensive model of the divertor region which is highly usable and which gives quantitatively accurate results. Therefore, it includes the key processes of: neutral recycling; impurity production and radiation; remote radiative cooling; neutral pumping; particle convection; ash effects; and the effects of divertor geometry and plate material. The fluid equations are solved for the plate temperature and density, and the divertor throat temperature, using a fixed point iteration routine with Gauss-Seidel updating and successive over-relaxation. Neutral particle modeling is accomplished with a simple model of a wedge-shaped section of plasma overlying the divertor plate and a simple slab attenuation model. The results of benchmarking the model developed here against four other divertor models was very successful and validates the approach taken.

CHAPTER 1

INTRODUCTION AND HISTORICAL REVIEW

The purpose of this thesis is twofold: (1) to present an overview of the methods and approaches to modeling fusion reactor divertors; and (2) to develop a simple, yet comprehensive, model which will allow divertor performance to be examined as a function of divertor geometry, core plasma properties, and pumping capability. With such a model the sensitivity of divertor performance to key parameters can be evaluated and, thus, modifications can be identified to achieve operational requirements.

1.1 Background

Much of the current research on tokamaks centers on the problem of handling plasma exhaust and impurity control. Plasma particles will eventually diffuse outward across magnetic flux surfaces until they encounter a physical boundary, for example, the reactor vessel first wall. On striking this wall the particles deposit energy and can also physically erode the wall through sputtering. These interactions increase the cooling requirements for the first wall and decrease its service lifetime. More significantly, the influx of sputtered wall material (impurities)

represents an energy sink in the plasma due to atomic ionization and radiation emission by repetitive collisional excitation and bremssstralung processes. These impurities also cause a fuel depletion effect by reducing the allowable density of fuel ions in the plasma. For a given plasma electron density, an impurity ionized to a $+Z$ state will take the place of Z fuel ions $(+1)$, reducing the amount of fuel available for fusion and thereby, reducing reactor power. This fuel depletion effect also occurs by virtue of the buildup of fusion reaction by-products (helium for a D-T plasma).

The problems of heat deposition, wall erosion, fuel depletion, and plasma cooling have provided the impetus for the development of several impurity control and exhaust handling concepts. Among the most successful of these is the divertor concept.

The divertor concept involves magnetically perturbing field lines near the edge of the core plasma such that they leave the main reactor chamber and enter a separate "divertor" chamber (Figure 1.1). Plasma particles (electrons, fuel, reaction products, and impurities) diffusing out of the core plasma region are swept along these field lines until they intercept a material target or plate. In this way, particles are intentionally impacted on a specially designed target plate rather than on the vessel

Figure 1.1   Divertor Diagram

first wall. It is assumed that servicing damaged divertor plates will be less of an impact on machine availability than servicing a damaged first wall. The neutral particles coming off the divertor plate can subsequently be pumped out of the divertor chamber. Major design considerations for the divertor system include; handling the large heat fluxes (radiation and particle), coping with potentially severe material erosion problems, and providing adequate neutral pumping to satisfy impurity exhaust requirements.

1.2 Rationale for Divertor Modeling

Divertor design requires development of models for the edge plasma and divertor regions which establish plasma properties and define plasma interaction with reactor components (walls, target plate, pumps). In general these models should include transport both across and along field lines. Among the most important plasma parameters for divertor design are the plasma density and temperature in front of the divertor plate. These parameters establish the heat and particle loads which determine the cooling requirements and erosion rates at the plate. In addition, modeling of the neutral particle transport is required to estimate the fraction of neutrals (D-T and He) coming off the divertor plate that escape through the plasma fan

overlying the plate and are pumped out of the divertor chamber. The gross amount of helium-ash pumped will then determine the steady state concentration of helium in the core plasma. The total heat exhausted into the divertor determines the fraction of the fusion alpha power that will be deposited on the reactor first wall. Plasma conditions in the divertor will influence the amount of impurities produced at the plate and their probability of transport into the main plasma, poisoning it.

The above discussion implies a substantial linkage between divertor operation and ultimate fusion reactor performance. This impact has made the modeling of the plasma edge and divertor regions an important area of study and one which has received significant attention.

1.3 Models Available and Approaches

The sophistication of impurity control modeling has increased greatly over the past 5-10 years. Beginning with simple, almost heuristic models, there has been an evolution to two dimensional (2D) computer codes employing realistic geometries. In general, most of these models start with a form of the plasma fluid equations originally derived by Braginskii[1] and vary in the number of dimensions considered, atomic processes modeled, and number of fluids assumed.

One early model by Mahdavi[2] (1981) solved the fluid equations in one dimension (1D), along field lines, for the scrapeoff region by assuming the dominance of parallel electron heat conduction. This assumption allowed analytic expressions to be derived for temperature and density. The predictions of this model compare qualitatively with experimental results in reproducing a strong dependence of scrapeoff temperature and density on main plasma boundary density and a weak dependence on fusion alpha power. This model did not, however, account for the significant effects of particle recycling at the divertor plate. Another 1D, one fluid model along field lines, by Harrison, Hotston, and Harbour[3] (1982), also assumed the dominance of electron parallel heat conduction, but included neutral particle recycling, pumping, and impurity radiation. It is this neutral particle recycling which cools the plasma in front of the divertor target plate, reducing the heat load and sputtering. This model's assumption of 100% electron heat conduction has limited its application to a narrow range of plasma conditions in which such an assumption is valid.

A 1D model by Harbour and Morgan[4] (1984), ZEPHYR, uses two sets of fluid equations (electron and ion) and solves them numerically for the ion and electron temperatures and densities along field lines from a "watershed" (or symmetry) point between divertors to the divertor plate(s). The

ZEPHYR model was used for the divertor design in the International Torus (INTOR) study. Peng and Galambos[5] (1984) numerically solved a 1D, one fluid, set of equations for the temperature and density at two points (divertor throat and plate). This "two-point" model was used for scaling/parametric studies of divertor performance, and, in combination with the ZEPHYR code, was used for particle escape studies of divertors[6]. In these studies the recycling coefficient, a key parameter, was not calculated, but rather, was taken as an input from the case being benchmarked.

Other codes have been developed as 2D or quasi-2D. ODDESSA by Prinja and Conn[7] (1984) is such a quasi-2D code, in which radial solutions of the fluid equations are coupled between a watershed point and the divertor recycling region. This approach has the advantage of giving the radial variation of plasma parameters and linkage between the core plasma edge region and the divertor region without entailing the use of more complex 2D solution methods. The PLANET code[8] of the Princeton Plasma Laboratory and the code of Braams[9-10] (1983), used to model the Next European Torus (NET), are examples of 2D codes employing realistic geometries.

One difficulty encountered in solving the fluid equations is that they represent a highly nonlinear set of equations

(even in 1D) which are normally not solvable by ordinary numerical means[11]. The least cumbersome models arrive at analytic expressions only by grossly simplifying the equations. The more sophisticated 1D and 2D models are computationally cumbersome, requiring specialized numerical methods on powerful computers. Even implemented as such, it is noted that these codes are not as computationally "robust" as desired (i.e. they do not always converge)[4].

1.4 Approach and Rationale for a Simple and Comprehensive Model

The development of a divertor model involves a tradeoff between making the model readily "usable" and making it "accurate" and "applicable" to a wide range of reactor designs and divertor conditions. If one simplifies the fluid equations and neglects modeling certain key processes in the divertor, the results will be qualitatively and quantitativley suspect. If one attempts to include all the physics of the divertor in more than one dimension, the code becomes computationally complex. In many instances, this complexity makes it necessary to run the code on a mainframe and requires a large amount of pre-run preparation time to configure the code for the problem at hand and to calculate and specify various parameters (diffusion coefficients,

ionization energies ,reaction rate parameters, ect.). In this way the code becomes less interactive and less "usable".

The purpose of the research described in this thesis is to produce a simple, yet comprehensive, model of the divertor region which can be implemented on a personal computer so as to retain an interactive capability. To achieve the desired goal, the model must satisfy three requirements. First, it must remain as analytic as possible so as to reduce the variety and complexity of any numerical methods used. This requirement will limit the number of dimensions in which the fluid equations are solved. Second, it should include the following significant processes in the divertor: neutral recycling, impurity production and radiation, line radiation, neutral pumping, particle convection, and the effect of divertor geometry and plate material. Finally, the model must yield results comparable to the more sophisticated models to validate the approach used.

1.5   Outline of Thesis

Chapter 2 of this thesis presents the diverse ingredients necessary for an impurity and particle control model, and highlights the essential issues and physics involved in these models. This chapter is included to give perspective

to the final choices made for the divertor model adopted here. Chapter 3 details these choices and develops the analytic expressions and the evaluation methods used in the final model. Chapter 4 is a description and discussion of the computer code which implements the divertor model, including the numerical methods employed. Chapter 5 compares the results of this model to those obtained by some of the previously described divertor models. Finally, a summary of this work and its major conclusions are presented in Chapter 6, together with suggestions for future work and refinements .

CHAPTER 2

MODELING OF THE PLASMA EDGE REGION

Models of the plasma edge region and divertor chamber
vary widely in their approach and included processes
depending on their application. They can vary from a point
model to three dimensional (3D), and may be based on kinetic
or fluid approximations. However, as discussed below, there
are certain basic components, and fundamental processes that
must be accounted for in the development of any model.[11]

First, the model must include a set of plasma transport
equations which are tailored to a specific or schematic
geometry. To solve the equations, a set of boundary
conditions must be applied. For a divertor, these boundary
conditions generally include the sheath condition present at
the target plate. The transport equations in many instances
include particle, momentum, and energy source (or sink)
terms that must be calculated. These source terms usually
arise from the recycling of neutrals from walls or the
divertor plate, or from refueling of the plasma. Obtaining
the spatial distribution of the neutrals involves detailed
neutral transport calculations, including neutral and ion
reflection from surfaces and neutral-ion interactions.
These distribution calculations in turn enter into the
determination of (1) the helium-ash pumping efficiency of

the divertor, and (2) the production of impurities by charge-exchange neutrals. An estimate of impurity production (by neutrals or ions) must be included as the impurities will alter plasma energy balances via ionization and radiation losses. From a design standpoint these estimates can also provide an evaluation of the erosion by self-sputtering of reactor walls and the target plates.

A final requirement is that all these individual components and processes must be linked together in an interactive way to obtain a self-consistant solution. What follows is a more detailed discussion of each of these components and processes.

2.1 Transport Equations

Traditionally, two different sets of transport equations have been applied to the plasma edge region; kinetic, and fluid. Each is derived from the first three moments of the Boltzmann equation. The applicability, or appropriateness, of either set can be determined by estimating the collisionality of the plasma being modeled.

The effective collisionality of a plasma, ν, can be defined as the ratio of the effective mean free path for 90^0 scatter collsions of ions and electrons, λ, to a characteristic length, L, $\nu = \lambda/L$. This collisionality could

also be called the Knudsen number from molecular gas dynamics. For an axisymetric toroidal device, L is the connection length L=πRq, where R is the plasma major radius, and q is the safety factor on edge. When $\nu \ll 1$, the plasma is highly collisional and the fluid approximation is appropriate. When $\nu \gg 1$, a kinetic treatment is warranted. Between these two limits, the fluid approach can be used, but with some caution.

The mean free path for cumulative 90° scatter can be written as:[11]

$$\lambda(m) \approx 5 \times 10^{16} T^2(eV) \ n_e(m^{-3})^{-1} \qquad (2.1)$$

where T is the plasma temperature and n_e is the plasma electron density.

Equation (2.1) is plotted below in Figure 2.1 as a function of T and n_e. For typical values of L, 10-50 m, the plot implies that the fluid approximation is valid for low temperatures and high densities, but not valid for low densities and high temperatures. It should be noted that typical parameters for the plasma edge region can be densities in the range 10^{16}-10^{20} m^{-3} and temperatures in the range 1-400 ev. However, for most operating or planned devices, the edge density and temperature should be in a

Figure 2.1   The Mean Free Path for 90° Scattering
             as a Function of n and T   [reference 11]

region where the fluid approximation is applicable.

The form of the fluid equations used in most models is generally derived from the formulation of Braginskii.[1] Neglecting a few terms these equations have the form of conservation equations for particles, momentum, and energy:

$$-\nabla \cdot \vec{\Gamma} + S_n = 0$$

$$-\nabla \cdot \vec{R} + S_p = 0 \qquad\qquad (2.2)$$

$$-\nabla \cdot \vec{Q} + S_e = 0$$

where Γ, R, and Q are the particle, momentum, and energy fluxes, respectively, and S_n, S_p, S_e are the associated source terms.

Several critical assumptions are required to arrive at the above form of the fluid equations and they include: the magnetic field at any point is externally determined; steady state conditions apply (which negates any microturbulence terms); and collisions and gyromotion are sufficient to maintain a Maxwellian distribution for the particles.[12]

The fluid equations can be expanded to more detail and written in a "semi-conservative" form in which as many terms as possible are expressed as the divergence of a flux. For circular magnetic flux surfaces the equations become:[11]

Continuity

$$\frac{\partial(nv_{\parallel})}{\partial\zeta} = \frac{1}{r}\frac{\partial}{\partial r}\,r\left(D_{\perp}\frac{\partial n}{\partial r} - nv_r\right) + S_n \qquad (2.3)$$

Momentum

$$\frac{\partial}{\partial\zeta}\left(p_i + p_e + mnv_{\parallel}^2 + 1.28\,\tau_i n\,T_i\,\frac{\partial v_{\parallel}}{\partial\zeta}\right) =$$

$$S_p + \frac{1}{r}\frac{\partial}{\partial r}\,r\left(mv_{\parallel}(-nv_r + D_{\perp}\frac{\partial n}{\partial r})\right) \qquad (2.4)$$

Ion Energy

$$\frac{\partial}{\partial\zeta}\left[\left(\frac{5}{2}\,T_i + \frac{1}{2}\,nm\,v_{\parallel}^2\right)nv_{\parallel} - n\chi_{\parallel}^i\frac{\partial T_i}{\partial\zeta}\right] =$$

$$-v_{\parallel}\frac{\partial}{\partial\zeta}(nT_e) + \frac{1}{r}\frac{\partial}{\partial r}\,r\left[n\chi_{\perp}^i\frac{\partial T_i}{\partial r} + \left(\frac{5}{2}\,T_i + \frac{1}{2}\,mv_{\parallel}^2\right)\cdot\right.$$

$$\left.\left(D_{\perp}\frac{\partial n}{\partial r} - nv_r\right)\right] + Q_{\Delta} + S_E^i \qquad (2.5)$$

and

Electron Energy

$$\frac{\partial}{\partial\zeta}\left(\frac{5}{2}\,T_e nv_{\parallel} - n\chi_{\parallel}^e\frac{\partial T_e}{\partial\zeta}\right) = v_{\parallel}\frac{\partial}{\partial\zeta}(nT_e) +$$

$$\frac{1}{r}\frac{\partial}{\partial r}\,r\left[\frac{5}{2}\,T_e\left(D_{\perp}\frac{\partial n}{\partial r} - nv_r\right) + n\chi_{\perp}^e\frac{\partial T_e}{\partial r}\right] - Q_{\Delta} + S_E^e$$

$$(2.6)$$

In these equations viscous effects have been neglected. The variable ζ is the coordinate along field lines, while r is the radial direction, the cross field direction. The velocity, $v_{\parallel}$, is the fluid velocity along field lines, v_r is the radial fluid velocity, n is the particle density, $T_{i,e}$

is the ion, electron temperature, m is the ion mass, τ_i is the ion collision time, $D_\perp$ is a radial density diffusion coefficient, $\chi_{\perp,\parallel}$ is a heat diffusivity (radial and parallel). The term Q_Δ is the classical ion-electron energy equipartition rate. The terms S_n, S_p, and S_e are, respectively, the density, momentum, and energy source terms from impurity and neutral atom collisions. The term $p_{i,e}$ is the ion, electron pressure (nT).

In the above equations, the requirement for plasma neutrality makes the continuity equations for the ions and electrons the same and the momentum balance equations for electrons and ion have been combined.

The fluid equations are four highly nonlinear, second order partial differential equations in n, $v_\parallel$, T_i, v_r, and T_e .They involve source terms which tend to be nonlinearly dependent on plasma parameters and are subject to their own modeling equations. Solution of these equations usually involves some degree of simplification (such as going to one dimension, or assuming the dominance of parallel electron conduction as the only energy transport mechanism) and an iterative process to converge on a solution because of the source terms. As a first step, though, a set of boundary conditions must be specified.

2.2   Boundary Conditions

Depending on the dimensionality of the problem, there may be as many as four boundaries to be considered in the computational mesh: the main plasma, the reaction chamber walls to which field lines are parallel, and two or more target plates. The symmetry of the problem can often be used to divide the edge plasma into two (or more) regions, each flowing to a target plate.

The boundary conditions of the main plasma can be set in several ways. The core-plasma edge density and temperatures (electron and ion) can be specified at a particular point (like the symmetry point). If the equations are only to be solved along the field lines, then these values could be used as radially representative across the entire edge region at that axial position. This would tend to overestimate the sputtering, recycling, and heat deposition on the target plate at most points since these represent peak radial values (T and n decrease radially). Another approach for a 1D solution would be to use a simple edge radial profile (exponential) in order to integrate for average values of density and temperature. This approach would tend to underestimate the heat flux to the target plate at some points (where T and n are larger than their average values) and overestimate it at others (where T and n are less than these average values). Using the same simple

radial profile, the 1D solution could be converted to a quasi-two dimensional one by solving the 1D equations stepwise across the edge region. If the full 2D equations were used, then a set of fluxes (particle, momentum, and energy) from the main plasma could be used as boundary conditions.

The boundary conditions at the wall would involve the influx of reflected charge-exchange neutrals and the impurities they produce by sputtering. These particles would represent a form of energy and momentum sinks, or particle sources. For a 2D solution the fluxes themselves could be used. For a 1D solution, the only way to include them would be as volumetric sources or sinks.

At the target plates an electrostatic potential forms. This sheath potential retards the electron flow so that ion and electron fluxes to the plate are equal, thus maintaining plasma neutrality. At the sheath the particle flow becomes collisionless, so the fluid approximation breaks down. The requirement for equal electron and ion fluxes leads to boundary conditions involving the particle and heat fluxes to the plates. From the continuity and momentum equations it can be shown that the fluid flow velocity cannot exceed the local sound speed as the plate is approached (i.e. $M = v_\parallel/C_s < 1$, where M is the mach number and C_s is the sound speed). The Bohm Criterion requires that the flow velocity

at the plate be at least sonic for a stable sheath to form.[11] Therefore, the usual modeling assumption is that the fluid velocity at the plate is the local ion sound speed; i.e. $\mathbb{M}=1$.

The power to the plate is usually expressed in terms of an energy transmission factor, γ , defined as the ratio of power flux to the plate to, particle flux times particle temperature. Thus,

$$\gamma_e = \frac{Q_e}{kT_e \Gamma_e} \qquad (2.7)$$

$$\gamma_i = \frac{Q_i}{kT_i \Gamma_i} \qquad (2.8)$$

$$\Gamma_e = \Gamma_i = n_e C_s \qquad (2.9)$$

$$C_s = \left(\frac{kT_e + kT_i}{m_i} \right)^{1/2} \qquad (2.10)$$

The form of the energy transmission coefficients can be expressed as:[11]

$$\gamma_e = \frac{2}{1-\nu_e} - .5 \ln\left[\left(2\pi \frac{m_e}{m_i} \right) \left(1 + \frac{T_i}{T_e} \right) \left(1 - \nu_e \right) \right] \qquad (2.11)$$

$$\gamma_i = \frac{2T_i}{T_e} \qquad (2.12)$$

where ν_e is the secondary electron yield per incident ion-electron pair.

Using the above energy transmission factors, the total power to the plate is:

$$Q_{plate} = \Gamma_p (kT_i \gamma_i + kT_e \gamma_e) \qquad (2.13)$$

where Γ_p is the particle flux at the plate. It should be noted that the above equation gives the energy flux that passes through the sheath to the target plate. It does not represent the actual energy deposited on the plate. This topic will be discussed in the next section along with recycling.

2.3 Neutral Particles and the Source Terms

The source terms in the fluid equations are usually derived from detailed neutral transport calculations. Neutrals can enter the plasma from several sources. The primary source of neutrals is the divertor target plate(s). Energetic hydrogen and helium ions are accelerated through the sheath and strike the divertor plate. Some of these particles are immediately backscattered as neutrals, retaining a large fraction of their original energy. The remaining particles are implanted in the target material where they come to rest as interstitial atoms. The helium atoms tend to become trapped in the material at grain

boundaries and dislocation sites. The hydrogen atoms are more mobile and can diffuse back out to the surface of the material where they recombine into molecular hydrogen and are emitted from the plate with an energy corresponding to the surface temperature of the target material. These molecules, however, are quickly dissociated and the resulting hydrogen atoms continue with an energy approximately equal to the Franck-Condon energy (3-5 ev). Because of this, the usual assumption is that the slow neutrals are emitted from the plate at the Franck-Condon energy. This flux of neutrals (fast and slow) diffuses through the plasma, undergoing excitation (emitting line radiation) and ionization by electron and ion impact. Until ionization take place, and a neutral appears as an ion with a given energy and momentum, the neutral acts as a momentum and energy sink. Thus, the spatial distribution of these neutrals and the associated excitation and ionization events serve as source/sink terms.

Once a neutral is ionized, it is swept back towards the target plate by the background plasma where it can once again impact the divertor plate. This process of repetitive neutralization at the plate and ionization near the plate is called recycling and is very dependent on plasma temperature and density since these parameters determine the reaction probabilities and rates. The recycling process is what

gives the divertor great potential for particle exhaust and impurity control. Its impact on divertor plasma parameters can be appreciated using a simple 1D recycling model, as discussed below.

Consider a plasma incident on a wall at x=a as shown in Figure 2.2. The continuity equation for the plasma is:[11]

$$\frac{\partial(nv)}{\partial x} = S = n_e \, n_o \, <\sigma v>_{ionization} \qquad (2.14)$$

where x is the direction along field lines, nv is a particle flux, n_e is the electron density, n_o is the neutral density, and $<\sigma v>$ is the electron impact ionization rate coefficient.

Integrating from the divertor entrance (x=0) to the divertor plate (x=a) yields:

$$\Gamma_a = \Gamma_o + \int_0^a n_e \, n_o \, <\sigma v> \, dx \qquad (2.15)$$

where $\Gamma_a = n_i v_a$ is the particle flux at the divertor plate (n_i is ion density), and Γ_o is the input particle flux at the divertor throat.

From the above expression it can be seen that the flux increases as the plate is approached (due to ionization of neutrals coming of the plate). A flux amplification factor

can be defined, $\mathring{A} = \Gamma_a/\Gamma_o$. Then the above equation becomes:

$$\mathring{A} = 1 + \frac{1}{\Gamma_o} \int_0^a n_e \; n_o \; <\sigma v> \; dx \; > 1 \qquad (2.16)$$

If the sheath boundary condition, $Q(a)=\gamma kT(a)\Gamma_a$ (where $\gamma = \gamma_i + \gamma_e$), is applied, where $Q(a)$ is the energy going to the plate at x=a, $kT(a)$ is the target plasma temperature (the ion and electron temperatures are assumed to be the same), and Γ_a is the target flux, and if the substitution $\Gamma_a = \Gamma_o\mathring{A}$ is made, we get:

$$kT = \frac{Q(a)}{\gamma \; \Gamma_a} = \frac{Q(a)}{\gamma \; \Gamma_o} \cdot \frac{1}{\mathring{A}} \qquad (2.17)$$

From equation (2.17) we can see that increasing $\mathring{A}$ decreases kT.

If $v_a = C_s \propto [T(a)]^{1/2}$ then:

$$Q(a) \sim \Gamma_a \; kT(a) \; \sim n(a)v_a kT(a)$$

$$Q(a) \sim n(a)[kT(a)]^{3/2} \quad \text{or}$$

$$n(a) \; \propto \frac{Q(a)}{[kT(a)]^{3/2}} \; \propto \mathring{A}^{3/2} \qquad (2.18)$$

Figure 2.2   Schematic Illustration of a Divertor Model

Thus, increasing the particle recycling increases n and decreases kT as noted before. Å>1 implies that each ion entering the divertor will, on average, impact the plate Å times. Therefore the energy per particle that goes to the plate is less. Another way of expressing recycling is with the recycling coefficient, R, defined by

$$R = \frac{\Gamma_a - \Gamma_o}{\Gamma_a} = \frac{\int_o^a n_e n_o <\sigma v>_{ion} dx}{\Gamma_a} \qquad (2.19)$$

and representing the fraction of particles hitting the plate which are recycled particles.

The result of recycling is a cool dense plasma in front of the target plate. Besides giving each entering particle several opportunities to deposit its energy on the divertor plate, the actual amount of energy to be deposited on the plate by particle impact is reduced because each time a particle recycles it has the chance to emit line radiation by collisional excitation prior to being ionized and going back to the plate. This energy loss by line radiation in the divertor is designated as "remote radiation cooling"[13] and is another advantage to the divertor because this radiated heat flux is distributed over the entire surface

of the divertor chamber. An empirical estimate by Harrison et al[4] of the energy loss due to ionization and radiation by each ionized neutral is:

$$\chi(eV) = 17.5 + \left(5 + \frac{37.5 \text{ eV}}{T_e}\right) \log_{10}\left(\frac{10^{21} m^{-3}}{n_e}\right) \quad (2.20)$$

Under most divertor conditions the magnitude of this energy loss is about 25 eV per ionized D-T neutral.

Post and Lackner[11] have solved the continuity equations for neutrals and ions, matching the fluxes at the plate. Using several assumptions they found two stable operating regimes for a divertor. One regime is found around $\AA \approx 1$ or $R \approx 0$ (low recycling) where neutrals stream (with little ionization) back to the main plasma or down pump ducts. For this regime the plasma temperature at the plate is high and the density low. The second stable regime is a high recycling one, where $\AA \gg 1$ or $R \approx 1$, and the divertor plasma is cooler and more dense. This is the preferred operating mode because the divertor plate heat load and sputtering is less than in the low recycling regime.

2.4 Impurities and the Source Terms

Impurities present in the plasma do not enter into the

particle source terms but at high enough densities can enter into the momentum and energy source terms by causing radiation losses via collisions. In this way impurities act as energy and momentum sinks. Low Z impurities will become fully stripped above several eV and, thereby, cease to be significant energy sinks. However, their presence in the main plasma can take the place of fuel atoms, due to plasma neutrality requirements and beta limits. The same is true for medium Z impurities which can radiate up to temperatures of around 2 keV (unlikely in a divertor). This means that until they are redeposited on a surface or pumped, they will continue to cause energy losses in the divertor plasma. Heavy impurities are capable of radiating from the core of the main plasma so they will also cause radiation losses in the divertor plasma. These heavy impurities, though, are quickly ionized so they should quickly return to the surface from which they were emitted.[11]

The primary source of impurities in the main plasma chamber (besides He) is the sputtered wall material resulting from the impact of charge-exchange neutrals on the walls. The precipitating slow neutrals could come from refueling atoms. The prime source of impurities in the divertor is obviously the divertor plates where the ions are intentionally impacted. A fraction, f , of the atoms that are sputtered off the plate will be quickly ionized and

carried back to the plate where they will redeposit and/or cause self-sputtering with a yield per impact of Y_s. Summing successive generations of self-sputtering and redeposition shows that if $fY_s < 1$ per incident ion, then the net impurity production rate, R_e, or sputtering of the plate is given by:

$$R_e = \Gamma_{H+} \, Y_{H+} \left(\frac{1}{1-fY_s} \right) \qquad (2.21)$$

where Γ_{H+} is the hydrogen ion (D or T) flux to the plate, Y_{H+} is the sputtering yield for hydrogen on the plate material, and f and Y_s are as defined above.

If $fY_s > 1$, the plate could potentially erode away very quickly due to runaway sputtering. However, at a local level, self-sputtering is a self-limiting process. An increase in sputtering will cause the plasma to cool down due to impurity radiation (described below) which will decrease the sheath potential and thereby reduce the impact energy of the D-T ions and impurity ions. This same cooling though, can allow impurities to escape into the main plasma, poisoning it. Sputtering of the divertor chamber walls can also occur as a result of charge-exchange neutrals that escape the divertor plasma.

As noted above, the major impact of impurities on the

plasma is to cool it via line radiation. Estimating the amount of impurity radiation is extremely difficult. Impurities in the divertor will radiate by: line radiation, recombination, and bremsstrahlung processes. Each of these processes is in turn dependent on the charge state of the impurity. In some cases the assumption of coronal equilibrium is made in which the rate equations for ionization and recombination to different charge states are solved based on a constant density and temperature plasma and no impurity-particle transport losses. The results of these calculations yields the following empirical expression for radiation power:[15,16]

$$P_{rad}(MW/m^3) = n_e n_{imp} \alpha(T) \; Z^\beta = n_e^2 f \; L_z \qquad (2.22)$$

where $n_e(m^{-3})$ is the electron density, n_{imp} is the impurity density, $\alpha(T)$ and β are fitting constants, Z is the atomic number of the impurity, f is the fractional impurity density, and L_z is the power parameter.

These expressions are valid for Z>6 and T> 1 keV. Little data exists for the lower temperatures anticipated in the divertor. Even if such data existed, the assumption of coronal equilibrium is suspect. The timescale for the onset of coronal equilibrium in a plasma is, in the case of a

divertor, greater than the timescale for ionization and return to the target plate. Preequilibrium values for the power parameter, L_z, can be 2-10 times the equilibrium values, depending on the impurity. Additionally, there are steep temperature and density gradients near the divertor plate which would also tend to invalidate coronal power estimates. This is an area which requires further research.

It is important to note that the impurity radiation can have a beneficial effect in the divertor by cooling the plasma while depositing the radiation energy over an area substantially greater than just the divertor plate. Some divertor designs include a provision for the intentional injection of medium Z impurities (e.g. xenon) into the divertor plasma to reduce the particle heat load on the target plate.

If the divertor is to operate effectively, divertor impurities must remain in the divertor. Impurity concentrations in the core plasma of as low as .01 % can fatally poison it. There are two dominant forces on an impurity ion which tend to pull in opposite directions. The first is the frictional drag of the background plasma as it flows into the divertor. The second is a thermal force pointing in the direction of higher temperature (i.e. out of the divertor to the core plasma).

Neuhauser[14] has identified a criterion which if

satisfied, implies that highly charged impurities will tend to be entrained and drift with the background plasma back to the divertor plate. Based on a model of the above forces, the criterion for impurity entrainment is:

$$\mathbb{M} > \frac{\lambda_I}{\lambda_T} \qquad (2.23)$$

where $\mathbb{M}$ is the plasma flow mach number, λ_I is the mean free path for coulomb collisions between impurity ions and the background plasma ions, and λ_T is the axial (along field lines) scale length for changes in the ion temperature. If the criterion is met, then the divertor will accrue the advantages of plasma cooling by impurity radiation without poisoning the core plasma.

CHAPTER 3

THE TWO POINT MODEL

As noted in Chapter 1, the development of a divertor model involves a tradeoff between simplicity, ease of implementation, and completeness. One immediate simplification that can be made is to develop the model in only one dimension. The choice of dimension adopted here is the direction along field lines. Using this dimension allows for linkage back to the core plasma. An additional consideration in this selection is that radial solutions to the fluid equations tend to be very sensitive to the value of the radial diffusion and thermal diffusivity coefficients which can only be estimated.

A second simplification is to solve the model equations at only two points, rather than continuouly along field lines. The two-point method of solution of the fluid equations involves integration along field lines between the divertor throat and target plate. By limiting the solution to the densities and temperatures at only these two points, the integrals of the particle, momentum, and energy source terms can be evaluated globally, greatly simplifying their representation and method of solution.

The two-point approach to modeling the divertor will yield values for the most critical divertor-plasma

parameters without requiring an inordinate amount of numerical computing effort.

This chapter of the thesis presents the derivation of the two point analytic equations for the throat and plate temperatures and densities, and the models and methods of evaluation for key terms in these analytic expressions.

3.1 Description/Geometry

The geometry of the two-point model assumes that the edge region of the plasma can be divided into two regions: one outside the divertor, and the other inside the divertor. An idealized elemental flux tube parallel to magnetic field lines (Figure.3.1) of length L_s (outside the divertor) and L_d (inside the divertor) is "unwound" from the torus. Both L_s and L_d are dependent on the geometry and magnetic topology of the reactor. The two point model is then applied to the region inside the divertor. Appendix C presents some simple analytic expressions for estimating plasma parameters between the symmetry (watershed) point and the divertor throat. These results for throat density and temperature are used as input for the model inside the divertor.

The steady state fluid equations which will be integrated along the straightened out field lines are,[5]

Figure 3.1   Two Point Model Geometry

Continuity $\quad \dfrac{d}{dx} \quad nv = -S_n$ $\hfill$ (3.1)

Momentum $\quad \dfrac{d}{dx} \left[nMv^2 + nT(1+r) \right] = S_p$ $\hfill$ (3.2)

Energy $\quad \dfrac{d}{dx} \left\{ x_o T^{2.5} \dfrac{dT}{dx} + nv \left[\dfrac{1}{2} Mv^2 + \dfrac{5}{2} T(1+r) \right] \right\} = S_e$ $\hfill$ (3.3)

where x is the direction along field lines, S_n, S_p, and S_e are, respectively, the particle, momentum, and energy source terms, n is the particle density, v is the plasma fluid flow speed, T is the electron temperature, M is the ion mass, r is the ion to electron temperature ratio (T_i/T_e), and x_o is the electron thermal conductivity coefficient (ion conduction is neglected).

The first term inside the brackets of the momentum equation, (3.2), accounts for the momentum due to fluid flow (convection) and the second term is the temperature (internal energy) contribution to momentum. The first term inside the brackets of the energy equation, (3.3), represents the energy conducted by electrons while the second term is the energy convected by ions and electrons. The energy source term is primarily derived from the recycling of neutrals at the plate, but can be artificially increased to mimic the losses due to impurity atoms. The addditional components required in the model, as outlined

in Chapter 2, will be presented as they arise in the derivation of the modeling equations and the description of the evaluation of terms.

3.2 Integration of the Fluid Equations Along Field Lines

Integration of the energy equation yields,

$$x_o T^{2.5} \frac{dT}{dx} + nv\left[\frac{1}{2}Mv^2 + \frac{5}{2}T(1+r)\right] = \int_p^x S_e dx + C \quad (3.4)$$

If the origin, (x=0), is at the plate, then the constant of integration, C, is found to be,

$$C = \left\{ x_o T^{2.5} \frac{dT}{dx} + nv\left[\frac{1}{2}Mv^2 + \frac{5}{2} T(1+r)\right] \right\} \Big|_t - \int_p^t S_e dx \quad (3.5)$$

where the first term on the right (in brackets) can be interpreted as Q_t, the energy flux that enters the throat, and the second term, as the energy loss/gain between the throat and the plate.

Integrating equation (3.4) results in

$$\left(\frac{T_t}{T_p}\right)^{7/2} - 1 = \frac{7 \; Q_t \; L_d \mu}{2 \; \kappa_o T_p^{7/2}} \qquad (3.6)$$

where T_t is the throat electron temperature, T_p is the plate electron temperature, and μ is the average fraction of energy transported in the divertor by conduction, and is given by,

$$\mu = 1 - \frac{1}{Q_t L_d} \int_p^t \left\{ \int_x^t S_e dx' + nv\left[\frac{1}{2}Mv^2 + \frac{5}{2}T(1+r)\right] \right\} dx \quad (3.7)$$

The next step in the derivation of the model equations is to eliminate the plate temperature from the right hand side of equation (3.6) using the sheath boundary condition[5],

$$Q_t - \int_p^t S_e dx = n_p v_p T_p (\gamma_e + r_p \gamma_i) \qquad (3.8)$$

where $\gamma_{e,i}$ is the sheath energy transfer factor for electrons, ions, n_p is the plate electron density, T_p is the plate electron temperature, v_p is the fluid speed at the divertor plate, and r_p is the ion to electron temperature ratio at the plate.

Solving for T_p and substituting the resulting expression

into equation (3.6) gives,

$$\left(\frac{T_t}{T_p}\right)^{7/2} - 1 = \left(\frac{n_p}{n_{\nabla T}}\right)^{7/3} \tag{3.9}$$

where $n_{\nabla T}$ is given by

$$n_{\nabla T} = \left(\frac{2\kappa_o}{7L_D\mu}\right)^{3/7} \frac{Q_t^{4/7}\left(1 - \frac{\int_p^t S_e dx}{Q_t}\right)}{\left(\gamma_e + r_p\gamma_i\right)} \left(\frac{M}{1+r_p}\right)^{1/2} \tag{3.10}$$

and can be interpreted as a temperature gradient threshold. In reference 5 it was found that if the throat density was less than this value, heat conduction tended to overwhelm the tendancy of recycling to produce a temperature gradient near the divertor plate. This means neutral recycling becomes less effective in lowering the plate temperature if the throat density falls below this threshold value. The momentum and continuity equations are now used to eliminate T_t and T_p from the left hand side of equation (3.9) as described below.

First the momentum equation is rewritten to include the fluid mach number ($\mathcal{M} = v/C_s$),

$$\frac{d}{dx}\left[Mn\tilde{m}^2C_s^2 + nT(1+r)\right] = S_p \qquad (3.11)$$

where C_s is the ion sound speed, and is given by

$$C_s = \left[\frac{T(1+r)}{M}\right]^{1/2} \qquad (3.12)$$

Integrating equation (3.11) and simplifying we obtain

$$nT(1+r)(1+\tilde{m}^2) = \int_p^x S_p dx + C \qquad (3.13)$$

If the integral on the right is evaluated at the plate (i.e. x=0) then,

$$C = n_p T_p (1 + r_p)(1 + \tilde{m}_p^2) = 2 n_p T_p (1+r_p)$$

where $\tilde{m}_p$ has been set equal to 1.0 as a boundary condition. Solving equation (3.13) for T we obtain

$$T = \frac{1}{n\left(1 + r\right)\left(1 + \tilde{m}^2\right)}\left[\int_p^x S_p dx' + 2n_p T_p\left(1+r_p\right)\right] \qquad (3.14)$$

Evaluating the integral of equation (3.14) out to the throat, point t, and dividing by T_p results in

$$\frac{T_t}{T_p} = \frac{1}{T_p n_t \left(1+r_t\right)\left(1+\bar{m}_t^2\right)} \left[\int_p^t S_p dx + 2n_p T_p\left(1+r_p\right) \right] \quad (3.15)$$

or rearranged as,

$$\frac{T_t}{T_p} = \frac{n_p}{n_t} \frac{1+r_p}{1+r_t} \frac{1}{1+\bar{m}_t^2} \left[2 + \frac{\int_p^t S_p dx}{n_p\left(1+r_p\right)T_p} \right] \quad (3.16)$$

The above expression can be further simplified by employing the following definitions:

R= fraction of ions hitting the plate which come from the ionization of neutrals and is equal to

$$R = \frac{\Gamma_p - \Gamma_t}{\Gamma_p} = \frac{\int_p^t S_n dx}{n_p v_p} = \frac{M^{1/2}\int_p^t S_n dx}{n_p\left[T_p\left(1+r_p\right)\right]^{1/2}} \quad (3.17)$$

where $\Gamma_{p,t}$ are, respectively, the particle fluxes at the plate and divertor throat.

$\overline{V}$ = average neutral velocity normalized to the ion speed at the plate, given by

$$\overline{V} = \frac{\frac{1}{M}\int_p^t S_p dx}{v_p \int_p^t S_n dx} = \frac{M^{-1/2}\int_p^t S_p dx}{\left[T_p\left(1+r_p\right)\right]^{1/2}\int_p^t S_n dx} \qquad (3.18)$$

Using R and $\overline{V}$ as defined above, equation (3.16) can be rewritten as

$$\frac{T_t}{T_p} = \frac{n_p}{n_t} \ \frac{1+r_p}{1+r_t} \ \frac{1}{1+ \tilde{m}^2_t} \left(2 + \overline{V}R\right) \qquad (3.19)$$

Finally, this equation can be inserted into equation (3.9) to give

$$\left[\frac{n_p}{n_t} \ \frac{1+r_p}{1+r_t} \ \frac{1}{1+\tilde{m}^2_t} \left(2 + \overline{V}R\right)\right]^{7/2} - 1 = \left(\frac{n_p}{n_{\nabla T}}\right)^{7/3} \qquad (3.20)$$

An expression for $\tilde{m}_t$ can be derived from the continuity equation, the definition of R, and equation (3.19). Thus,

$$\bar{M}_t = \left(\frac{a}{1-a} \right)^{1/2} \tag{3.21}$$

where
$$a = \frac{n_p}{n_t} \left(1-R \right)^2 \left(\frac{1}{2+\bar{V}R} \right)$$

Equation (3.20) uses information from all three fluid equations in it derivation. This equation, along with equation (3.8) and a simplification of equation (3.18), can be used to solve for three of the four primary plasma parameters; T_p, n_p, T_t, and n_t. Before this can be done though, methods for evaluating the integrals of the source terms, the conduction fraction (μ), and the recycling coefficient (R) must be determined.

3.3 Evaluation of the Integrals of the Source Terms

3.3.1 Introduction

The evaluation of the integrals of the particle, momentum, and energy source terms requires a detailed understanding of divertor physics. The source terms are primarily derived from the recycling of neutrals produced at the divertor plate. Plasma ions are accelerated through the sheath, strike the divertor plate, and are neutralized. A fraction (R_n) of these particles is immediately

backscattered, retaining a large fraction (R_e) of their impact energy (see Appendix A for expressions for R_n and R_e). The remaining fraction ($1-R_n$) is implanted in the target material where the particles come to rest as interstitial atoms. The normal assumption is that at equilibrium the implanted hydrogen atoms diffuse back out to the surface of the divertor plate where they recombine into hydrogen molecules and are emitted with an energy corresponding to the plate temperature. Dissociation by electron impact occurs quickly near the plate after emission so another assumption often used is that these neutrals are emitted from the plate as atoms (rather than molecules) with an energy equivalent to the Franck-Condon energy (3-5 eV). This flux of fast and slow neutrals then diffuses through the plasma undergoing excitation (emitting line radiation), charge exchange, and ionization (by electron impact). Each of these processes will be considered in the derivation of the integrals of the source terms.

3.3.2 Integral of the Particle Source Term

The only source of D-T particles in the divertor region is the ionization of neutrals. The value of the particle source term can be expressed as a function of the recycling coefficient defined in this chapter and Chapter 2. Thus,

$$\int_p^t S_n dx = R\Gamma_p = Rn_p\left[\frac{T_p\left(1+r_p\right)}{M}\right]^{1/2} \qquad (3.22)$$

The evaluation of the recycling coefficient is accomplished by modeling neutral transport and will be discussed in Section 3.5.

3.3.3 Integral of the Momentum Source Term

The integral of the momentum source term must account for the two energy groups of neutral particles, slow and fast. After leaving the target plate, each neutral particle can undergo charge exchange, ionization, or escape to the divertor plenum where it may return to the plasma or be pumped. Charge exchange and ionization events both contribute to the momentum source term while escape/pump events contribute nothing. Considering only these two contributing processes, F_{ion}, the fraction of neutrals coming directly from the plate which undergoes ionization rather than charge exchange, is given by,

$$F_{ion} = \frac{<\sigma v>_{ion}}{<\sigma v>_{ion} + <\sigma v>_{cx}} \qquad (3.23)$$

where $<\sigma v>_{ion}$ is the reaction rate coefficient for electron impact ionization (ground state and excited state combined) and $<\sigma v>_{cx}$ is the charge exchange rate coefficient (see Appendix A for evaluation of these quantities).

Each neutral that is ionized contributes an average of $Mv_o \sin\theta$ to the momentum source. This is derived from the assumption of perpendicular emission of the neutrals from the plate. The velocity of the neutral in this perpendicular direction is V_o, while θ is the angle of incidence of the magnetic field lines to the plate (see Figure 3.2). The neutral velocity in the field line direction is $v_o \sin\theta$.

For the fast group the neutral velocity is given by

$$v_f = \left(\frac{2 R_e E_o}{R_n M}\right)^{1/2} = \left(\frac{2 R_e T_p \gamma_i}{R_n M}\right)^{1/2} \qquad (3.24)$$

where E_o is the incident energy of the ion. For the slow group the neutral velocity would be

Figure 3.2   Momentum Source Term Geometry

$$v_s = \left(\frac{2\ E_{fc}}{M} \right)^{1/2} \tag{3.25}$$

where E_{fc} is the Franck-Condon energy.

The relative fraction that undergoes charge exchange is,

$$F_{cx} = 1 - F_{ion} \tag{3.26}$$

Charge exchange represents a change in momentum because incoming ions change places with neutral particles of different speeds and directions. The calculation of this component of the momentum source term depends on whether neutrals are modeled with their own set of fluid equations or included in the single fluid considered here. If neutrals are accounted for separately, the contribution to the momentum source would be,

$$M(v_o \sin\theta + v_{avg}) \tag{3.27}$$

where M is the ion mass, $v_o \sin\theta$ is the neutral velocity in the field direction, and v_{avg} is the average ion velocity between the throat and plate. The neutralization of the incoming ion causes an average loss of momentum of Mv_{avg},

where v_{avg} is calculated as,

$$v_{avg} = \frac{1}{2}\left[\left(\frac{T_t\left(1+r_t\right)}{M}\right)^{1/2}\hat{n}_t + \left(\frac{T_p\left(1+r_p\right)}{M}\right)^{1/2}\right] \quad (3.28)$$

This approach to calculating the momentum source term assumes that there is no change in direction of the initial neutral (now an ion) as a result of the charge exchange interaction. If the resulting neutral from this interaction is subsequently ionized then the momentum of the neutral (Mv_{avg}) is regained making a negative addition to the source term. If neutral particles are not accounted for separately with a set of fluid equations then the neutral contribution to the source term must be added to the ion component. This makes the charge exchange component $Mv_o\sin\theta$, the same as for ionization.

Based on the above expressions, and whether neutrals are independently modeled, the final expression(s) for the integral of the momentum source term can be written as

$$\int_p^t S_p dx = M n_p v_p R \left\{ R_n \left[F_{ion-f} v_f \sin\theta + F_{cx-f} \left(v_f \sin\theta + v_{avg} \right) \right] + \left(1 - R_n \right) \left[F_{ion-s} v_s \sin\theta + F_{cx-s} \left(v_s \sin\theta + v_{avg} \right) \right] \right\}$$

If neutral momentum pressure is included in the D-T ion equations, this expression reduces to

$$\int_p^t S_p dx = M n_p v_p R \left[R_n v_f \sin\theta + (1-R_n) v_s \sin\theta \right] \qquad (3.29)$$

where $n_p v_p$ represents the neutral particle flux coming off the plate at steady state and the other terms are as described previously.

Here the recycling coefficient (R) is being used as a measure of the fraction of neutral flux that undergoes interaction. Although this is a reasonable use for R, it does imply that the contribution to the momentum source term of ionized or charge exchanged neutrals coming from the divertor plenum is negligible.

Numerical evaluation of the integral of the momentum source term for a variety of divertor conditions resulted in values which are small compared to the total momentum of the D-T particles as they flow to the plate and thus, this

term has little effect on the final solution of the fluid equations. It is noted that in some models[2,3,22] this term is neglected altogether. The divertor code developed in this thesis gives the user the option of including this term or setting it to zero.

3.3.4 Integral of the Energy Source Term

The integral of the energy source term includes contributions from radiation, ionization, and charge exchange. To account for radiation and ionization losses, the average energy loss per ionization event, χ, defined previously, is used

$$\chi(eV)=17.5 + \left(5 + \frac{37.5}{T_e(ev)}\right) \log_{10}\left(\frac{10^{21}m^{-3}}{n_e}\right) \ ev$$

For a neutral produced at the target and moving through the plasma fan in front of the divertor plate, the use of an energy loss per ionization event assigns the entire energy loss to the point of ionization. In reality it will radiate throughout its trajectory due to excitation by electron impact. Over a wide range of operating conditions, the value of χ does not vary much from a value of around 25-26 eV for hydrogen. Its value could be artificially increased to

include losses due to the radiation and ionization of impurities. This enhancement would be proportional to the amount of sputtering, impurity type, and mean free paths for impurity ionization and excitation. As noted in Chapter 2, evaluating the magnitude of this energy loss increment is difficult. Therefore, in the divertor model code this increment is treated as a multiplicative parameter, $\chi' = Imp \cdot \chi$, where Imp is a multiplicative factor, increasing D-T radiation losses to account for impurity energy losses.

Charge exchange also contributes to the energy source term. Incoming ions change places with neutrals which have different energies. The total energy of an incoming ion can be written as[5]

$$E_{ion} = 3/2 \ T + 1/2 Mv^2 \qquad (3.30)$$

where T is the plasma temperature and v is the flow speed.

If the assumption is made that the energy of the fast neutrals is approximately the same as that of the incoming ions, then the charge exchange of neutrals of this energy group contributes nothing to the energy source term. If, in addition, it is assumed that the energy of the slow neutrals is negligible compared to the energy of the incoming ions, then charge exchange represents the total loss of the

incoming ion's energy. Based on these assumptions, the integral of the energy source term can be expressed as,

$$\int_p^t S_e \, dx = n_p v_p \left[R\chi' + \left(1 - R_n\right) F_{cx-s} \left(\frac{3}{2} T_{avg} + \frac{1}{2} M v_{avg}^2 \right) \right] \quad (3.31)$$

where T_{avg} is the average plasma temperature between the throat and plate and V_{avg} is the average flow velocity.

In equation (3.31) above, χ' is multiplied by the recycling coefficient since this represents the total fraction of neutral flux that is ionized. The second term is not multiplied by R because this term pertains only to slow neutrals. The fraction of slow neutrals that is ionized is much larger than the combined fraction of slow and fast. Therefore it is assumed that 100% of the slow neutrals undergo some sort of interaction (i.e. $R_{slow} \approx 1$).

3.4 Evaluation of the Conduction Fraction

The conduction fraction introduced in Section 3.2 (eqn 3.7) is the average fraction of energy transported in the divertor by electron conduction. Thus

$$\mu = 1 - \frac{1}{Q_t L_d} \int_p^t \left\{ \int_x^t S_e dx' + nv \left[\frac{1}{2} Mv^2 + \frac{5}{2} T(1+r) \right] \right\} dx \quad (3.32)$$

Evaluation of this quantity requires a knowledge of the density, temperature, mach number, and energy source (sink) term profiles in the divertor region. The two point model does not provide this profile information so the following assumptions must be made to evaluate μ.

The first assumption is to ignore the integral of the energy source term. The major contribution to this integral comes from a narrow band near the divertor plate. While this term might be significant near the plate, it represents a small contribution to the second integral. Numerical integration of this integral has confirmed the insignificance of the source term.

The second assumption concerns the profiles of the density and ion to electron temperature ratio, (r). A previous study, using more sophisticated models[5], has shown a reasonable distribution for these two quantities has the following form, $f(x)$,

$$f(x) = f(0) + \left[f(L) - f(0) \right] \left[1 - \left(1 - \frac{x}{L} \right)^\alpha \right] \quad (3.32)$$

where α is a polynomial shape factor.

Using the continuity equation, (3.1), the mach number can be expressed in terms of n and r as

$$\bar{M}(x) = \left(1-RR'\right)\left[\frac{n_p\left(T_p(1+r_p)\right)^{1/2}}{n\left(T(1+r)\right)^{1/2}}\right] \quad (3.33)$$

where R' is the fraction of ionization up to x and is given by

$$R' = \frac{\int_p^x S_n dx'}{\int_p^t S_n dx'} \quad (3.34)$$

Equation (3.33) can be used along with the momentum equation, (3.2), to yield the temperature profile,

$$T(x) = \left[\left(\bar{V}R\right)' + 2 - \left(1-RR'\right)^2 \frac{n_p}{n}\right]\frac{n_p T_p(1+r_p)}{n T(1+r)} \quad (3.35)$$

where $(\bar{V}R)'$ is the fraction of momentum source up to the point x and is given by

$$(\overline{V}R)' = \overline{V}R \; \frac{\int_p^x S_p dx'}{\int_p^t S_p dx'} \qquad (3.36)$$

Evaluation of R' and $(\overline{V}R)'$ requires additional assumptions about the distribution of the particle and momentum sources. One intuitively simple method is to assume an exponentially decreasing distribution for these sources. Thus

$$S_n \; \alpha \; \left[R_n EXP\left(\frac{-x}{\lambda_1}\right) + \left(1-R_n\right) EXP\left(\frac{-x}{\lambda_2}\right) \right] \qquad (3.37)$$

and

$$S_p \alpha \; R_n \left[F_{ion-f} v_f \sin\theta EXP\left(\frac{-x}{\lambda_1}\right) + F_{cx-f}\left(v_f \sin\theta + \right. \right.$$
$$\left. v_{avg}\right) EXP\left(\frac{-x}{\lambda_3}\right) \right] + \left(1-R_n\right)\left[F_{ion-s} v_s \sin\theta EXP\left(\frac{-x}{\lambda_2}\right) + \right.$$
$$\left. F_{cx-s}\left(v_s \sin\theta + v_{avg}\right) EXP\left(\frac{-x}{\lambda_4}\right)\right] \qquad (3.38)$$

or in its simplified form (neutral momentum included)

$$S_p \alpha \ R_n \ v_f \sin\theta \ \text{EXP}\left(\frac{-x}{\lambda_1}\right) \ + \ \left(1- R_n\right) v_s \sin\theta \ \text{EXP}\left(\frac{-x}{\lambda_2}\right)$$

$$(3.39)$$

where λ_j is the mean free path (MFP) for; fast neutral ionization (j=1); slow neutral ionization (j=2); fast neutral charge exchange (j=3); and slow neutral charge exchange (j=4). Each mean free path is calculated as,

$$\lambda_j = \frac{v_j}{n_{av}<\sigma v>_j \sin\theta} \qquad (3.40)$$

where n_{av} is the average throat to plate density, $<\sigma v>_j$ is the appropriate reaction rate coefficient, and v_j is the particle velocity. The $\sin\theta$ term adjusts the MFP to account for the fact that the integration is being performed along field lines while the particles are assumed to come off the divertor plate perpendicularly.

Given a shape factor, α, the above set of equations can be numerically integrated to give a value for the conduction fraction, μ.

3.5 Evaluation of the Recycling Coefficient

3.5.1   Introduction

The recycling coefficient, R, was defined in Section 3.2 as the fraction of ions hitting the plate that come from the recycling of neutrals. Those neutrals that are not ionized in their first pass through the plasma, but escape to the plenum region of the divertor can eventually meet one of three fates: 1.) return to the plasma and be ionized after scattering around the divertor plenum (the probability that a neutral makes it back through the plasma to the plate , reflects, and escapes again is very small); 2.) be pumped out of the divertor plenum; or 3.) escape out the divertor throat to the core plasma where they are ionized. The contribution of this third channel is small so, to first order, what is not pumped out of the divertor chamber is eventually recycled to the divertor plate. Based on this phenomenological description the global recycling coefficient can be approximated as,

$$R = 1 - \bar{p}f \qquad (3.41)$$

where $\bar{p}$ is the average neutral escape probability (energy group and position averaged) and f is the ratio of neutrals pumped to those reaching the divertor plenum.

For the purposes of this model, the pumped fraction will be varied as a free parameter. One does have some control

over the value of this parameter based on pump speed, geometry of the pump ducts (conductance) and divertor plenum, and plenum wall materials. Calculation of the pumped fraction would be the subject of future study. Thus, the evaluation of R requires the determination of the neutral escape probability, $\bar{p}$.

3.5.2 Calculating the Neutral Escape Probability

The method used to calculate $\bar{p}$ is based on a wedge shaped section of plasma overlying the divertor plate and a simple slab attenuation approach (see Figure 3.3). First the MFP for ionization of a neutral by electron impact is calculated for slow and fast neutrals using

$$\lambda = \frac{v}{n\langle\sigma v\rangle_{ion}} \qquad (3.42)$$

where v is the fast or slow velocity, n is the electron density, and $\langle\sigma v\rangle$ is the combined ground state and excited state electron impact ionization reaction rate coefficient. The MFPs can be calculated using plate or average quantities.

The probability that a neutral of given velocity and angular direction will be ionized after being emitted from a

Figure 3.3   Geometry of Neutral Escape Probability
             Calculation

point on the divertor plate is given by

$$p(x,\phi) = EXP\left(\frac{-l(x,\phi)}{\lambda}\right) \qquad (3.44)$$

where $l(x,\phi)$ is the distance to the plasma surface (beginning of plenum) along the direction ϕ from the point x and λ is the energy/velocity dependent MFP. It should be noted that no particular allowance has been made for the effect of charge exchange events. A similar approach to calulating $\bar{p}$ (reference 3) found that this contribution to $\bar{p}$ is small so it is neglected here.

Several methods for summing these probabilities over all directions and points on the plate have been examined in this thesis. Each has been included in the final divertor model programs as options.

The first method entails calculating an average distance, $\bar{l}(x)$, to the plasma surface for each of a mesh of points on the divertor plate. At each point, l is expressed as a function of angle ϕ, point position (x), width of the divertor plate(x_t), and angle of incidence of the field lines to the plate (θ). This function is then integrated between $\phi=o$ and $\phi=ARC$, where ARC is the angle back to the throat of the divertor. Any neutral that is emitted in a direction greater than ARC is assumed to be ionized. This

method gives the following result

$$\overline{l}(x) = \frac{\int_0^{ARC} l(\phi)d\phi}{\int_0^{ARC} d\phi} = \frac{TAN\phi(x-x_t)}{ARC} \int_0^{ARC} \frac{d\phi}{ACOS\phi + BSIN\phi}$$

where A is $TAN\theta$ and B is 1.0. The explicit result is,

$$\overline{l}(x) = \frac{TAN\theta \ (x-x_t)}{\left(A^2 + B^2\right)^{1/2} ARC} \left\{ ln\left[TAN\frac{1}{2}(ARC+\theta)\right] - ln\left[TAN\left(\frac{\theta}{2}\right)\right] \right\}$$

$$(3.45)$$

The neutral escape probability for neutrals emitted from a point on the plate is then

$$p(x) = \frac{ARC}{\pi} \left[R_n EXP\left(\frac{-\overline{l}(x)}{\lambda_f}\right) + \left(1-R_n\right) EXP\left(\frac{-\overline{l}(x)}{\lambda_s}\right) \right] \quad (3.46)$$

where λ_f and λ_s are the fast and slow neutral ionization MFPs.

This escape probability is then calculated for a mesh of points along the divertor plate and the average, $\overline{p}$, defined as the global escape probability. The advantage to this

method lies in the fact that the integral used has an explicit solution which speeds calculation for a mesh of points. The disadvantage is that the exponential of an *average escape distance* is not the same as the integral of the escape probability averaged over all possible directions.

The second method involves numerically evaluating the integral of the escape probability as a function of angle. Thus,

$$p(x) = \int_0^{ARC} EXP\left(\frac{-1(\phi)}{\lambda}\right) \frac{ARC}{\pi} \, d\phi \qquad (3.47)$$

This integral is evaluated for slow and fast neutrals and the escape probability at x calculated as

$$p(x) = R_n p(x)_{fast} + \left(1 - R_n\right) p(x)_{slow} \qquad (3.48)$$

Again, this evaluation must be performed for a mesh of points along the plate and the average escape probability, $\bar{p}$, calculated.

Another option included in the *divertor model program* is an angular probability for reflection in the integral of the second method. Some experiments have found that particle

reflection from a smooth surface was not isotropic for 90° incidence but showed a cosine distribution. Use of this option decreases the escape probability because most of the particles that escape do so by escaping from the tip of the plasma wedge. Weighting the directional escape probabilities with a cosine distribution decreases the contribution of those particles which are emitted in a direction towards this tip.

A program was written to compare the results of each of these methods against one another and against the results in reference 3. A detailed comparison of the three methods (l_{avg}, integral, and integral with a cosine distribution) can be found in Appendix D. Typical results are shown in Figure 3.4, giving the escape probalility as a function of plate position for the integral with cosine method. As seen in this figure, the escape probability increases as the thickness of the plasma overlying the plate decreases (see Figure 3.3 for geometry). Also, it is noted that the escape probability is much less for slow neutrals than for fast neutrals due to their smaller ionization MFP. Below, the results of the three methods are compared to the result of reference 3.

Figure 3.4   Neutral Escape Probability versus Plate
Position

Table 3.1
Neutral Escape Probability Comparison

Approach	$\bar{p}$
l_{avg}	.067
integral	.095
integral w/cosine	.074
Ref 3	.077

For these results, plate quantities (T_p and n_p) were used. It is noted that in reference 3 a cosine distribution was employed.

3.6 Helium Effects

The steady state concentration of helium in the core plasma has a great influence on the power output of the reactor. Additionally, helium in the divertor can significantly increase the sputtering of the divertor plate and increase radiative cooling of the divertor plasma. The concentration in the core plasma and in the divertor is a function of the helium-ash removal rate from the divertor. Helium ions flow with the plasma into the divertor and impact the divertor plate where they are neutralized (some

may become permanently implanted) and return to the divertor plasma. Just as with D-T neutrals, some of the helium neutrals will be ionized and recycled to the plate while others will escape to the divertor plenum and may be pumped or return to the plasma to be ionized. Analogous to the D-T recycling coefficient, a global helium recycling coefficient can be defined as

$$R_{He} = 1 - \bar{p}_{He} f_{He} \qquad (3.49)$$

where $\bar{p}_{He}$ is the average helium neutral escape probability and f_{He} is the helium pumping probability. This pumping, probability, f_{He}, may differ from the D-T pumping probability depending on pump type, plenum and duct configuration, and neutral particle (D-T or He) energy distribution. Just as with the pumping probability for D-T, f_{He} is also varied as a free parameter in the divertor model code. The escape probability for helium can be calculated using the same equations presented in section 3.5 by replacing the D-T ionization rate coefficient with the helium ionization rate coefficient.

The helium ions which originally enter the divertor are normally in the +2 charge state. The recycled helium ions, however, can be in charge state +1 or +2. This distribution of charge states will have an impact on the concentration of

helium at the plate and on the sputtering of the plate due to the sheath potential. The probability, P_{12}, that a singly charged helium ion will be ionized to the +2 state can be estimated as[3]

$$P_{12} = 1 - EXP\left(\frac{-t_{res}}{\tau_i}\right) \qquad (3.50)$$

where t_{res} is the residence time of the He^+ ion in the divertor, and τ_i ($\sim 3 \times 10^{-5}$ sec) is a characteristic time for the ionization step He^+ to He^{++}.

An upper limit on this residence time can be obtained by neglecting the effects of local electric fields and expressing it as

$$t_{res} = t_t + t_{drift} \qquad (3.51)$$

where t_t is a thermal equilibration time ($\sim 10^{-5}$ sec) for ion-ion collisions and t_{drift} is the ion drift time at the fluid velocity (assumed to be the plate sound speed, C_p) and is estimated as

$$t_{drift} = \frac{MFP_{ion}}{C_p} \qquad (3.52)$$

The ionization probability, P_{12}, can be used to estimate the fractional concentration of helium at the divertor plate. At steady state, the helium which enters the divertor must be equal to the helium pumped. This condition can be expressed as

$$\xi_{He}(t)\Gamma_t = \xi_{He}(p)\Gamma_p(1-R_{He}) \qquad (3.53)$$

where ξ_{He} is the fractional concentration of helium (singly and doubly charged) relative to the electron density and $\Gamma_{t,p}$ is the electron flux at the throat/plate.

The helium concentration at the throat is normally taken to be the core plasma concentration. The D-T ion flux at both locations, throat and plate, is less than the electron flux due to the presence of helium. At the throat

$$\Gamma_{t,D-T} = n_e\left(1 - 2\ \xi_{He}(t)\right)C_t \bar{m}_t \qquad (3.54)$$

and at the plate

$$\Gamma_{p,D-T} = n_e \left[1 - \left(1 + P_{12} \right) \xi_{He}(p) \right] C_p \qquad (3.55)$$

So, at the plate, part of the D-T ion flux is replaced by helium flux which will increase sputtering due to its greater mass and possible +2 charge state.

The exhaust performance of the divertor can be characterized in terms of the helium enrichment factor, ε, expressed as

$$\varepsilon = \frac{\Gamma_{He}(pump) / \ \Gamma_{D-T}(pump)}{\Gamma_{He}(t) \ / \ \Gamma_{D-T}(t)} \qquad (3.56)$$

or expressed in the quantities defined above

$$\varepsilon = \frac{\left(1 - R_{He} \right) \xi_{He}(p)}{\left(1 - R \right) \left[1 - \left(1 + P_{12} \right) \xi_{He}(p) \right]} \cdot \frac{\left(1 - 2\xi_{He}(t) \right)}{\xi_{He}(t)}$$

In addition to causing a fuel depletion effect and increased sputtering, the helium which is recycled in the divertor can add to the radiation energy losses, cooling the plasma. In the present calculations this radiation component has been estimated as

$$\chi_{He}(ev) = 15 + P_{12}\left(70 + \frac{3300}{T_e}\right) \qquad (3.57)$$

where χ_{He} is the energy loss per ionized helium particle and T_e is the local electron temperature. The 15 eV term corresponds to the energy loss in going from He^O to He^+, while the remainder of the χ_{He} expression is for ionization to He^{++}. The energy loss in the divertor plasma due to helium recycling (to be added to equation (3.31)) is

$$P_{Rad-He}(eV) = n_p v_p \xi_{He}(p) \chi_{He} R_{He} \qquad (3.58)$$

Any charge exchange component to this energy loss has been neglected.

3.7 Sputtering

One of the critical concerns in designing a divertor is the sputtering rate of the target plate material. This rate will determine the service lifetime of the plate, and as noted in Chapter 2, impurity production can have a great impact on the viability of the divertor design. Once the plasma model has determined the plate temperature and density (with an estimated impurity increment), these parameters can be used to estimate the plate sputtering.

Some iterative process might be necessary to make the result self-consistent.

The sputtering rate (including self sputtering) at a point on the target plate, as expressed in Chapter 2, is

$$R_e = \Gamma_p Y \left(\frac{1}{1-fY_s} \right)$$

where Γ_p is a particle flux at a point on the plate, Y is the sputtering yield for the particular particle (incident energy and plate material dependent), Y_s is the self sputtering yield, and f is the fraction of impurities returned to the plate. The above equation is valid for $fY_s < 1$.

The sputtering yields can be determined using a sputtering model by Smith et al[21] which can be expressed as

$$Y(E_o) = \frac{C}{40} z_1^{.75} \left(z_2 - 1.8 \right)^2 \left(\frac{M_1 - .8}{M_2} \right) \frac{E_o - E_{th}}{\left(E_o - E_{th} + 50 z_1^{.75} z_2 \right)^2}$$

$$(3.59)$$

where

$$
\begin{aligned}
C \quad &= 2000 \text{ for incident hydrogen } (^1H)\\
&= 400 \text{ for all other particles}
\end{aligned}
$$

Z_1 = atomic number of incident particle

Z_2 = atomic number of plate material

M_1 = mass number of incident particle

M_2 = mass number of plate material

E_0 = incident particle energy (eV)

E_{th} = threshold energy for sputtering (eV)

The threshold energy for sputtering is given by

$$E_{th} = \frac{\left(4M_1 + M_2\right)^2}{4\ M_1 M_2} U_0 \tag{3.60}$$

where U_0 is the binding energy of the plate material (eV). Appendix A includes a table of values for Z, M, and U_0 for various plate materials.

The incident energy of particles impacting the plate can be expressed as a function of the sheath energy transmission coefficients. Thus,

$$E_0 = r_p \left(E_p + ZT_p(\gamma_i - 2) \right) \tag{3.61}$$

where E_p is the energy of the particles prior to sheath acceleration (which has a Maxwell-Boltzmann distribution at the plate), T_p is the electron temperature at the plate, and

Z is the charge of the particle.

If the temperature of the plasma is well above the sputtering threshold, then $E_p=2T_p$ can be used,[3] and evaluating the sputtering is very straight-forward. In most instances, though, the plate temperature is less than the sputtering threshold. However, this does not imply that there is no sputtering. Particles in the high temperature tail of the Maxwell-Boltzmann distribution may still cause sputtering. Therefore, the calculation of the sputtering rate must take account of this particle distribution. Thus,

$$R_e= \Gamma_p\left(\frac{1}{1-fY_s}\right) \cdot \int_{E'}^{\infty} P(E)Y(E_o)dE \qquad (3.62)$$

where P(E) is the Maxwell-Boltzmann distribution

$$P(E) = \left(\frac{E}{T_p}\right)^{1/2} EXP \left(\frac{-E}{T_p}\right)$$

and E' is the particle energy at which $E_o=E_{th}$

$$E' = E_{th}/r_p - ZT_p(\gamma_i-2)$$

Equation (3.62) can be numerically integrated to give the

sputtering rate.

The sputtering rate can be converted to an erosion rate (cm/yr, 100% duty) by dividing R_e by the plate material number density (cm^{-3}) and multiplying by the number of seconds in a year

$$d_e(\text{cm/yr}) = \frac{R_e}{\rho} \cdot 3.15 \times 10^7 \qquad (3.63)$$

The code for the divertor model includes a subroutine which calculates sputtering of the target plate due to deuterium, tritium, and helium (+1 and +2). An assumption necessary to implement this model is that sputtered plate material atoms return to the plate in the +1 charge state. The erosion and sputtering rates are calculated at each of 50 points across the divertor plate and the peak erosion rate outputed, along with the total impurity production rate per length of divertor.

3.8 Impacts of Radial Variations

The simplication of the fluid equations to consider only the axial direction introduces certain inaccuracies in calculating neutral escape probabilites and plate sputtering. These quantities are sensitive to the plate

density and temperaure. Use of the axial approximation
makes it necessary to assume a constant plasma density and
temperature across the divertor plate. To remedy this a
literature search was conducted to determine how to
introduce radial variation of these parameters into the
divertor model.

The results of most models[9,13,17,18,19,20] show that
radial density and temperature profiles are approximately
exponential in both the upstream region (throat and beyond),
and in the downstream region (in the divertor) and can be
expressed as

$$P(r) = P_o \ EXP\left(\frac{-r}{\lambda_a}\right) \qquad (3.64)$$

where P is the parameter of interest (T or n), and λ_a is
the fall-off distance for that parameter.

For density, the fall-off distance can be approximated as

$$\lambda_n = \left(D \ \tau_\parallel\right)^{1/2} \qquad (3.65)$$

where D is the radial diffusion coefficient (m^2/sec) (in
this work experimental values have been used) and $\tau_\parallel$ is a
characteristic transport time, approximated as

$$\tau_{\parallel} = \frac{L}{v} \qquad\qquad (3.66)$$

where L is a connection length in the region for which λ_n is being calculated, and v is an average fluid velocity in the region.

For λ_n at the target plate, L is the divertor connection length, L_d, and v is the sound speed at the plate (even though the mach number at the throat is normally small, the sound speed is large, so C_p represents a reasonable average).

The temperature fall off distance is more difficult to calculate and has been modeled many different ways. In reference 17 the ratio λ_T/λ_n was found to be an increasing function of $\chi_{\perp}/D$ and a decreasing function of the sheath energy transmission factor. Rather than attempt to calculate λ_T, the ratio λ_T/λ_n can be varied as a free parameter, A.

To test the validity of using exponential profiles for the temperature and density at the plate a separate program was written which evaluated these profiles in the pressure balance equation derived from the continuity and momentum fluid equations,

$$n_t T_t \left(1 + r_t\right)\left(1 + \tilde{m}_t^2\right) = 2\, n_p T_p \left(1 + r_p\right) \qquad (3.67)$$

On the basis of this investigation, it was concluded that the pressure balance equation could be satisfied radially with exponential profiles for density and temperature. In the computer model λ_n at the plate is calculated and A is an input parameter. The radial profiles for temperature and density have been added to the calculations of the recycling coefficient (including weighting each escape probability along the plate by the flux incident at that point) and sputtering rate.

CHAPTER 4

DESCRIPTION OF THE COMPUTER MODEL

To yield results, the divertor model described in Chapter
3 must be implemented on a computer using various numerical
computing techniques to solve for the parameters of
interest. Section 4.1 of this chapter discusses the
possible solution techniques and the rationale for the
selection of a fixed-point iteration approach. Section 4.2
then describes the implemented model code, DIV, in detail
including; program logic and structure, data input
requirements, and program output.

4.1 Discussion of Numerical Solution Techniques

Solution of the model equations given in the previous
chapter involves the simultaneous solution of a system of
nonlinear equations. There are several techniques that can
be used to solve such a system. The first is a straight
forward fixed-point iteration approach. The advantage to
this method is the simplicity of implementation. While the
convergence of this method is only linear to super-linear
(better than linear, less than quadratic), the final
solution set need not be accurate to greater than about 1%
since the model is only an approximation. Given a good set

of initial guesses for the solution variables, the only concern would be the stability of the solution. The disadvantage to this method is the requirement for good initial guesses. If the initial guesses are too far from the solution values, then the results might diverge, or converge to an unstable set.

Other more sophisticated methods are based on Newton-Raphson approaches which require the evaluation or estimation (via the secant method) of the partial derivatives of the equation set . These methods involve the use of matrix operations to solve the system of equations. Such methods will normally converge more quickly than the fixed-point method (quadratic convergence) and can be written in ways to increase the chance for convergence even with poor initial guesses. However, this increase in "power" is bought at the cost of much increased complexity and computing time. Reference 5 used a software package program, HYBRID, to solve a set of model equations. Solution of this similar set required .2 seconds of Cray computer time. For the model described in this thesis, a fixed point iteration approach with some improvements has been adopted.

4.2 Computer Model DIV Description

The computer model DIV, written in IBM Fortran for an IBM-PC/AT (or compatible), uses a fixed point iteration routine to solve the model equations for the plate density and temperature, and the throat temperature using the following fixed-point equations:

$$n_p = \left[\left(\frac{n_p}{n_{\nabla T}} \right)^{7/3} + 1 \right]^{2/7} \left[\frac{n_t \left(1 + r_t \right) \left(1 + \overline{m}_t^2 \right)}{\left(2 + \overline{V}R \right) \left(1 + r_p \right)} \right] \qquad (4.1)$$

derived from equation (3.20),

$$T_p = \left[\left(Q_t - \int_p^t S_e \, dx \right) \frac{M^{1/2} \left(\gamma_e + r_p \gamma_i \right)}{n_p \left(1 + r_p \right)^{1/2}} \right]^{2/3} \qquad (4.2)$$

derived from equation (3.8), and

$$T_t = \frac{\left(2 + \overline{V}R \right) \left(1 + r_p \right) T_p n_p}{\left(1 + \overline{m}_t^2 \right) \left(1 + r_t \right) n_t} \qquad (4.3)$$

derived from equation (3.19)

The throat density is held constant.

Input for the code (Table 4.1) requires starting values for n_p, T_p, and T_t. The user has the option of specifying the recycling coefficient, R, and/or the conduction

Table 4.1

Program DIV Input

Inputs	Definition	Units
QT	Power flux into the divertor	W/m^2
LD	Divertor connection length	m
M	D-T ion mass	amu
XT	Divertor plate width	m
THETA	Angle of incidence of magnetic field lines to the divertor plate	radians
EL	D-T reflection coefficient reduced energy	
TP	Plate electron temperature	eV
TT	Throat electron temperature	eV
NP	Plate electron density	$x10^{19}m^{-3}$
NT	Throat electron density	$x10^{19}m^{-3}$
RP	Plate ion to electron temperature ratio	
RT	Throat ion to electron temperature ratio	
G1	Electron sheath energy transmission coefficient	
G2	Ion sheath energy transmission coefficient	
R	Recycling coefficient	

Table 4.1 cont.

Input	Definition	Units
U	Conduction fraction	
F	D-T pump fraction	
IMP	Impurity increment	
D	Radial diffusion coefficient	m^2/sec
A	Temperature to density fall-off distance ratio	
CT	Fractional concentration of helium at the throat	
FHE	Helium pump fraction	
ELM	Helium reflection coefficient reduced energy	
SHP	Shape factor, α, for the conduction fraction	
METH	Method for $\bar{p}$ calculation 1=Lavg 2=integral	
DIST	Distribution for $\bar{p}$ calculation 1=none 2=cosine	
TOL	Convergence tolerance	
SOR	Over or under relaxation constant	

fraction, μ, (which will then be held constant) and of setting the momentum source term equal to zero. Otherwise these variables will be calculated. Most of the variables inputed are known quantities or can be calculated using methods presented in Appendices A and C. Others, such as the ion to electron temperature ratios and pump fractions, can be estimated from the results of other models or experiments. The only parameter for which there is no physical or calculational basis is the shape factor, α, used in calculating the conduction fraction. However, experience with the code has shown the final solution set to be insensitive to the value of α except for very low recycling cases.

After the initial data entry, the program (see flowchart of Figure 4.1) first calculates initial and intermediate quantities, such as $\widetilde{m}_t$, μ, R, and $\overline{V}$, based on the initial values for T_p, n_p, and T_t. The program then calculates the first of the fixed point parameters, applies successive over or under relaxation,

$$A'_{n+1} = SOR\left(A_{n+1}\right) + \left(1-SOR\right)A_n \qquad (4.4)$$

where A' is the relaxed variable and SOR is the over/under relaxation constant, and then updates the intermediate

Figure 4.1   Program DIV Flowchart

variables prior to calculating the next fixed point parameter (a la Gauss Seidel). This relaxation method was added to the fixed point routine to preclude wide oscillations (if SOR <1 is used) or to speed convergence (if SOR >1 is used) of the iterations.

The newly calculated value for the plate density is then compared to the old value using a relative error check for convergence (the user specifies the tolerance). The plate density was chosen as the convergence parameter because its equation includes information from all three fluid equations and, by practice, was found to be the most difficult parameter to get to converge. If the convergence criterion is met, then the program recalculates the intermediate parameters based on the solution set and displays this set and the intermediate parameters (Table 4.2). If the criterion is not met, then the program loops back to start another iteration. After each iteration is complete the most current values for the fixed-point parameters are displayed on the screen so the user can observe if the results are converging or diverging. After ten iterations with no convergence the user is prompted to continue or stop iterations and return to data entry. If convergence is achieved, the user is asked if sputtering should be calculated. Sputtering calculations require additional data entry (Table 4.3). The sputtering subroutine canalso be

F/G 18/1   NL

Table 4.2

Program DIV Output

Output	Definition	Units
TP	Plate temperature	eV
NP	Plate density	$m^{-3} x 10^{-19}$
TT	Throat temperature	eV
NT	Throat density	$m^{-3} x 10^{-19}$
MT	Throat mach number	
U	Conduction fraction	
ISE	Radiation loss fraction	
R	Recycling coefficient	
CP	Fractional helium at the plate	
HER	Helium enrichment	
P12	Ionization probability of $He^{+} \rightarrow He^{++}$	
LNP	Density fall distance at the plate, λ_n	

directly accessed after the initial data entry, bypassing the divertor calculations.

An extensive number of runs with the DIV code for a variety of input data has allowed the inclusion of a number of error checks in the program to stop execution of the code if certain parameters are diverging. This has eliminated most realtime fatal errors. Appendix B includes a complete

Table 4.3

Sputtering Input Data

Input	Definition	Units
UO	Plate material binding energy	eV
Z3	Plate material atomic number	
M3	Plate material mass number	
NM	Plate material number density	$cm^{-3}x10^{-24}$
IE	Multiple of TP for upper limit to maxwell-boltzmann integration	

listing of the DIV computer code. It also has a description of each of the subroutines displayed in Figure 4.1.

CHAPTER 5

BENCHMARKING THE DIVERTOR MODEL

5.1 Introduction

As stated in Chapter 1, the goal of this research is to produce a simple, comprehensive, and accurate model of the divertor region. The requirements to limit the complexity of the model and to include all key processes have been met as described in Chapters 3 and 4. How close the model has come to satisfying the third requirement, accuracy (i.e. to yield results comparable to those of more sophisticated models), will now be discussed. In this chapter the computer code DIV is benchmarked against four other models: a model by the JAERI team[22], the Harrison et al model[3], the ZEPHYR code[4], and the Braam's code[9]. The results displayed in the comparison tables reflect only the parameters reported by each of these codes which are also calculated by DIV. Complete data input and output for each benchmark case can be found in Appendix E.

5.2 JAERI Team Model Benchmark

This model is a one fluid, 1D (axial) plasma edge model which includes remote radiative cooling, recycling, and

particle shielding at the main plasma surface. The particle, momentum, and energy source terms are evaluated by a neutral transport code. In reference 22 the code is described, and results for modeling of Doublet III compared (favorably) to experimental results. To obtain the DIV results listed in Table 5.1 the following assumptions were made: the momentum source term was set to zero, and the radiative power loss was artificially increased (by making IMP=1.45) to mimic the oxygen impurity radiation included in the JAERI calculations. Additionally, the recycling coefficient was calculated, in the absence of any divertor plate data, by assuming a plate width of .25 m and a theta of .35 radians. The pump fraction, f, was arrived at by back-calculation using the reported recycling coefficient and divertor plasma results. The remainder of the input data for DIV was the same as that used by the JAERI team for its results. The results of this comparison are listed in Table 5.1.

Table 5.1
JAERI Team Benchmark Case

Parameter	JAERI Team	DIV
T_p(eV)	4.0	3.8
n_p($\times 10^{19}$ m^{-3})	9.1	9.2
T_t(eV)	37.0	35.0
n_t($\times 10^{19}$ m^{-3})	1.8	1.8
Throat Mach Number, $\bar{m}_t$	.26	.34
Radiation fraction	.50	.51
Recycling Coefficient, R	.81	.80

The results of Table 5.1 indicate that DIV compares extremely well with the JAERI team model. The largest deviation in any fixed point parameter is less than 6%. The sensitivity of these results to changes in impurity radiation and the shape factor was also examined. A 5% increase in the impurity increment, increasing the radiation fraction by a like amount, caused about a 20% decrease in T_p and a corresponding increase in n_p. Variation of the shape factor, α, from 3 to 4, caused a 15% change in n_p and T_p. Both these sensitivities were expected. Experience with the DIV code has shown that T_p becomes more sensitive to the

impurity increment as the impurity fraction increases. In this case, the radiation fraction, is fairly large (~.5). Alternatively, it has been found that sensitivity to the shape factor decreases as the recycling coefficient increases (or as the conduction fraction increases). The recyling coefficient for this case, .81, is rather low, correlating to the sensitivity to the shape factor observed.

5.3 Harrison, et al Model Benchmark

This model is also 1D and one fluid. It includes neutral particle transport, remote radiation cooling, helium effects, and impurity radiation. The data and results presented in reference 3 are for INTOR under "standard conditions". One of this model's assumptions is that electron conduction is the only energy transport mechanism. The modeling assumptions for DIV in this case were that impurity radiation was zero (it was found to be negligible in reference 3) and the momentum source term was equal to zero. Table 5.2 gives the results of this comparison.

Table 5.2
Harrison et al Model Benchmark Case

Parameter	Reference 3	DIV
$T_p(eV)$	25.5	23.8
$n_p(\times 10^{19}\ m^{-3})$	9.6	9.2
$T_t(eV)$	66.0	63.0
$n_t(\times 10^{19}\ m^{-3})$	6.97	6.97
Conduction Fraction, μ	1.00	.99
Radiation Fraction	.13	.16
Helium Enrichment, ε	3.18	2.23
Recycling Coeffient, R	.99	.99
Plate Helium Concentration	.05	.025

The DIV results compare very well with the Harrison et al results. The largest deviation of any of the parameters is for the radiation fraction (23%) and the helium enrichment (30%), but the deviation for the parameters of most interest, T_p and n_p, is less than 7%. One difference between the two models is that the Harrison model assumes that the concentration of helium at the plate is the same as the concentration in the core plasma while DIV calculates

this quantity. This difference was accounted for in the calculation of the helium enrichment but was not sufficient to account for the difference in values of the helium enrichment. Some additional runs were made to try to make the two radiation fractions equal by adjusting the impurity increment. Setting the impurity increment (IMP) equal to .85 (from an initial value of 1.0) succeeded in matching these parameters, but increased the plate temperature slightly and decreased the plate density. However, there appears to be no physical basis on which to decrement the D-T radiation value.

The results above were found to be fairly sensitive to the energy transmission factors (γ_i and γ_e). An increase in both of about 20% caused a 28% decrease in T_p and a 39% increase in n_p. The percentage changes and the directions of the changes were reversed for a 20% decrease in the energy transmission factors. The results were also found to be insensitive to the shape factor due to the large recycling coefficient and conduction fraction.

5.4 ZEPHYR Benchmark

ZEPHYR is an axial 1D, two fluid numerical divertor model developed at Culham laboratories. It includes: a simple 1D neutral model; neutral recycling; D-T radiation; particle

and energy convection; fluid viscosity; and electron/ion equipartition. It solves the fluid equations along field lines between a symmetry point and the divertor plate. The results presented in reference 4 are for an INTOR-like device. The specific results to which DIV is compared is the "Search 13A" case (one of the many results in this parametric study). The only assumption made to benchmark against this case was to set the momentum source term equal to zero. The input data values for DIV were, for the most part, all taken from the reported ZEPHYR input or ZEPHYR results (such as ion to electron temperature ratios and Q_t value). The recycling coefficient was set to the .471 value used by ZEPHYR. Benchmarking for the pump fraction value, as was done for the JAERI case, yielded a pump fraction greater than 1.0 (an impossibility). Therefore, iterative calculation of the recycling coeffcient was not possible. This benchmarking result indicates a significant difference between the neutral particle models of the two divertor models. It should be noted that the reported recycling coefficient for this case, .471, is extremely low considering the reported plate temperature (10.8 eV) and density ($8.6 \times 10^{19} \text{ m}^{-3}$). One final note is that helium effects were neglected. Table 5.3 displays the comparison to the ZEPHYR results.

TABLE 5.3
ZEPHYR Benchmark Case

Parameter	ZEPHYR	DIV
T_p(eV)	10.8	10.5
n_p($\times 10^{19}$ m^{-3})	8.6	8.68
T_t(eV)	26.7	28.0
n_t($\times 10^{19}$ m^{-3})	3.66	3.66
Throat Mach Number, $\mathcal{M}_t$	.73	.70
Radiation Fraction	.15	.16
Recycling Coefficient, R	.471	.471

The largest deviation from the ZEPHYR values was in the radiation fraction which was only 8% different. As expected, the DIV results were somewhat sensitive to the shape factor due to the low value of the conduction fraction ($\sim$.14). The results above are for α=5. Changing this to α=6 caused T_p/n_p to increase/decrease by about 6%. A similar sensitivity was arrived at when the shape factor was decreased to a value of 4. The results are also very sensitive to changes in the sheath energy transmission factors (though the values used for the results above were

the same as those used in reference 4). A 10% increase in
the radiation fraction (by setting IMP=1.1) had only a
slight effect on the temperature and density at the plate
($\leq 6\%$). Because the radiation fraction is only 15% in this
case, radiative cooling does not play an important role in
determining the plate conditions.

5.5 Braam's Code Benchmark

This model solves the Braginskii fluid equations for
electrons and ions in two dimensions (axially and radially)
from a symmetry point (between divertors) to the divertor
plates. The code includes particle/energy convection,
viscosity, equipartition, axial variation in the radial
thickness of the edge plasma (i.e. cross-sectional area),
radiation, and helium effects. The results of this model,
reported in the NET Report #50, reference 9, are for a
NET/INTOR-like device for both the inner and outer divertor
plates. In doing this benchmark case it was necessary to
convert the radial results for temperature and density into
average values at the plate and throat for both data input
and comparison. The modeling assumptions made include: the
momentum source term is zero, and the pump fractions for D-T
and helium are the same. Another inherent assumption in
this approach is that the average values themselves

represent a solution to the fluid equations. Some of the specific input data requirements had to be satisfied using the calculational methods of Appendix C. The pump fractions were back-calculated as described in Section 5.2, using the plate data given in the NET report. Table 5.4 reports the results of this comparison.

Table 5.4
NET Report #50 (outer target) Benchmark

Parameter	Report #50	DIV
T_p(eV)	7.6	11.0
n_p($\times 10^{19}$ m^{-3})	14.0	13.4
T_t(eV)	67.3	64.8
n_t($\times 10^{19}$ m^{-3})	5.0	5.0
Radiation Fraction	.17	.21
Recycling Coefficient, R	.998	.998
Plate Helium Concentration	.011	.025
Helium Enrichment, ϵ	1.0	.99

The plate temperature for this case is 45% higher than it should be and the plate concentration of helium is more than twice the Report #50 value. Additionally, the radiation

fraction is somewhat high (which makes this an unlikely candidate for lowering T_p). Numerous runs were made in an attempt to improve the results with no success. The conclusion arrived at is that the assumption, that average values represent a solution, may in fact not be valid. The disperity between the two reported helium plate concentrations may be due to the assumption the $f_{He}=f_{D-T}$ used in DIV. In some other models the pump fraction for helium is larger than that for D-T. This would tend to decrease the plate concentration bringing it closer to the Report #50 value.

The results tended to be sensitive to the sheath energy transmission factors. As expected, the results were insensitive to the shape factor (R was large) and the radiation fraction (which was low, ~21%).

5.6 Benchmarking Conclusions

In general, the divertor model DIV yields very good results when compared to other 1D axial models. Some problems arise, due to the average value assumption, when comparison is made to a 2D model. The sensitivity of the results to three input parameters, the shape factor, energy transmission factors, and radiation fraction (via the impurity increment), was examined and qualitative

dependencies identified as listed in Table 5.5 and discussed below. The most sensitive of these three parameters was the

Table 5.5
Parameter Sensitivities

Parameter	Sensitivity of T_p and n_p	
	Small	Large
Sheath Energy Transmission Factors, γ_i and γ_e	-	Always
Impurity Increment, IMP	If radiation fraction is small	If radiation fraction is large
Shape Factor, α	If R or μ is large	If R or μ is small

sheath energy transmission factors which directly control the rate at which energy can be exhausted to the divertor plate. Any increase in these factors will decrease the plate temperature, and increase the plate density. The next most sensitive parameter was the radiation fraction. This quantity could be adjusted using the impurity increment. The greatest sensitivity was found when the impurity fraction was high. This observation implies that the final plate temperature is very dependent on the total power lost by radiative processes. When the radiation fraction is low,

the sensitivity is much decreased. Finally, the sensitivity to the shape factor was found to be a function of the recycling coefficient. As R increases, the mach number at the throat decreases, decreasing the fluid flow velocity, and thereby, energy convection. This forces the conduction fraction to increase. As μ increases it becomes less sensitive to the shape factor. In general, an increase in the shape factor would independently decrease the conduction fraction, but the interplay with the other variables tends to make the net effect an increase in μ.

Several other comments are warrented as a result of the benchmarking and other program runs. The pressure at the divertor plate ($\propto n_p T_p$) is ultimately determined by the energy flux (Q_t) into the divertor. The effect of the sheath energy transmission factors and radiation fraction is only to alter the relative value of these parameters, not their product. This implies that there is only so much that can be done with the injection of impurities to reduce heat deposition and sputtering. This impurity injection approach, though, sensitizes the plate density and temperature to changes in the magnitude of the radiation fraction. Any mechanism which might cause fluctuations in the amount of radiation produced in the divertor (such as flow reversal) will cause wide variation in plate density and temperature.

Another comment concerns the inclusion of the the calculation of R in the program. The ability to allow R to vary as the program iterates has improved the convergence characteristics of the numerical techniques used and gives a more self-consistent final solution. It also appears that the low recycling regime is not accessible for some combinations of input data. In most cases, if the initial guesses for the fixed-point parameters were poor the program tended to move towards the high recycling regime. Whether this indicates a greater amount of stability for this regime, or is just a numerical quirk is not known.

Finally, a few comments about sensitivities, other than those noted in the benchmarking section, are warranted. In most cases the results of a converged run are sensitive to the throat density, n_t. As n_t increases, the plate density will increase, with a corresponding decrease in plate temperature (this is with Q_t constant). An increase in Q_t tends to increase the plate temperature. The response of the radiation energy loss mechanisms is normally not great enough to compensate for an increase in the energy flux, so the plate temperature must increase to reflect the greater amount of energy that much be exhausted to the divertor plate.

CHAPTER 6

SUMMARY, CONCLUSIONS, AND FUTURE WORK

6.1 Motivation and Objective

If fusion by magnetic confinement is ever to become a viable energy source, the problems associated with impurity production and exhaust must be solved. The divertor concept represents an attractive solution to these problems by exhausting D-T particles and helium-ash into a separate chamber, away from the core plasma, where they can be impacted on a target plate, neutralized, and pumped out of the reactor. The performance of a given divertor design, though, can presently, only be assessed with the use of plasma edge models. Expensive experimentation must eventually be performed to verify the results of these models.

The modeling itself is a complex process both because it involves a strong coupling between numerous reactor systems (core plasma, first wall, divertor, pumping, etc..) and because the fluid equations used are highly nonlinear. Some models oversimplify both the equations and processes included in order to obtain analytical expressions. While some of these simple models can identify certain dependencies, they do not yield quantitatively accurate

results. Other models attempt to include all the physics and solve the fluid equations in two dimensions (axially and radially) resulting in computer codes which are highly numerical and complex. The objective of this thesis has been to develop a simple, comprehensive, model of the divertor region that is highly usable and gives quantitatively accurate results.

The approach has been to solve the fluid equations in the axial direction (along field lines) with a two point technique in which only throat and plate quantities are of interest. This allows the particle, momentum, and energy source terms to be evaluated globally, simplifying their calculation. This approach has also limited the complexity of the numerical techniques needed to solve for the parameters of interest. The model includes the key processes of: neutral recycling; impurity production and radiation; remote radiation cooling; neutral pumping; particle convection; helium effects; and the effects of divertor geometry and plate material. Neutral particle modeling was accomplished using a simple model of a wedge-shaped section of plasma overlying the divertor plate, and a simple slab attenuation model. Additionally, a simple exponential radial profile was introduced for the plate temperature and density to make the calculations of neutral recycling and sputtering more realistic. Implementation of

the model was accomplished in Fortran on a PC to make the code highly "usable" and responsive. The numerical techniques used to solve for the plate temperature and density, and the throat temperature were a fixed-point iteration routine with Gauss-Seidel updating and successive over-relaxation. Convergence with this method is fairly quick, usually requiring less than twenty iterations. The quality of the results was examined using a series of benchmarking cases, as discussed next.

6.2 Benchmarking Results

The divertor model code, DIV, was benchmarked against four other divertor models. The results of the benchmarking validated the approach taken in this research. DIV compares extremely well with the three 1D (axial) divertor models examined. The largest deviation in any of the fixed point parameters (T_p, n_p, and T_t) was less than 8%. Comparison with the results of a 2D model was less successful but not poor. One explanation for this might be that the assumption, that averages of the radial solutions of the 2D model represent an axial solution, is not valid. The sensitivity of the results to variations in a variety of parameters was examined and qualitative dependencies identified. The only input parameter which cannot be

calculated or evaluated beforehand is the shape factor used in the calculation of the conduction fraction. However, at the high recycling regimes anticipated for effective divertor operation, the results become insensitive to the value of this parameter.

6.3 Applications

The inclusion of all key processes and the interactive calculation of the recycling coefficient, helium concentration, and divertor plasma parameters, along with its PC implementation, makes DIV especially useful for conducting parametric studies of divertor designs. Once plasma results are generated, they can be input into the sputtering module to evaluate erosion rates and impurity production. Additionally, the ability to input different materials in both the divertor code and sputtering module allows for self-consistent assessments of divertor material options.

Another versatility of DIV is the variety of allowable inputs to the code which makes it possible to match other model results. Once a given model's results are matched, the effect of slight changes to the original design or input can be determined quickly.

6.4 Future Work

In conducting the research and in development of the model, certain information was found to be lacking in the literature, and certain expediencies had to be adopted. These deficiencies represent avenues for future work, as noted below.

1. Noncoronal equilibrium impurity radiation data is nonexistent. The timescale for the return of impurities to the divertor plate is smaller than that for the onset of coronal equilibrium, invalidating the coronal equilibrium assumption made by some models. There appears to be little definitive work on noncoronal equilibrium radiation. This gap has made it impossible to link the sputtering rate at the plate to the impurity radiation.

2. Some of the input data for DIV could be calculated by the program rather than calculated off-line as done now. These might include the energy flux to the divertor (Q_t) and the sheath energy transmission factors.

3.   The present model does not allow for a variation
        in the cross-sectional area of the plasma as it
        flows to the plate. This variation could have a
        significant impact on the heat deposition on the
        plate. Such an improvement would allow for a
        more realistic magnetic field line topology at
        the plate rather than the simple topology currently
        used.

4.   Models for the D-T and helium pump fractions
        (f and f_{He}) would make the final divertor
        solutions more self-consistent and increase
        accuracy in calculating the recycling
        coefficient and helium enrichment.

5.   An investigation of flow reversal and its impact
        on divertor operations would be desireable.
        Flow reversal has been identified as occuring
        when the local recycling coefficient is greater
        than 1.0.[23] The escape of divertor impurities
        into the main plasma made possible by this flow
        reversal could make operation of the divertor
        in the high recycling regime undesireable.

LITERATURE CITED

1. S.I. Braginskii, <u>Reviews of Plasma Physics</u> vol. 1, ed. M.A. Leontovich, Consultants Bureau, N.Y.,205 (1965).

2. M.A. Mahdavi et al., "A Reviewnof the Recent Expanded Boundary Divertor Experiments in the Doublet III Device," Journal of Nuclear Materials 111 & 112, 355 (1982).

3. M.F.A. Harrison et al., "Plasma Characteristics and Gas Transport in the Single-null Poloidal Divertor of the International Tokamak Reactor," Nuclear Technology/Fusion, vol. 3, 432 (1983).

4. P.J. Harbour et al., "Models and Codes for the Plasma Edge Region," CLM-RR/E4/3, Culham Laboratory, Oxfordshire, England, (December, 1982).

5. J.D. Galambos and Y-K. M. Peng, " Two Point Model for Divertor Transport," ORNL/FEDC-83/14, Fusion Engineering Design Center, Oak Ridge National Laboratory, (April, 1984).

6. J.D. Galambos ,Y-K. M. Peng, D. Heifetz, " Coupled Plasma-Neutral Transport Model for the Scrape-off Region," ORNL/FEDC-84/6, Fusion Engineering Design Center, Oak Ridge National Laboratory, (March, 1985).

7. A.K. Prinja and R.W. Conn, " An Axially Averaged-Radial Transport Model of Tokamak Edge Plasmas," Journal of Nuclear Materials 128 & 129, 135 (1984).

8. D.E. Post and R.F. Mattas, " Impurity Control Systems for Reactor Experiments," pp1101-1147, Physics of Plasma-wall Interactions in Controlled Fusion, Plenum Press, N.Y. (1986).

9. M.F.A. Harrison and E.S. Hotson, " Plasma Edge Physics for NET/INTOR," NET Report #50, (December, 1985).

10. B.J. Braams, "11th European Conference on Controlled Fusion and Plasma Physics," EPS 7D, Part II, p431., Aachen,(September 1983).

11. D.E. Post and K. Lackner, " Plasma Models for Impurity Control Experiments," pp627-693, Physics of Plasma-wall Interactions in Controlled Fusion, Plenum Press, N.Y. (1986).

12. C.E. Singer, " Plasma Transport Near Material Boundaries," pp607-625, Physics of Plasma-wall Interactions in Controlled Fusion, Plenum Press, N.Y. (1986).

13. F. Wagner and K. Lackner, "Divertor Tokamak Experiments," pp931-1004, Physics of Plasma-wall Interactions in Controlled Fusion, Plenum Press, N.Y. (1986).

14. J. Neuhauser et al., " Impurity Transport in the Tokamak Scrapeoff Layer," Nuclear Fusion vol. 24 no. 1, 39 (1984).

15. D.E. Post et al., " Steady-state Radiative Cooling Rates for Low-density, High Temperature Plasmas," Atomic Data and Nuclear Data Tables, 20, 397 (1977).

16. H. Vernickel and J. Bohdansky, " A General Formula for Impurity Radiation Loss of Fusion Plasmas in Corona Equilibrium," Nuclear Fusion vol. 18 no. 10, 1467 (1978).

17. P.C. Stangeby, " The Plasma Sheath," pp41-97, Physics of Plasma-wall Interactions in Controlled Fusion, Plenum Press, N.Y. (1986).

18. M. Keilhacker et al., " The Plasma Boundary Layer in Limiter and Divertor Tokamaks," Physica Scripta T2/2, 443 (1982).

19. M.F.A. Harrison et al., " A Study of the Boundary Layer of INTOR," Journal of Nuclear Materials 93 & 94, 454 (1980).

20. M. Ulrickson and D.E. Post, " Particle and Energy Transport in the Plasma Scrape-off Zone and its Impact on Limiter Design," Journal of Vacuum Science Technology A, vol. 1 no. 2, 907 (April-June 1983).

21. D.L. Smith et al., " A Physical Sputtering Code for Fusion Applications," 9th Symposium on Engineering Problems of Fusion Research, vol. I , Chicago, Illinois, (1981).

22. M. Shimada and the JAERI team, " Modeling of Dense and Cold Divertor Plasma in D-III," Journal of Nuclear Materials 121, 184 (1984).

23. L. Spitzer, <u>Physics of Fully Ionized Gases</u>, 2nd ed., John Wiley & Sons, N.Y. 1983.

24. K.L. Bell et al., CLM-R216, Culham Laboratory, Oxfordshire, England, (1981).

25. P. Mioduszewski, " Advanced Limiters," pp.891-929, Physics of Plasma-wall Interactions in Controlled Fusion, Plenum Press, N.Y. (1986).

APPENDIX A

INPUT DATA FOR DIVERTOR MODELING

A.1 Thermal Conduction

The Spitzer[23] electron thermal conductivity coefficient $(x=x_0 T^{2.5})$ was used in the energy equation, (3.3), and the derivatives of this equation. The value of x_0 is calculated as,

$$x_0 = \frac{31500}{<Z>\ln\Lambda} \quad W(eV)^{-7/2} m^{-1} \qquad (A.1)$$

where $<Z>$ is the effective charge of the plasma (taken to be 1.25) and $\ln\Lambda$ is the coulombic logrithm (value of 13 used).

A.2 Surface Reflection

The reflection coefficients, R_n and R_e, for particles (D-T and helium) normally incident at energy E_0 on a surface were evaluated using the empirical relationships of reference 3.

For Particles

$$R_n = .19 - .237\log_{10}(E_o/EL) \qquad (A.2)$$

For Energy

$$R_e = 0.06 - .22\log_{10}(E_o/EL) \qquad (A.3)$$

where EL is a material, and particle, dependent reduced energy given by

$$EL(eV) = \frac{\left(M_1 + M_2\right)\left(Z_1 Z_2\right)\left(Z_1^{2/3} + Z_2^{2/3}\right)^{1/2}}{.03255\, M_2} \qquad (A.4)$$

where $M_{1,2}$ is the mass of the incident particle/target material, and $Z_{1,2}$ is the atomic number of the incident particle/target material.

A.3 Electron Impact Ionization Rates for Hydrogen

The equation for the rate coefficient for electron impact ionization of D-T from the ground state ($<\sigma v>_{ion}$) was taken from the divertor model, ZEPHYR[4], and is given by

$$\langle \sigma v \rangle_{ion,D-T} = EXP \left\{ \sum_{n=0}^{6} a_n \left[\ln(kT) \right]^n \right\} \qquad (A.5)$$

where kT is the electron plasma temperature in ev and a_n are fitting constants given by

$$a_O = -45.56 \qquad a_4 = 7.43 \times 10^{-2}$$

$$a_1 = 11.44 \qquad a_5 = 4.15 \times 10^{-3}$$

$$a_2 = 3.83 \qquad a_6 = -9.49 \times 10^{-5}$$

$$a_3 = .705$$

The collisional radiative ionization rate coefficient for D-T (ionization of an excited atom) can be expressed as[3]

$$\langle \sigma v \rangle_{cr,D-T} = \langle \sigma v \rangle_{ion,D-T} \left[1 + \frac{10}{kT} \left(\frac{n}{10^{20}} \right)^\beta \right] \qquad (A.6)$$

where kT is the plasma temperature in eV, n is the electron plasma density in m^{-3}, and β is,

$$\beta = .5 \left[1 - 1.36 \ EXP \left(\frac{-n}{10^{19}} \right) \right]$$

A.4 Charge Exchange Rates for Hydrogen

The charge exchange rate coefficients were evaluated using the expressions given in reference 3. For a D-T plasma at average temperature T_{avg} (eV), the coefficients are:

For one particle at rest (slow neutral CX)

$$<\sigma v>_{cx-s} = \left[\left(.4282 \ T_{avg} \right)^{.3338} \right] X \ 10^{-14} \ m^3 sec^{-1} \quad (A.7)$$

For both particles at T_{avg} (fast neutral CX)

$$<\sigma v>_{cx-f} = \left[\left(.8426 \ T_{avg} \right)^{.3369} \right] X \ 10^{-14} \ m^3 sec^{-1} \quad (A.8)$$

A.5 Electron Impact Ionization Rates for Helium

The expression for the electron impact ionization rate for neutral helium was taken from reference 24 and is given by

$$\langle\sigma v\rangle_{ion,He} = EXP\left(\frac{-I}{kT}\right)\left(\frac{kT}{I}\right)^{1/2}\sum_{n=0}^{5}a_n\left[\log_{10}\left(\frac{kT}{I}\right)\right]^n m^3 sec^{-1}$$

(A.9)

where kT is the electron plasma temperature in eV, I is the ionization energy of neutral helium in eV (24.6 eV) and a_n are fitting coefficients given below:

$$a_0 = 1.5\times10^{-8} \qquad a_3 = -3.59\times10^{-9}$$
$$a_1 = 5.67\times10^{-10} \qquad a_4 = 1.55\times10^{-9}$$
$$a_2 = -6.08\times10^{-9} \qquad a_5 = 1.32\times10^{-9}$$

The collisional radiative ionization rate coefficient for neutral helium can be expressed as[3]

$$\langle\sigma v\rangle_{cr,He} = \langle\sigma v\rangle_{icn,He}\left[1 + \left(\frac{10}{kT}\right)\left(\frac{I(He)}{I(D-T)}\right)\left(\frac{n}{10^{20}}\right)^{\beta}\right]$$

(A10)

where I is the ionization energy for helium (24.6 eV) and D-T (13.6 eV), and β is as given above.

A.6 Sputtering Data

The parameters for calculation of physical sputtering yields used in equations (3.59) and (3.60) are listed in Table A.1 below.[21]

Table A.1
Material Sputtering Parameters

Wall Material	Z	M	Uo(eV)
Be	4	9.0	3.4
B	5	10.8	5.7
C	6	12.0	7.4
Ti	22	47.9	4.9
V	23	50.9	5.3
Fe	26	55.9	4.3
Ni	28	58.7	4.4
Cu	29	63.5	3.5
Nb	41	92.9	7.6
Mo	42	95.9	7.8
Ta	73	180.9	10.4
W	74	183.9	11.1

Equation (2.21) presented in Chapter 2 for the

calculation of the sputtering rate due to a hydrogen ion flux can be derived based on summing the sputtering yields over a number of generations. An impacting hydrogen ion will produce Y (sputtering yield) impurity neutrals. If a fraction, f, of these plate material atoms then return to the plate, each will cause another Y_s (self sputtering yield) impurity neutrals. The total yield due to the impact of a single hydrogen ion can be represented over a number of generations by

$$\text{Total Yield} = Y + YfY_s + YfY_s\left(fY_s\right) + Y\left(fY_s\right)^3 + \ldots$$

If fY_s is < 1 then this can be rewritten as

$$\text{Total Yield} = Y\left(\frac{1}{1-fY_s}\right) \qquad (A.11)$$

So the sputtering rate due to a flux, Γ_{H+}, of hydrogen ions would be, as given by equation (2.21)

$$R_e = \Gamma_{H+}Y\left(\frac{1}{1-fY_s}\right)$$

APPENDIX B

PROGRAM DIV SUPPORT MATERIALS

This appendix contains a list of the variables in the program DIV along with a description of the subroutines in the program. Enclosed with the appendix is a printout of a sample run and the program itself.

B.1 Program Variables

Each of the significant variables used in the divertor model program DIV is described below along with its dimensions. Items with a star are data entries.

Variable	Description
* A	Ratio of temperature to density scale lengthes
ARC	Angle from a point on the divertor back to the throat (Radians)
CHE	Energy loss by radiation and ionization per recycled helium particle (eV)
CHI	Energy loss by radiation and ionization per recycled D-T particle (eV)
CP	Fractional plate concentration of helium

*	CT	Fractional throat concentration of helium
*	D	Particle diffusion coefficient (m^2/sec)
*	EL	Reflection coefficient reduced energy for D-T particles (eV)
*	ELM	Reflection coefficient reduced energy for helium particles (eV)
	ELOSS	Average energy loss per recycled neutral (eV)
*	DIST	Neutral reflection distribution to be used for the neutral escape probability calculation, 1=cosine, 2=none.
*	F	D-T Pump fraction, the fraction of neutrals pumped that reach the divertor plenum
*	FHE	Helium pump fraction
	FCXF	Relative probability of CX versus ionization for fast neutrals
	FCXS	Relative probability of CX versus ionization for slow neutrals
	FIF	Relative probability of ionization versus CX for fast neutrals
*	G1	Sheath energy transmission factor for electrons
*	G2	Sheath energy transmission factor for ions
	HER	Helium enrichment
*	IE	Upper integration limit as a multiple of plate temperature for sputtering calculations

*	IMP	Impurity radiation increment, a multiplicative factor
	ISE	Integral from plate to throat of the energy source term
*	LD	Divertor connection length (m)
	LCXF	Mean free path in field line direction for fast neutral CX (m)
	LCXS	MFP in field line direction for slow neutral CX (m)
	LDAF	MFP for fast neutral ionization(m)
	LDAS	MFP for slow neutral ionization(m)
	LF	MFP in field line direction for fast neutral ionization (m)
	LNP	Density scale length at the plate (m)
	LS	MFP in field line direction for slow neutral ionization (m)
*	M	D-T particle mass (amu)
*	M3	Atomic mass of plate material (amu)
*	METH	Method to be used for calculation of neutral escape probability, 1= integral, 2=lavg.
	MLT	Multiple of $<\sigma v>_{ion}$ to get total ionization rate (includes ground state and excited state rates)
	MT	Throat mach number
	NAV	Throat to plate average electron density (m^{-3})
	NDT	Temperature gradient density threshold (m^{-3})
*	NM	Plate material number density(m^{-3})

*	NP	Plate electron density (m^{-3})
*	NT	Throat electron density (m^{-3})
	P12	Ionization probability of He^+ to He^{++}
	PBAR	Neutral escape probability
	PFT	Total fast neutral escape probability
	PH	Neutral helium escape probablity
	PST	Total slow neutral escape probability
*	QT	Energy flux entering the throat (W/m^2)
*	R	Recycling coefficient
	RE	Energy reflection coefficient
	RHE	Helium recycling coefficient
	RN	Particle reflection coefficient
*	RP	Ion to electron temperature ratio at the plate
*	RT	Ion to electron temperature ratio at the throat
*	SHP	Shape factor for μ calculation
	SI	$\langle\sigma v\rangle_{ion}$ for groundstate ionization
*	SOR	Successive under or over relaxation coefficient
	TAV	Average throat to plate electron temperature
*	THETA	Angle of incidence of field lines to divertor plate (radians)
*	TOL	Tolerance for convergence

*	TP	Plate electron temperature (eV)
*	TT	Throat electron temperature (eV)
*	U	Conduction fraction
*	UO	Binding energy for plate material (eV)
	VAVG	Average plasma flow speed (m/sec)
	VBAR	Average neutral velocity normalized to plate ion sound speed
	VF	Fast neutral speed (m/sec)
	VS	Slow neutral speed (m/sec)
	XC	Point along divertor plate (m)
*	XT	Width of divertor plate (m)
*	Z3	Atomic number of plate material

Other variables found in the program are intermediate variables. Those with a "O" suffix are original entry values retained for comparison. Any prefix with "ANS" after it is a response to a "yes" or "no" query.

B.2 Subroutine Description

This section briefly describes the subroutines included in the divertor model program DIV. The more important of these appeared on the program flow diagram, Figure 4.1.

Subroutine	Description
ICALC	Performs initial calculation

	of basic quantities used throughout the program
ESC	Calculates the neutral escape probability and recycling coefficient for D-T using ROMBERG, EVAL1 and EVAL2.
HESC	Calculates the neutral escape probability and recycling coefficient for helium using ROMBERG, EVAL1, and EVAL2.
SRVBAR	Calculates VBAR
SRMT	Calculates MT
SRNDT	Calculates ISE and NDT
MU	Calculates the conduction fraction (μ) using ROMBERG and EVAL3.
ROMBERG	Evaluates an integral using Romberg integration.
EVAL1	Function evaluation for the integral calculation of ESC and HESC for slow neutrals
EVAL2	Function evaluation for the integral calculation of ESC and HESC for fast neutrals
PROB	Function evaluation for ESC and HESC for the lavg method
EVAL3	Function evaluation for the integral of MU
SPUD	Sputtering subroutine

B.3   DIV Program Listing (attached)

PROGRAM DIV

```fortran
C       Specifications Block

        REAL TP,TT,NP,NT,RP,RT,LD,QT,M,SHP,F,G1,
     2       G2,XT,THETA,EL,DIST,METH
        REAL MT,VBAR,PBAR,R,ISE,U,NDT,TPO,TTO,NPO,
     2       NTO,UO,RO,SOR,D,A,LNP
        REAL X(101),Y(101),Z(101),PROD,ANS,RANS,
     2       UANS,TOL,CT,CP,FHE,RH
        REAL TAV,NAV,SI,SCXS,SCXF,FIF,FCXF,FCXS,RN,
     2       RE,VF,VS,LDAS,LDAF
        REAL LCXF,LCXS,MLT,CKANS,IMP,VANS,ELH,HER,P12,TANS

C       Common Blocks- used to pass common data between
C       subroutines

        COMMON /INPUT/ TP,TT,NP,NT,RP,RT,LD,QT,M,SHP,F,G1,G2,
     2          DIST,METH,IMP,VANS,D,A,CT,FHE,ELH,THETA,EL
        COMMON /CALC/ TAV,NAV,SI,SCXS,SCXF,FIF,FCXF,FCXS,
     2          LDAS,LDAF,LCXS,LCXF,MLT,LNP,RN,RE,VF,VS
        COMMON /SR/ PBAR,R,VBAR,ISE,MT,U,NDT,RHE,CP,P12

        CHARACTER*64 FNAME

C       Format Block

100     FORMAT(' Input known parameters,QT,LD,M,XT,THETA,EL')
200     FORMAT(' Input guesses,TP,TT,NP,NT,RP,RT')
250     FORMAT(' Input plasma constants,G1,G2,R,U,F,IMP')
300     FORMAT(' Input calc parameters,SHP,METH,DIST,TOL,SOR')
400     FORMAT(' Change known parameters? 1=yes 2=no')
500     FORMAT(' Change guesses? 1=yes 2=no')
550     FORMAT(' Change plasma constants? 1=yes 2=no')
600     FORMAT(' Change shape/plasma parameters? 1=yes 2=no')
700     FORMAT(' Another calculation? 1=yes 2=no')
800     FORMAT(' 10 loops complete, continue? 1=yes 2=no')
900     FORMAT(' Store iterations? 1=yes 2=no')
1000    FORMAT(' Enter data file name')

C       Diagnostic Error Statements, all cause iterations
C       to stop

1100    FORMAT(' MT was negative')
1200    FORMAT(' NDT was Negative')
1300    FORMAT(' PROD is LT 1')
1400    FORMAT(' QT-ISE is negative')
1500    FORMAT(A)
1600    FORMAT(I4,3X,E10.4,3X,E10.4,3X,E10.4)
1700    FORMAT(' Convergence to ',E9.4,' achieved')
```

```
1800    FORMAT(' TP=',E9.4,' NP=',E9.4,' TT=',E9.4,' NT=',
      2          E9.4)
1900    FORMAT(' MT=',E9.4,' U=',E9.4,' ISE=',E9.4,' R=',E9.4)
1950    FORMAT(' CP=',E9.4,'HER=',E9.4,' P12=',E9.4,'LNP=',
      2          E9.4)
2000    FORMAT(' Iteration #-',I4)
2100    FORMAT(' U is negative on TT change')
2600    FORMAT(' NP=',E10.4,' TT=',E10.4,'TP=',E10.4)
2700    FORMAT(' U is negative, TP decremented -1')
2800    FORMAT(' Do you want to calculate R? 1=yes 2=no')
2900    FORMAT(' Do you want to calculate U? 1=yes 2=no')
3000    FORMAT('ICALC')
3100    FORMAT(' SRVBAR')
3200    FORMAT(' SRMT')
3300    FORMAT(' MU=',E10.4)
3400    FORMAT(' SRNDT')
3500    FORMAT(' ESC, R=',E10.4)
3600    FORMAT(' Want to check MU? 1=yes 2=no')
3700    FORMAT(' Change input data? 1=yes 2=no')
3800    FORMAT(' Want to check R? 1=yes 2=no')
3900    FORMAT(' Change input data? 1=yes 2=no')
4000    FORMAT(' VBAR=0? 1=yes 2=no')
4100    FORMAT(' Radial/HE data,enter D,A,CT,FHE,ELH')
4200    FORMAT(' Change radial/He data? 1=yes 2=no')
4300    FORMAT(' Do you want to calculate sputtering?
      2          1=yes 2=no')
4400    FORMAT(' Jump to Sputtering? 1=yes 2=no')
4500    FORMAT(' Do you want to hold TT constant? 1=yes 2=no')
C              Prompt for Inputs

        WRITE(*,100)
        READ(*,*) QT,LD,M,XT,THETA,EL
        WRITE(*,200)
        READ(*,*) TPO,TTO,NPO,NTO,RP,RT
        WRITE(*,250)
        READ(*,*) G1,G2,RO,UO,F,IMP
        WRITE(*,4100)
        READ(*,*) D,A,CT,FHE,ELH
        WRITE(*,300)
        READ(*,*) SHP,METH,DIST,TOL,SOR

C       Initialization

70      K=1
        MT=.1
        TP=TPO
        NP=NPO
        TT=TTO
        NT=NTO
        U=UO
```

```fortran
      R=RO
      RHE=RO
      X(1)=NPO
      Y(1)=TTO
      Z(1)=TPO

C     Prompt for Jump to Sputtering Subroutine
      WRITE(*,4400)
      READ(*,*) ANS
      IF(ANS.LT.1.5) THEN
      CALL ICALC
      CP=CT
      P12=0.0
      CALL SPUD
      GOTO 65
      ENDIF

C     Prompts for calculation of VBAR, R, Mu,TT
      WRITE(*,4000)
      READ(*,*) VANS
      WRITE(*,4500)
      READ(*,*) TANS
      WRITE(*,2800)
      READ(*,*) RANS
      IF(RANS.LT.1.5) THEN
      WRITE(*,3800)
      READ(*,*) CKANS
      IF(CKANS.LT.1.5) THEN
      CALL ICALC
      CALL ESC
      WRITE(*,3500) R
      WRITE(*,3900)
      READ(*,*) CKANS
      IF(CKANS.LT.1.5) GOTO 75
      ENDIF
      ENDIF
      WRITE(*,2900)
      READ(*,*) UANS
      IF(UANS.LT.1.5) THEN
      WRITE(*,3600)
      READ(*,*) CKANS
      IF(CKANS.LT.1.5) THEN
      CALL ICALC
      CALL SRVBAR
      CALL SRMT
      CALL MU
      WRITE(*,3300) U
      WRITE(*,3700)
      READ(*,*) CKANS
      IF(CKANS.LT.1.5) GOTO 75
```

```
        ENDIF
        ENDIF

C       Do loop for 10 Fixed Point iterations
20      DO 10 J=1,10
        K=K+1

80      CALL ICALC
        WRITE(*,3000)
        IF(RANS.LT.1.5) THEN
        CALL ESC
        CALL HESC
        ENDIF
        WRITE(*,3500) R
        CALL SRVBAR
        WRITE(*,3100)

        CALL SRMT
        WRITE(*,3200)
        IF(MT.LT.0.0) THEN
        WRITE(*,1100)
        GOTO 60
        ENDIF

        IF(UANS.LT.1.5) THEN
        CALL MU
        WRITE(*,3300) U
C       This decrements TP by 1 if Mu is negative
        IF(U.LT.0.0) THEN
        WRITE(*,2700)
        TP=TP-1.
        IF(TP.LT.3) GOTO 60
        GOTO 80
        ENDIF
        ENDIF

        CALL SRNDT
        WRITE(*,3400)
        IF(NDT.LT.0.0) THEN
        WRITE(*,1200)
        GOTO 60
        ENDIF

C       Use Fixed point iteration to get NP,TT,TP

        PROD=(2.+VBAR*R)*(1.+RP)/NT/(1.+RT)/(1.+MT*MT)

C       X(K) is NP
        X(K)=(((NP/NDT)**2.33333+1.)**.285714)/PROD
```

```fortran
      NP=SOR*X(K)+(1.-SOR)*X(K-1)
C     Check for Convergence on NP, if satisfied output
C     updated results

      IF(ABS((X(K)-X(K-1))/X(K)).LT.TOL) THEN

      WRITE(*,1700) TOL
      WRITE(*,1800) TP,NP,TT,NT
      HER=(1.-RHE)/(1.-R)
      WRITE(*,1900) MT,U,ISE,R
      WRITE(*,1950) CP,HER,P12,LNP*SIN(THETA)
      GOTO 60
      ENDIF

C     Now all variables are updated on most current NP
      CALL ICALC
      WRITE(*,3000)
      IF(RANS.LT.1.5) THEN
      CALL ESC
      CALL HESC
      ENDIF
      WRITE(*,3500) R
      CALL SRVBAR
      WRITE(*,3100)

      CALL SRMT
      WRITE(*,3200)
      IF(MT.LT.0.0) THEN
      WRITE(*,1100)
      GOTO 60
      ENDIF

      IF(UANS.LT.1.5) THEN
      CALL MU
      WRITE(*,3300) U
      IF(U.LT.0.0) THEN
      WRITE(*,2700)
      TP=TP-1.
      IF(TP.LT.3) GOTO 60
      GOTO 80
      ENDIF
      ENDIF

      CALL SRNDT
      WRITE(*,3400)
      IF(NDT.LT.0.0) THEN
      WRITE(*,1200)
      GOTO 60
      ENDIF
```

```fortran
C         Y(K) is TT
          IF(TANS.LT.1.5) GOTO 35
          Y(K)=(2.+R*VBAR*(1.+RP))*NP*TP*(1.+RP)/(NT*(1.+RT)*
     2        (1.+MT*MT))
          TT=SOR*Y(K)+(1.-SOR)*Y(K-1)
C         Now all variables are updated using most current TT
          CALL ICALC
          WRITE(*,3000)
          IF(RANS.LT.1.5) THEN
          CALL ESC
          CALL HESC
          ENDIF
          WRITE(*,3500) R
          CALL SRVBAR
          WRITE(*,3100)

          CALL SRMT
          WRITE(*,3200)
          IF(MT.LT.0.0) THEN
          WRITE(*,1100)
          GOTO 60
          ENDIF

          IF(UANS.LT.1.5) THEN
          CALL MU
          WRITE(*,3300) U
          IF(U.LT.0.0) THEN
          WRITE(*,2700)
          TP=TP-1.
          IF(TP.LT.3) GOTO 60
          GOTO 80
          ENDIF
          ENDIF

          CALL SRNDT
          WRITE(*,3400)
          IF(NDT.LT.0.0) THEN
          WRITE(*,1200)
          GOTO 60
          ENDIF

          IF((QT-ISE).LT.0.0) THEN
          WRITE(*,1400)
          GOTO 60
          ENDIF

C         Z(K) is TP
35        Z(K)=(6.355E-5*(QT-ISE)/(NP*SQRT((1.+RP)/M)
     2        *(G1+RP*G2)))**.66667
          TP=SOR*Z(K)+(1.-SOR)*Z(K-1)
```

```fortran
C        Now output results of most current iteration
         WRITE(*,2000) K
         WRITE(*,2600)NP,TT,TP

10       CONTINUE

C        prompt to do ten more loops
         WRITE(*,800)
         READ(*,*) ANS
         IF(ANS.LT.1.5) GOTO 20

C        Prompt for storing iterations
60       WRITE(*,900)
         READ(*,*) ANS
         IF(ANS.LT.1.5) THEN
         WRITE(*,1000)
         READ(*,1500) FNAME
         OPEN(2,FILE=FNAME)
         DO 30 I=1,K
         WRITE(2,1600) I,Z(I),Y(I),X(I)
30       CONTINUE
         CLOSE(2)
         ENDIF

C        Prompt for Sputtering calculations
         WRITE(*,4300)
         READ(*,*) ANS
         IF(ANS.LT.1.5) CALL SPUD

C        Prompts for another calculation and data changes
65       WRITE(*,700)
         READ(*,*) ANS
         IF(ANS.GT.1.5) GOTO 50
75       WRITE(*,400)
         READ(*,*) ANS
         IF(ANS.LT.1.5) THEN

         WRITE(*,100)
         READ(*,*) QT,LD,M,XT,THETA,EL
         ENDIF
         WRITE(*,500)
         READ(*,*) ANS
         IF(ANS.LT.1.5) THEN
         WRITE(*,200)
         READ(*,*) TPO,TTO,NPO,NTO,RP,RT
         ENDIF
         WRITE(*,550)
         READ(*,*) ANS
         IF(ANS.LT.1.5) THEN
```

```
         WRITE(*,250)
         READ(*,*) G1,G2,RO,UO,F,IMP
         ENDIF
         WRITE(*,4200)
         READ(*,*) ANS
         IF(ANS.LT.1.5) THEN
         WRITE(*,4100)
         READ(*,*) D,A,CT,FHE,ELH
         ENDIF
         WRITE(*,600)
         READ(*,*) ANS
         IF(ANS.LT.1.5) THEN
         WRITE(*,300)
         READ(*,*) SHP,METH,DIST,TOL,SOR
         ENDIF

         GOTO 70
50       STOP
         END



C*************************************************************

         SUBROUTINE ICALC

C        This subroutine does initial calculations which go
C        into the CALC common block

            REAL TP,TT,NP,NT,RP,RT,LD,QT,M,SHP,F,G1,G2,
       2       XT,THETA,EL,DIST,METH
          REAL TAV,NAV,SI,SCXS,SCXF,FIF,FCXS,FCXF,
       2       RN,RE,VF,VS,LDAS,LDAF,ELH
          REAL LCXS,LCXF,MLT,Z,ZS,IMP,VANS,D,A,LNP,CT,FHE

          COMMON /INPUT/ TP,TT,NP,NT,RP,RT,LD,QT,M,SHP,
       2          F,G1,G2,XT,THETA,EL,DIST,METH,IMP,VANS,
       3          D,A,CT,FHE,ELH
          COMMON /CALC/ TAV,NAV,SI,SCXS,SCXF,FIF,FCXF,
       2          FCXS,RN,RE,VF,VS, LDAS,LDAF,LCXS,LCXF,MLT,LNP

         TAV=(TP+TT)/2.
         NAV=(NP+NT)/2.
         LNP=SQRT(D*LD/9822.27/(TP*(1.+RP)/M)**.5)/SIN(THETA)
         RN=.19-.237*ALOG10(3.*TP/EL)
         RE=.06-.22*ALOG10(3.*TP/EL)
         VF=9822.27*SQRT(6.*TP*RE/M/RN)
C          VS is based on a Franck-Condon energy of 3 ev
         VS=9822.27*SQRT(6./M)
         Z=ALOG(TAV)
         ZS=((((((-9.49e-5*Z+4.15e-3)*Z-7.43e-2)*Z
```

```
2    +.705)*Z-3.83)*Z+11.44)*Z-31.74
 SI=EXP(ZS-13.82)
 MLT=2.0+(10./TAV)*(NAV/10.)**(.5*(1.-1.36*EXP(-NAV)))
 SCXS=((.4282*TAV)**.3338)*1.e-14
 SCXF=((.8426*TAV)**.3369)*1.e-14
 FIF=MLT*SI/(MLT*SI+SCXF)
 FCXF=1.-FIF
 FCXS=SCXS/(SCXS+MLT*SI)
 LDAS=VS/(NAV*1.e19*MLT*SI)/SIN(THETA)
 LDAF=VF/(NAV*1.e19*MLT*SI)/SIN(THETA)
 LCXS=VS/(NAV*1.e19*SCXS)/SIN(THETA)
 LCXF=VF/(NAV*1.e19*SCXF)/SIN(THETA)
 RETURN
 END


C****************************************************************


      SUBROUTINE SRVBAR

C     This subroutine calculates VBAR

      REAL TP,TT,NP,NT,RP,RT,LD,QT,M,SHP,F,G1,
     2     G2,XT,THETA,EL,DIST,METH
      REAL MT,VBAR,PBAR,R,ISE,U,NDT,VANS,D,A,
     2     LNP,RHE,CT,FHE,CP
      REAL TAV,NAV,SI,SCXS,SCXF,FIF,FCXF,FCXS,
     2     RN,RE,VF,VS,LDAS,LDAF
      REAL LCXF,LCXS,MLT,FVBAR,SVBAR,VAVG,IMP,ELH,P12

      COMMON /INPUT/ TP,TT,NP,NT,RP,RT,LD,QT,M,SHP,FHE,ELH,
     2        F,G1,G2,XT,THETA,EL,DIST,METH,IMP,VANS,D,A,CT
      COMMON /CALC/ TAV,NAV,SI,SCXS,SCXF,FIF,FCXF,FCXS,
     2        RN,RE,VF,VS,
LDAS,LDAF,LCXS,LCXF,MLT,LNP
      COMMON /SR/ PBAR,R,VBAR,ISE,MT,U,NDT,RHE,CP,P12

C     Calculate VBAR

      VAVG=4911.13*(MT*SQRT(TT*(1.0+RT)/M)+
     2     SQRT(TP*(1.0+RP)/M))

      FVBAR=RN*VF*SIN(THETA)
      SVBAR=(1.-RN)*VS*SIN(THETA)

      VBAR=(FVBAR+SVBAR)/(9822.27*SQRT(TP*(1.0+RP)/M))
      IF(VANS.LT.1.5) VBAR=0.0
      RETURN
      END


C****************************************************************
```

```fortran
      SUBROUTINE SRMT

C     This subroutine calculated MT, the throat mach number
      REAL TP,TT,NP,NT,RP,RT,LD,QT,M,SHP,F,G1,G2,
     2     XT,THETA,EL,DIST,METH
      REAL MT,VBAR,PBAR,R,ISE,U,NDT,MTO,A,IMP,
     2     VANS,D,AA,CT,FHE,RHE,CP
      REAL ELH,P12

      COMMON /INPUT/ TP,TT,NP,NT,RP,RT,LD,QT,M,
     2          SHP,F,G1,G2,XT,THETA,EL,
     3          DIST,METH,IMP,VANS,D,AA,CT,FHE,ELH
      COMMON /SR/ PBAR,R,VBAR,ISE,MT,U,NDT,RHE,CP,P12

C     Calculate MT

15    A=NP*(1.0-R)*(1.0-R)/(NT*(2.0+R*VBAR))
      IF(A.GT.1.0) THEN
      MT=-1.0
      RETURN
      ENDIF
      MTO=SQRT(A/(1-A))
C     This loop is to adjust VBAR using the most current MT
      IF(ABS((MTO-MT)/MTO).GT..05) THEN
      MT=MTO
      CALL SRVBAR

      GOTO 15
      ENDIF
      MT=MTO

      RETURN
      END


C*****************************************************************

      SUBROUTINE SRNDT

C     This subroutine calculated NDT and most energy loss
C     related terms

      REAL TP,TT,NP,NT,RP,RT,LD,QT,M,SHP,F,G1,G2,XT,
     2     THETA,EL,DIST,METH
      REAL MT,VBAR,PBAR,R,ISE,U,NDT,VANS,D,A,LNP,CT,
     2     FHE,RHE,CP,CHE,ELH
      REAL TAV,NAV,SI,SCXS,SCXF,FIF,FCXF,FCXS,RN,
     2     RE,VF,VS,LDAS,LDAF
      REAL LCXF,LCXS,MLT,CHI,ELOSS,VAVG,IMP,TRES,P12
```

```fortran
      COMMON /INPUT/ TP,TT,NP,NT,RP,RT,LD,QT,M,SHP,
     2         F,G1,G2,XT,THETA,EL,
     3         DIST,METH,IMP,VANS,D,A,CT,FHE,ELH
      COMMON /CALC/ TAV,NAV,SI,SCXS,SCXF,FIF,FCXF,
     2         FCXS,RN,RE,VF,VS,
     3         LDAS,LDAF,LCXS,LCXF,MLT,LNP
      COMMON /SR/ PBAR,R,VBAR,ISE,MT,U,NDT,RHE,CP,P12

100   FORMAT(' ELOSS=',E10.4)

      CHI=17.5+(5.+37.5/TAV)*ALOG10(100./NAV)
      TRES=3.64*(RN*LDAF+(1.-RN)*LDAS)*SIN(THETA)/
     2     9822.27/SQRT(TP*(1+RP)/M)
      P12=1.-EXP(-(1.e-5+TRES)/3.e-5)
      CHE=15.+P12*(70+3360./TP)
      CP=CT*NT*MT*SQRT(TT*(1.+RT)/TP/(1.+RP))/(1.-RHE)/NP
      VAVG=4911.13*(MT*SQRT(TT*(1.0+RT)/M)+
     2     SQRT(TP*(1.0+RP)/M))

      ELOSS=IMP*(1.-(1.+P12)*CP)*(CHI+(1.-RN)*(1.
     2       -R)*FCXS*(1.5*TAV+
     2   5.183E-9*M*VAVG*VAVG-3.)/R)+RHE*CHE*CP/R
      WRITE(*,100) ELOSS
      ISE=R*NP*9822.27*SQRT(TP*(1.0+RP)/M)*ELOSS*1.602

      IF(ISE/QT.GT.1.0) THEN
      NDT=-1.0
      RETURN
      ENDIF
      NDT=(553.83/(U*LD))**.42857*(QT**.57143)*(1.0-ISE/QT)*
     2   SQRT(M/(1.0+RP))*6.35515E-5/(G1+RP*G2)

      RETURN
      END


C***************************************************************


      SUBROUTINE ESC

C     This subroutine calculates PBAR and R for D-T. It
C     calculates the escape probability for particles based
C     on simple exponential attentuation at 50 points across
C     the divertor plate and averages the PBAR values by
C     weighting them with the local plate particle flux

      REAL PS,PF,PST,PFT,PBAR,XC,INCR,ARC,TN,RST,
     2     R,EF1,EF2,LDS,LDF,ELH
      REAL TP,TT,NP,NT,RP,RT,LD,QT,M,SHP,F,G1,G2,
     2     XT,THETA,EL,DIST,METH
      REAL TAV,NAV,SI,SCXS,SCXF,FIF,FCXF,FCXS,RN,
```

```fortran
2       RE,VF,VS,LDAS,LDAF,CP
 REAL LCXS,LCXF,MLT,VBAR,ISE,MT,U,NDT,IMP,VANS,
2       D,A,LNP,CT,FHE,RHE
 REAL NPO,TPO,TPR,NPR,VFR,RNR,RER,MLTR,P12,FXT

 COMMON /INPUT/ TP,TT,NP,NT,RP,RT,LD,QT,M,SHP,
2       F,G1,G2,XT,THETA,
3   EL,DIST,METH,IMP,VANS,D,A,CT,FHE,ELH
 COMMON /CALC/ TAV,NAV,SI,SCXS,SCXF,FIF,FCXF,FCXS,
2       RN,RE,VF,VS,LDAS,LDAF,LCXS,LCXF,MLT,LNP
 COMMON /SR/ PBAR,R,VBAR,ISE,MT,U,NDT,RHE,CP,P12
 COMMON /SUBESC/ ARC,XC,LDF,LDS

 INTEGER JL

C    Initialize Parameters

 XC=0.0
 PST=0.0
 PFT=0.0
 PS=0.0
 PF=0.0
 EF1=1.0
 EF2=2.0
 FXT=0.0
C    Initial Calculations

 INCR=XT/50.
 TN=TAN(THETA)
 NPO=XT*NP/LNP/(1.-EXP(-XT/LNP))
 TPO=XT*TP/A/LNP/(1.-EXP(-XT/A/LNP))
C    Do Loop to Calculate Escape Probability for a mesh of
C    points

 DO 50 JL=1,49

 XC=XC+INCR
 TPR=TPO*EXP(-XC/A/LNP)
 NPR=NPO*EXP(-XC/LNP)
 RNR=.19-.237*ALOG10(3.*TPR/EL)
 RER=.06-.22*ALOG10(3.*TPR/EL)
 VFR=9822.27*SQRT(6.*TPR*RER/M/RNR)

 Z=ALOG(TPR)
 ZS=(((((-9.49e-5*Z+4.15e-3)*Z-7.43e-2)*Z
2    +.705)*Z-3.83)*Z+11.44)*Z-31.74
 SI=EXP(ZS-13.82)
 MLT=2.0+(10./TPR)*(NPR/10.)**(.5*(1.-1.36*EXP(-NPR)))
 LDS=VS/(NPR*1.e19*MLT*SI)
 LDF=VFR/(NPR*1.e19*MLT*SI)
```

```
            ARC=3.1416-ACOS(XC/SQRT(XT*XT*TN*TN+XC*XC))

            IF(METH.LT.1.5) THEN
            CALL RMBG(0.0,ARC,EF1,RST)
            PS=RST/ARC
            ENDIF

            IF(METH.GT.1.5) CALL PROB(LDS,PS,THETA,XT)

            PST=PST+NPR*SQRT(TPR)*PS*(1.-RNR)

            IF(METH.LT.1.5) THEN
            CALL RMBG(0.0,ARC,EF2,RST)
            PF=RST/ARC
            ENDIF

            IF(METH.GT.1.5) CALL PROB(LDF,PF,THETA,XT)

            PFT=PFT+NPR*SQRT(TPR)*PF*RNR
            FXT=FXT+NPR*SQRT(TPR)
   50       CONTINUE

   C        Calculate final escape probability
            PBAR=(PFT+PST)/FXT
            R=1.-PBAR*F
            RETURN
            END


   C*************************************************************

            SUBROUTINE HESC

   C        This subroutine does the same thing as ESC but for He

            REAL PS,PF,PST,PFT,PBAR,XC,INCR,ARC,TN,RST,R,
          2      EF1,EF2,LDS,LDF,ELH
            REAL TP,TT,NP,NT,RP,RT,LD,QT,M,SHP,F,G1,G2,XT,
          2      THETA,EL,DIST,METH
            REAL TAV,NAV,SI,SCXS,SCXF,FIF,FCXF,FCXS,RN,RE,
          2      VF,VS,LDAS,LDAF,CP
            REAL LCXS,LCXF,MLT,VBAR,ISE,MT,U,NDT,IMP,VANS,
          2      D,A,LNP,CT,FHE,RHE
            REAL NPO,TPO,TPR,NPR,VFR,RNR,RER,MLTR,VSH,PH,P12

            COMMON /INPUT/ TP,TT,NP,NT,RP,RT,LD,QT,M,
          2          SHP,F,G1,G2,XT,THETA,
          3          EL,DIST,METH,IMP,VANS,D,A,CT,FHE,ELH
            COMMON /CALC/ TAV,NAV,SI,SCXS,SCXF,FIF,FCXF,
          2          FCXS,RN,RE,VF,VS,
```

```fortran
3               LDAS,LDAF,LCXS,LCXF,MLT,LNP
      COMMON /SR/ PBAR,R,VBAR,ISE,MT,U,NDT,RHE,CP,P12
      COMMON /SUBESC/ ARC,XC,LDF,LDS

      INTEGER JL

C     Initialize Parameters

      XC=0.0
      PST=0.0
      PFT=0.0
      PS=0.0
      PF=0.0
      EF1=1.0
      EF2=2.0
      FXT=0.0
C     Initial Calculations

      INCR=XT/50.
      TN=TAN(THETA)
      NPO=XT*NP/LNP/(1.-EXP(-XT/LNP))
      TPO=XT*TP/A/LNP/(1.-EXP(-XT/A/LNP))
C     Do Loop to Calculate Escape Probability for a mesh of
C     points

      DO 50 JL=1,49

      XC=XC+INCR
      TPR=TPO*EXP(-XC/A/LNP)
      NPR=NPO*EXP(-XC/LNP)
      RNR=.19-.237*ALOG10(3.*TPR/ELH)
      RER=.06-.22*ALOG10(3.*TPR/ELH)
      VFR=9822.27*SQRT(6.*TPR*RER/4./RNR)
      VSH=9822.27*SQRT(6./4.)
      Z=ALOG10(TPR/24.6)
      ZS=(((((1.3207e-9*Z+1.5529e-9)*Z-3.59e-9)*Z
2     -6.082e-9)*Z+5.666e-10)*Z+1.5e-8

      SI=EXP(-24.6/TPR)*SQRT(TPR/24.6)*ZS*1.e-6
      MLT=2.0+(18.1/TPR)*(NPR/10.)**(.5*(1.-1.36*EXP(-NPR)))
      LDS=VSH/(NPR*1.e19*MLT*SI*0.55)
      LDF=VFR/(NPR*1.e19*MLT*SI*0.55)

      ARC=3.1416-ACOS(XC/SQRT(XT*XT*TN*TN+XC*XC))

      IF(METH.LT.1.5) THEN
      CALL RMBG(0.0,ARC,EF1,RST)
      PS=RST/ARC
      ENDIF
```

```
        IF(METH.GT.1.5) CALL PROB(LDS,PS,THETA,XT)

        PST=PST+NPR*SQRT(TPR)*PS*(1.-RNR)

        IF(METH.LT.1.5) THEN
        CALL RMBG(0.0,ARC,EF2,RST)
        PF=RST/ARC
        ENDIF

        IF(METH.GT.1.5) CALL PROB(LDF,PF,THETA,XT)

        PFT=PFT+NPR*SQRT(TPR)*PF*RNR
        FXT=FXT+NPR*SQRT(TPR)
50      CONTINUE

C       Calculate final escape probability
        PH=(PFT+PST)/FXT
        RHE=1.-PH*FHE
        RETURN
        END
C******************************************************************
C       This subroutine evaluates an integral A-B of EF using
C       Romberg integration. It is used in ESC, HESC, MU, and
C       SPUD

        SUBROUTINE RMBG(A,B,EF,RESULT)

        REAL A,B,H,V,FF,R1(12),R2(12),RA,RB,RV,EF,RESULT

        INTEGER K,J,L,M,I
C       Initial Calculations
        DO 50 I=1,12
        R1(I)=0.0
        R2(I)=0.0
50      CONTINUE

        H=B-A
C       Calculate R1,1
        IF(EF.LT.1.5) THEN
        CALL EVAL1(A,RA)
        CALL EVAL1(B,RB)
        ENDIF
        IF(EF.GT.1.5) THEN
        IF(EF.LT.2.5) THEN
        CALL EVAL2(A,RA)
        CALL EVAL2(B,RB)
        ENDIF
        ENDIF
        IF(EF.GT.2.5) THEN
        IF(EF.LT.3.5) THEN
```

```fortran
      CALL EVAL3(A,RA)
      CALL EVAL3(B,RB)
      ENDIF
      ENDIF
      IF(EF.GT.3.5) THEN
      CALL EVAL4(A,RA)
      CALL EVAL4(B,RB)
      ENDIF
      R1(1)=H*(RA+RB)/2.0
      DO 400 I=2,10
      L=2**(I-2)
      FF=0.0
      DO 100 K=1,L
      V=A+(FLOAT(K)-0.5)*H
      IF(EF.LT.1.5) THEN
      CALL EVAL1(V,RV)
      ENDIF
      IF(EF.GT.1.5) THEN
      IF (EF.LT.2.5) THEN
      CALL EVAL2(V,RV)
      ENDIF
      ENDIF
      IF(EF.GT.2.5) THEN
      IF(EF.LT.3.5) THEN
      CALL EVAL3(V,RV)
      ENDIF
      ENDIF
      IF(EF.GT.3.5) THEN
      CALL EVAL4(V,RV)
      ENDIF
      FF=FF+RV
100   CONTINUE
      R2(1)=0.5*(R1(1)+H*FF)
      DO 200 J=2,I
      R2(J)=((4.0**FLOAT(J-1)*R2(J-1))-R1(J
     2      -1))/(4.0**FLOAT(J-1)-1.0)
      IF(EF.LT.3.5) THEN
      IF(ABS(R2(J)).LT.1.e-2) THEN
      R2(J)=0.0
      GOTO 500
      ENDIF
      ENDIF
      IF(ABS((R2(J)-R2(J-1))/R2(J)).LT.1.0E-3) GOTO 500
200   CONTINUE

      H=H/2.0
      DO 300 M=1,I
      R1(M)=R2(M)
300   CONTINUE
400   CONTINUE
```

```
500      RESULT=R2(J)
         RETURN
         END

C********************************************************

         SUBROUTINE EVAL1(X,RST)

C        This subroutine is function evaluation for fast
C        particle calculations of method 1 of ESC

         REAL L,ARC,XC,TN,RST,LDF,LDS,D,A,LNP,CT,FHE
         REAL TP,TT,NP,NT,RP,RT,LD,QT,M,SHP,F,G1,G2,XT,
     2       THETA,EL,DIST,METH
         REAL IMP,VANS

         COMMON /SUBESC/ ARC,XC,LDF,LDS
         COMMON /INPUT/ TP,TT,NP,NT,RP,RT,LD,QT,M,SHP,F,
     2           G1,G2,XT,THETA,EL,DIST,METH,
     3           IMP,VANS,D,A,CT,FHE,ELH

         TN=TAN(THETA)
         L=TN*(XT-XC)/(SIN(X)+TN*COS(X))
         RST=(ARC/3.1416)*EXP(-1.0*L/LDS)

         IF(DIST.LT.1.5) RST=SIN(X)*RST

         RETURN
         END

C********************************************************

         SUBROUTINE EVAL2(X,RST)

C        This subroutine is function evaluation for slow
C        particle calculations of method 1 of ESC

         REAL L,ARC,XC,TN,RST,LDF,LDS,D,A,CT,FHE,LNP
         REAL TP,TT,NP,NT,RP,RT,LD,QT,M,SHP,F,G1,G2,
     2       XT,THETA,EL,DIST,METH
         REAL IMP,VANS

         COMMON /SUBESC/ ARC,XC,LDF,LDS
         COMMON /INPUT/ TP,TT,NP,NT,RP,RT,LD,QT,M,SHP,
     2           F,G1,G2,XT,THETA,
     3           EL,DIST,METH,IMP,VANS,D,A,CT,FHE,ELH

         TN=TAN(THETA)
         L=TN*(XT-XC)/(SIN(X)+TN*COS(X))
         RST=(ARC/3.1416)*EXP(-1.0*L/LDF)
```

```
      IF(DIST.LT.1.5) RST=SIN(X)*RST

      RETURN
      END


C*************************************************************

      SUBROUTINE PROB(LDA,P,THETA,XT)

C     This subroutine is function evaluation for method 2
C     of ESC

      REAL LDA,XC,P,ARC,PT1,PT2,LAVG,TN,THETA,
     2     XT,DIST,LDF,LDS

      COMMON /SUBESC/ ARC,XC,LDF,LDS

C     Initial Calculations

      TN=TAN(THETA)

C     Calculate LAVG
      PT1=ALOG(TAN(THETA/2.0))
      PT2=ALOG(TAN((THETA+ARC)/2.0))
      LAVG=TN*(XT-XC)*(PT2-PT1)/(SQRT(1.0+TN*TN)*ARC)

C     Calculate Escape Probility
      P=(ARC/3.1416)*EXP(-1.0*LAVG/LDA)

      RETURN
      END
C*************************************************************

      SUBROUTINE MU

C     This subroutine calculates the conduction fraction

      REAL PBAR,R,VBAR,ISE,MT,U,NDT,RST,EF,IMP,VANS,
     2     D,A,RHE,CT,FHE,CP,P12
      REAL NP,TP,NT,TT,RP,RT,LD,QT,M,SHP,F,G1,G2,
     2     XT,THETA,EL,DIST,METH

      COMMON /SR/ PBAR,R,VBAR,ISE,MT,U,NDT,RHE,CP,P12
      COMMON /INPUT/ TP,TT,NP,NT,RP,RT,LD,QT,M,SHP,
     2        F,G1,G2,XT,THETA,EL,
     2   DIST,METH,IMP,VANS,D,A,CT,FHE,ELH

      CALL RMBG(0.0,LD,3.,RST)
      U=1.-RST/QT/LD
      RETURN
```

```fortran
      END

C*****************************************************************

      SUBROUTINE EVAL3(X,RST)

C     This is function evaluation for romberg integration
C     of MU

      REAL PBAR,RCY,VBAR,ISE,MT,U,NDT,RST,IMP,
     2     BOT,VANS,D,A,LNP,RHE,FHE
      REAL NP,TP,NT,TT,RP,RT,LD,QT,M,SHP,F,G1,
     2     G2,XT,THETA,EL,DIST,METH
      REAL TAV,NAV,SI,SCXS,SCXF,FIF,FCXF,FCXS,RN,
     2     RE,VF,VS,LDAS,LDAF,CP
      REAL LCXF,LCXS,MLT,FC,N,R,T,MA,RPR,TOP,
     2     VRPR,VAVG,LF,LS,P12

      COMMON /SR/ PBAR,RCY,VBAR,ISE,MT,U,NDT,RHE,CP,P12
      COMMON /INPUT/ TP,TT,NP,NT,RP,RT,LD,QT,M,SHP,F,
     2         G1,G2,XT,THETA,EL,
     3           DIST,METH,IMP,VANS,D,A,CT,FHE,ELH
      COMMON /CALC/ TAV,NAV,SI,SCXS,SCXF,FIF,
     2         FCXF,FCXS,RN,RE,VF,VS,
     3         LDAS,LDAF,LCXS,LCXF,MLT,LNP

      FC=(1.-(1.-X/LD)**SHP)
      N=NP+(NT-NP)*FC

      R=RP+(RT-RP)*FC

      LF=LDAF
      LS=LDAS

      RPR=(LF*RN*(1.-EXP(-X/LF))+(1.-RN)*LS*(1.-EXP(-X/LS)))
     2    /(LF*RN*(1.-EXP(-LD/LF))+(1.-RN)*LS*(1.-EXP(
     3    -LD/LS)))

      VAVG=4911.13*(MT*SQRT(TT*(1.+RT)/M)+
     2     SQRT(TP*(1.+RP)/M)

      TOP=RN*(FIF*SIN(THETA)*VF*(1.-EXP(-X/LF))
     2    +FCXF*(VF*SIN(THETA)+VAVG*(1.-RCY))*
     3    (1.-EXP(-X/LCXF)))+(1.-RN)*VAVG*(1.-RCY)
     4    *FCXS*(1.-EXP(-X/LCXS))

      BOT=RN*(FIF*SIN(THETA)*VF*(1.-EXP(-LD/LF))
     2    +FCXF*(VF*SIN(THETA)+VAVG*(1.-RCY))
     3    *(1.-EXP(-LD/LCXF)))+(1.-RN)*VAVG
     4    *(1.-RCY)*FCXS*(1.-EXP(-LD/LCXS))
```

```
      VRPR=RCY*VBAR*TOP/BOT

      T=(VRPR+2.-(1-RCY*RPR)**2.*NP/N)*NP*TP
     2   *(1.+RP)/(N*(1.+R))

      MA=(1.-RCY*RPR)*(NP/N)*SQRT(TP*(1.+RP)/T/(1.+R))

      RST=N*MA*SQRT(T*(1.+R)/M)*(MA*MA*T*(1.+R)*.5+2.5*T*
     2   (1.+R))*1.5735E4

      RETURN
      END


C*****************************************************************

      SUBROUTINE SPUD

C     This subroutine calculates sputtering on the divertor
C     plate based on an exponential profile. You can used
C     the average local temperature for each of 50 points
C     across the plate or integration of the MB distribution
C     and Yield at each.

      REAL UO,Z3,M3,NPO,TPO,X,INC,ETH1,ETH2,ETH3,
     2     TPR(51),NPR(51)
      REAL SP(51),Y1,Y2,Y3,YT,SPT,ANS,DIST,METH,
     2     IMP,VANS,D,A,CT,FHE
      REAL PBAR,RCY,VBAR,ISE,MT,U,NDT,RHE,CP,
     2     LDAS,LDAF,LCXS,LCXF,MLT
      REAL TP,TT,NP,NT,RP,RT,LD,QT,M,SHP,F,
     2     G1,G2,XT,THETA,EL,P12,LNP
      REAL TAV,NAV,SI,SCXS,SCXF,FIF,FCXF,
     2     FCXS,RN,RE,VF,VS,NM,PEAK
      REAL FLAG,SDT(51);SHE(51),EI,TPRC,IE,
     2     E1,E2,E3,RST1,RST2,RST

      COMMON /SR/ PBAR,RCY,VBAR,ISE,MT,U,NDT,RHE,CP,P12
      COMMON /INPUT/ TP,TT,NP,NT,RP,RT,LD,QT,M,SHP,
     2        F,G1,G2,XT,THETA,EL,
     3        DIST,METH,IMP,VANS,D,A,CT,FHE,ELH
      COMMON /CALC/ TAV,NAV,SI,SCXS,SCXF,FIF,
     2        FCXF,FCXS,RN,RE,VF,VS,
     3        LDAS,LDAF,LCXS,LCXF,MLT,LNP
      COMMON /MB/ TPRC,FLAG,M2,M3,UO,Z3,ETH1,ETH2

      CHARACTER*64 FNAME

C     FORMAT BLOCK
100   FORMAT(' Input plate material data,
     2        UO,Z3,M3,NM(xE24),IE ')
```

```
200     FORMAT(' Peak sputtering rate is',E10.4,' CM/YR  TP=',
       2         E9.4,' NP=',E9.4)
300     FORMAT(' Sputtering Yield per meter is',E10.4,' xE19')
400     FORMAT(' Enter sputtering data file.prn')
500     FORMAT(A)
600     FORMAT(I5,3X,E10.4,3X,E10.4,3X,E10.4,
       2         3X,E10.4,3X,E10.4)
700     FORMAT(' Do another plate material? 1=yes 2=no')
800     FORMAT(' Use average temps or integrate MB? 1=avg
       2         =integrate')
900     FORMAT(' Do you want to store data? 1=yes 2=no')
1000    FORMAT(' Impurity yield is GT 1.0 set = 0.0')
350     WRITE(*,100)
        READ(*,*) UO,Z3,M3,NM,IE
        WRITE(*,800)
        READ(*,*) ANS
        NPO=XT*NP/LNP/(1.-EXP(-XT/LNP))
        TPO=XT*TP/A/LNP/(1.-EXP(-XT/A/LNP))
        SPT=0.0
        X=0.0

        INC=XT/50.
        ETH1=UO*(4.*M+M3)*(4.*M+M3)/4./M/M3
        ETH2=UO*(16.+M3)*(16.+M3)/16./M3
        ETH3=UO*6.25

C       This block evaluates sputtering using MB integration
        IF(ANS.GT.1.5) THEN
        DO 150 I=1,50
        Y3=0.0
        SHE(I)=0.0
        SDT(I)=0.0
        TPR(I)=TPO*EXP(-X/A/LNP)
        TPRC=RP*TPR(I)
        NPR(I)=NPO*EXP(-X/LNP)
        E3=(G2-2.)*RP*TPR(I)
        IF(E3.GT.ETH3) THEN
        Y3=YLD(UO,400.,Z3,Z3,M3,M3,E3,ETH3)
        IF(Y3.GT.1.0) THEN
        WRITE(*,1000)
        Y3=0.0
        ENDIF
        ENDIF
        EI=.5*(ETH1-(G2-2.)*RP*TPR(I))
        IF(EI.LT.0.0) EI=0.0
        IF(EI.LT.IE*TPRC) THEN
        FLAG=1.

        IF(EI.LT.1.5*TPRC) THEN
        CALL RMBG(EI,1.5*TPRC,4.,RST1)
```

```
      CALL RMBG(1.5*TPRC,IE*TPRC,4.,RST2)
      ENDIF
      IF(EI.GT.1.5*TPRC) THEN
      CALL RMBG(EI,IE*TPRC,4.,RST1)
      ENDIF
      RST=RST1+RST2
      RST1=0.0
      RST2=0.0
      SDT(I)=(1.-(1.+P12)*CP)*RST*NPR(I)*SQRT(TPR(I)*
     2       (1.+RP)/M)*11083.6/(1.-Y3)
      ENDIF
      EI=.5*(ETH2-2.*(G2-2.)*RP*TPR(I))
      IF(EI.LT.0.0) EI=0.0
      IF(CP.LT:0.001) GOTO 550

      IF(EI.LT.IE*TPRC) THEN
      FLAG=2.
      IF(EI.LT.1.5*TPRC) THEN
      CALL RMBG(EI,1.5*TPRC,4.,RST1)
      CALL RMBG(1.5*TPRC,IE*TPRC,4.,RST2)
      ENDIF
      IF(EI.GT.1.5*TPRC) THEN
      CALL RMBG(EI,IE*TPRC,4.,RST1)
      ENDIF
      RST=RST1+RST2
      RST1=0.0
      RST2=0.0
      SHE(I)=P12*CP*RST*NPR(I)*SQRT(TPR(I)*(1.+RP)/M)
     2       *11083.5/(1.-Y3)
      ENDIF
      EI=.5*(ETH2-1.*(G2-2.)*RP*TPR(I))
      IF(EI.LT.0.0) EI=0.0
      IF(CP.LT.0.001) GOTO 550

      IF(EI.LT.IE*TPRC) THEN
      FLAG=3.
      IF(EI.LT.1.5*TPRC) THEN
      CALL RMBG(EI,1.5*TPRC,4.,RST1)
      CALL RMBG(1.5*TPRC,IE*TPRC,4.,RST2)
      ENDIF
      IF(EI.GT.1.5*TPRC) THEN
      CALL RMBG(EI,IE*TPRC,4.,RST1)
      ENDIF
      RST=RST1+RST2
      RST1=0.0
      RST2=0.0
      SHE(I)=SHE(I)+(1.-P12)*CP*RST*NPR(I)*
     2       SQRT(TPR(I)*(1.+RP)/M)*11083.5/(1.-Y3)
      ENDIF
550   SP(I)=SDT(I)+SHE(I)
```

```
          SPT=SPT+0.02*XT*SP(I)
          X=X+INC

150       CONTINUE
          ENDIF

C         This block evaluates sputtering using average local
C         temp
          IF(ANS.LT.1.5) THEN
          DO 450 I=1,50
          Y1=0.0
          Y2=0.0
          Y3=0.0
          SDT(I)=0.0
          SHE(I)=0.0
          TPR(I)=TPO*EXP(-X/A/LNP)
          TPRC=TPR(I)
          NPR(I)=NPO*EXP(-X/LNP)
          E1=TPR(I)*G2*RP
          E2=TPR(I)*2.*RP*(G2-1.)
          E3=TPR(I)*RP*(G2-1.)
          IF(E3.GT.ETH3) THEN
          Y3=YLD(UO,400.,Z3,Z3,M3,M3,E3,ETH3)
          IF(Y3.GT.1.0) THEN
          WRITE(*,1000)
          Y3=0.0
          ENDIF
          ENDIF
          IF(E1.GT.ETH1) THEN
          Y1=YLD(UO,400.,1.,Z3,M,M3,E1,ETH1)
          ENDIF
          IF(E2.GT.ETH2) THEN
          Y2=YLD(UO,400.,2.,Z3,4.,M3,E2,ETH2)
          ENDIF
          SDT(I)=9822.27*NPR(I)*SQRT(TPR(I)*(1.+RP)/M)*Y1*(1.
     2          -(1.+P12)*CP)/(1.-Y3)
          SHE(I)=9822.27*NPR(I)*SQRT(TPR(I)*(1.+RP)/M)*
     2          Y2*CP/(1.-Y3)
          SP(I)=SDT(I)+SHE(I)
          SPT=SPT+.02*XT*SP(I)
          X=X+INC
450       CONTINUE
          ENDIF

C         On screen Output of results
          PEAK= SP(1)*.0315/NM
          WRITE(*,200) PEAK,RP*TPR(1),NPR(1)
          WRITE(*,300) SPT

C         Prompt for storage of  sputtering rates for each of 50
```

```fortran
C       points
        WRITE(*,900)
        READ(*,*) ANS
        IF(ANS.LT.1.5) THEN
        WRITE(*,400)
        READ(*,500) FNAME
        OPEN(3,FILE=FNAME)
        DO 250 J=1,50
        WRITE(3,600) J,SP(J),SDT(J),SHE(J),TPR(J),NPR(J)

250     CONTINUE
        CLOSE(3)
        ENDIF
C       Prompt for another calculation
75      WRITE(*,700)
        READ(*,*) ANS
        IF(ANS.LT.1.5) GOTO 350
        RETURN

        END


C***********************************************************

        REAL FUNCTION YLD(UO,C,Z1,Z2,M1,M2,EO,ETH)

C       This is sputtering yield function evaluation based on
C       D.L. Smith's model

        REAL UO,C,Z1,Z2,M1,M2,EO,ETH

        YLD=C*Z1**.75*(Z2-1.8)*(Z2-1.8)*((M1-.8)/M2)
     2     **1.5*(EO-ETH)/UO/(EO-ETH+50.*Z2*Z1**.75)**2.
        RETURN

        END


C***********************************************************

        SUBROUTINE EVAL4(E,RST)

C       This is function evaluation for MB integration of
C       SPUD
        REAL TP,TT,NP,NT,RP,RT,LD,QT,M,SHP,F,G1,
     2       G2,XT,THETA,EL,DIST,METH
        REAL IMP,VANS,D,A,CT,FHE,ELH,TPRC,FLAG,
     2       M2,M3,UO,Z3,ETH1,ETH2,EO
        REAL RST,E

        COMMON /INPUT/ TP,TT,NP,NT,RP,RT,LD,QT,M,SHP,F,
     2          G1,G2,XT,THETA,EL,
```

```fortran
3          DIST,METH,IMP,VANS,D,A,CT,FHE,ELH
   COMMON /MB/ TPRC,FLAG,M2,M3,UO,Z3,ETH1,ETH2

   IF(FLAG.LT.1.5) THEN

   EO=2.0*E+TPRC*(G2-2.)

   RST=SQRT(E/TPRC)*EXP(-E/TPRC)*
2      YLD(UO,400.,1.,Z3,M,M3,EO,ETH1)/TPRC
   ENDIF
   IF(FLAG.GT.1.5) THEN
   IF(FLAG.LT.2.5) THEN
   EO=2.*E+2.*TPRC*(G2-2.)
   RST=SQRT(E/TPRC)*EXP(-E/TPRC)*
2      YLD(UO,400.,2.,Z3,4.,M3,EO,ETH2)/TPRC
   ENDIF
   ENDIF
   IF(FLAG.GT.2.5) THEN
   EO=2.*E+1.*TPRC*(G2-2.)
   RST=SQRT(E/TPRC)*EXP(-E/TPRC)*
2      YLD(UO,400.,2.,Z3,4.,M3,EO,ETH2)/TPRC
   ENDIF
   RETURN
   END
```

APPENDIX C

GENERIC DIVERTOR MODELING

The best approach in modeling a divertor is to use as many known data values as possible. However, in the absence of knowledge about the value of a particular parameter some sort of estimate must be made in order to continue modeling. The purpose of this appendix is to present calculational methods for the estimation of some DIV input parameters and reasonable ranges for others.

C.1 Power Flux into the Divertor, Q_t

The power flux into the divertor can be estimated using the equation

$$Q_t \ (W/_{m^2}) = \frac{P}{N \ A_{\parallel,d}} \qquad (C.1)$$

where P (W) is the total power to be exhausted, N is the number of divertor plates (a reactor may have more than one divertor, each with more than one plate), and $A_{\parallel,d}(m^2)$ is the cross-sectional area of the plasma as it flows into the divertor.

The power to be exhausted and the number of divertor plates are usually known, so determining Q_t depends on finding the plasma cross sectional area. For a Tokamak, this area can be estimated as[3]

$$A_{\|,d}(m^2) = \frac{F_e 2\pi \, a \, \Delta_s}{q} \qquad (C.2)$$

where a(m) is the plasma minor radius, Δ_s(m) is the scapeoff thickness (normally several heat flux scale lengthes, λ_Q), q is the safety factor on edge, and F_e is a flux expansion factor at the throat to account for the normal expansion of magnetic field lines as they enter the divertor. Reference 3 gives a value for F_e of about 1.4. The heat flux scale length, λ_Q(m), is often a given parameter. If it is not given, it can be estimated using[25]

$$\lambda_Q = \frac{\lambda_n \lambda_T}{\frac{3}{2}\lambda_n + \lambda_T} = \frac{A\lambda_n}{\left(\frac{3}{2} + A\right)} \qquad (C.3)$$

where A is the ratio of temperature to density scale lengthes. The density scale length, λ_n, would be calculated as given in Section 3.8 using some estimate of the fluid velocity ($\sim$.3-.5 of the sound speed).

C.2 The Divertor Connection Length, L_D

This connection length is the distance along field lines between the divertor throat and the target plate. It is a function of the magnetic field line topology and sensitive to the plate position being considered. If its value is unknown, some fraction (.2-.3) of the outside connection length can be used. The outside connection length, L_s, is

$$L_s(m) = \frac{2\pi\ Rq}{N} \qquad (C.4)$$

where $R(m)$ is the plasma major radius and N is the number of divertors. Thus

$$L_D(m) \approx .25\ L_s \qquad (C.5)$$

C.3 The Throat Electron Plasma Temperature, T_t

If the symmetry point electron temperature, T_s, is specified, this value can be extrapolated forward to the divertor throat using an equation based on 100% electron thermal conduction[3]

$$T_T^{7/2}(eV) = T_s^{7/2}(eV) - \frac{7P\,L_s}{4A_{\parallel,s}N\,\kappa_o} \qquad (C.5)$$

where P and L_s are as previously defined, N is the number of divertor plates, $A_{\parallel,s}(m^2)$ is the cross-sectional area of the plasma outside the divertor (i.e. no flux expansion factor), and κ_o is the Spitzer electron thermal conductivity coefficient ($\sim 2000\ W(eV)^{-7/2}m^{-1}$).

C.4 The Throat Electron Density, n_t

The pressure balance equation can be used to estimate the throat electron density, once the throat temperature has been calculated. Thus,

$$n_t(m^{-3}) = \frac{n_s\,T_s}{T_t} \qquad (C.6)$$

where $n_s(m^{-3})$ is the symmetry point electron density. The mach numbers squared ($\mathbb{M}^2$) at both locations are assumed to be small and can be neglected. If after a computer run the mach number at the throat is found not to be small, then this value could be used to adjust the throat density (divide by $1+\mathbb{M}_t^2$).

C.5 Estimates for the Plate Electron Temperature and

Density, T_p and n_p

Another equation based on the assumption of 100% electron thermal conduction can be used to get an initial estimate of T_p.[3] Thus,

$$T_p^{7/2}(eV) = T_t^{7/2}(eV) - \frac{7Q_t L_D}{2 x_o} \qquad (C.7)$$

and the plate electron density estimated using the pressure balance equation,

$$n_p(m^{-3}) = \frac{n_t T_t \left(1 + r_t\right)}{2T_p \left(1 + r_p\right)} \qquad (C.8)$$

where the mach number at the throat has been assumed to be zero and the mach number at the plate set equal to 1.0. If a sample run shows the mach number at the throat not to be small, then the plate density can be adjusted by multiplying by $(1 + \tilde{m}_t^2)$.

C.6 Reasonable Ranges for Other Input Parameters

Based on a review of the literature and experience with the DIV code, Table C.1 below displays reasonable ranges for other input parameters for which no calculation or estimate has been given in the body of this thesis or this appendix.

Table C.1
Parameter Ranges

Parameter	Units	Range
Pump Fractions f and f_{He}	-	0-.5
Diffusion Coefficient, D	m^2/sec	.8-1.5
Scale Length Ratio, A	-	.7-1.1
Shape Factor, α	-	3-8
Field Line Angle of Incidence, θ	Radians	.09-.79 ($5^\circ-45^\circ$)

A few additional comments regarding other parameter values are warranted. The mass the the D-T ions is usually taken to be 2.5 amu. If you are going to calculate R and μ in the DIV program, then these input values do not matter.

APPENDIX D

DISCUSSION OF NEUTRAL ESCAPE PROBABILITY

As stated in Chapter 3, the recycling coefficient, R, can be approximated as $1-\bar{p}f$, where f is the pumped fraction, and $\bar{p}$ is the average neutral escape probability. Section 3.5 outlined the various calculational approaches to determining $\bar{p}$. This appendix presents a discussion of the effects of variations in certain parameters on the neutral escape probability and a comparison of the three calculational methods.

D.1 Effects of Varying Parameters

The parameters required to calculate the neutral escape probability are:

X_t - the width of the divertor plate (M)

θ - the angle of incidence of the field lines to the divertor plate (radians)

T   - the temperature of the plasma in front of the plate (eV). This could be the plate temperature or an average of the throat and plate tempertures.

n   - the electron density in front of the plate. (m^{-3}) Again, this could be the plate or an average quantity.

EL   - the material and particle dependent reduced energy for the calculation of the reflection

coefficients (eV).

I   - Number of mesh points along the divertor plate

Each of these parameters was varied to examine its effect on the neutral escape probability. In each case, the effect on $\bar{p}$ was qualitatively predictable. These effects are discussed below.

X_t - As X_t increased the escape probability decreased. This was due to the fractional decrease in the tip area of the plasma wedge. Most of the particles that escape do so out of the tip of the plasma wedge. Increasing the width of the divertor plate just increases the area from which particles do not escape.

θ - As θ increased the escape probability decreased. This makes sense, since increasing θ increases the effective thickness of the plasma.

T   - As T increased, the escape probability decreased. The temperature is used in the calculation of particle ionization MFP, appearing in both the numerator (velocity term), and the denominator (in the reaction rate coefficient). This result implies that the $<\sigma v>_{ion}$ term is more sensitive to temperature than the velocity term.

n   - As the density increased $\bar{p}$ decreased. This is because the MFP for ionization scales as $1/n$ for density. Increasing n decreases the MFP and thereby the escape probability.

EL   - As EL increases so does $\bar{p}$. For a larger reduced energy the fraction of particles in the fast group is greater. Particles from this group make up most of those that escape, so increasing their fraction increases the escape probability.

I   - Past an I of 50 (especially for larger escape probabilities) the difference between calculated escape probabilities is less than 5%. Based on

this an I of 50 was used for the escape
probability subroutine in the divertor model
program DIV.

D.2 Comparison of Methods

As described in Section 3.5, there are three different
methods that can be used in the divertor model program to
calculate $\bar{p}$. The "l_{avg}" method calculates an average escape
distance (distance to the plenum) for each mesh point. The
escape probability for a particle emitted from a point is
then, $p=\exp[-\bar{l}(x)/\lambda]$, where λ is the appropriate energy
group ionization MFP. The second method, "integral",
integrates   the   escape   probability, $p=\exp[-l(x,\phi)/\lambda]$,
directly to arrive at $\bar{p}$.   The third method, "Integral
w/cosine distribution", is the same as the second but adds a
cosine angular distribution probability for the reflected
particles.

Figure D.1 presents the results of calculating $\bar{p}$ using
each of the three methods for a range of electron densities
from 5×10^{18} to 5×10^{20} m^{-3}. At high escape probabilities
(corresponding to low recycling) the l_{avg} and Integral
methods yield very similar values for $\bar{p}$ while the Integral
w/cosine method is 50-60% lower. The l_{avg} and Integral
methods continue to be close in value down to values of .5
for $\bar{p}$. Beyond this point the methods are not far apart in

absolute value but as fractions of each other the difference increases to about 30% at small values of $\bar{p}$. The Integral w/cosine method produces a value for $\bar{p}$ lower than the other two methods except for $\bar{p} < .1$. In this region the l_{avg} method is a reasonable approximation for the Integral w/cosine method (assumed to be the most realistic predictor of the actual escape probability because it takes angular probability into account) and takes much less computational time. All three methods are available in the DIV program.
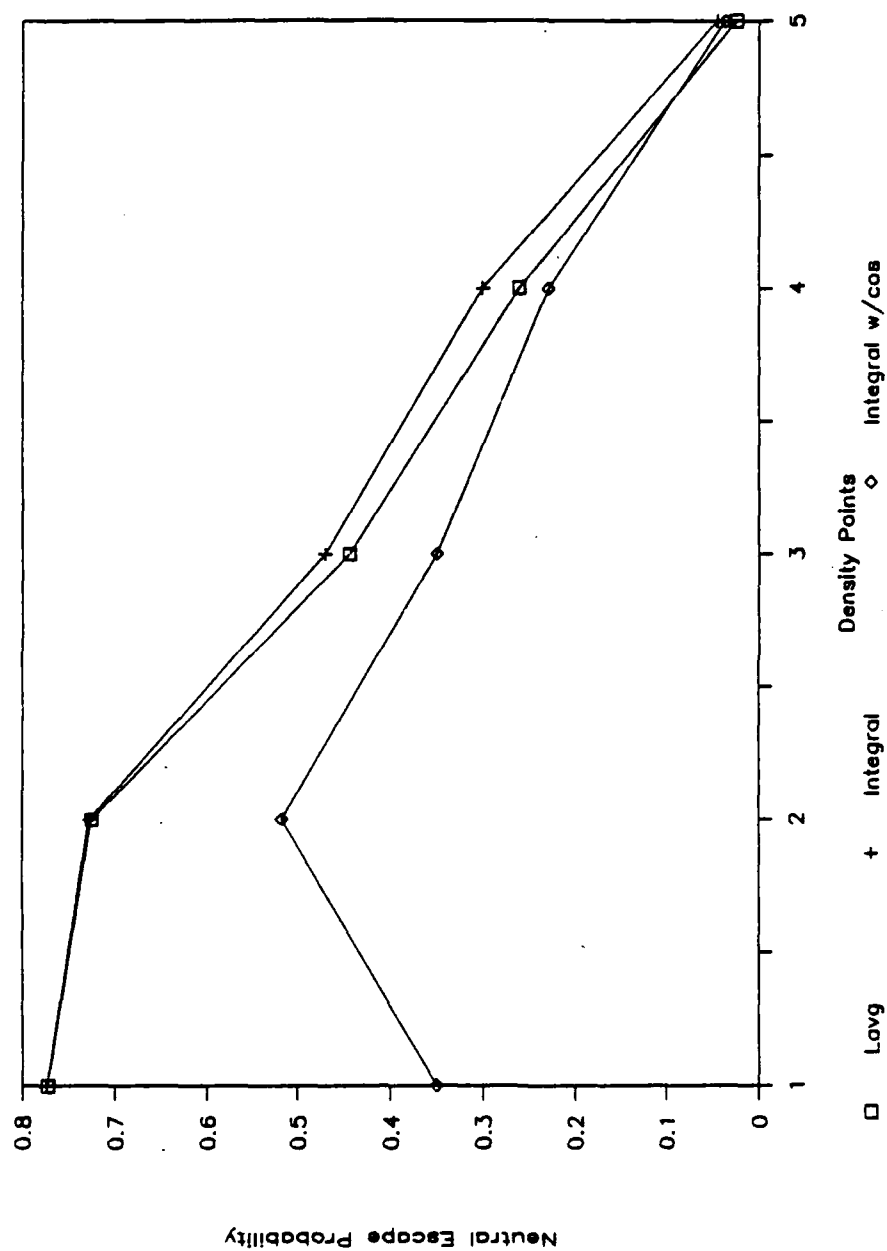
Figure D.1   Neutral Escape Probability Calculation
Method Comparison

APPENDIX E

BENCHMARKING INPUT AND OUTPUT DATA

This appendix tabulates the DIV input data used in the benchmarking cases presented in Chapter 5, along with the output from the divertor model code. The symbols used in the tables that follow are the same DIV program variables presented in Tables 4.1 and 4.2 of Chapter 4.

Table E.1

JAERI Case Input and Output Data

Input Parameter	Value	Parameter	Value	Output Parameter	Value
QT	17e6	R	.81	TP	3.8
LD	13.33	U	-	NP	9.1
M	2.0	F	1.14	TT	35.0
XT	.29	IMP	1.45	NT	1.8
THETA	.35	D	1.0	MT	.34
EL	9660	A	.7	U	.61
TP	4.0	CT	0.0	ISE	.51
TT	37.0	FHE	1.14	R	.8
NP	9.1	ELH	20400	CP	NA
NT	1.8	SHP	3.0	HER	NA
RP	1.0	METH	2.0	P12	NA
RT	1.0	DIST	2.0	LNP	NA
G1	3.9	TOL	1e-3		
G2	3.9	SOR	1.0		

Note: NA means "Not Applicable"

Table E.2

Harrison et al Case Input and Output Data

Input				Output	
Parameter	Value	Parameter	Value	Parameter	Value
QT	107e6	R	.99	TP	23.8
LD	10.0	U	–	NP	9.2
M	2.5	F	.028	TT	63.0
XT	.27	IMP	1.0	NT	6.97
THETA	.26	D	1.0	MT	$8.1e{-}4$
EL	9660	A	.7	U	.99
TP	25.5	CT	.05	ISE	.16
TT	66.0	FHE	.031	R	.99
NP	9.24	ELH	20400	CP	.025
NT	6.97	SHP	4.0	HER	2.23
RP	1.0	METH	2.0	P12	.30
RT	1.0	DIST	2.0	LNP	.021
G1	3.0	TOL	$1e{-}3$		
G2	3.0	SOR	1.0		

Table E.3

ZEHPYR Case Input and Output Data

Input				Output	
Parameter	Value	Parameter	Value	Parameter	Value
QT	31e6	R	.471	TP	10.5
LD	15.0	U	-	NP	8.68
M	2.5	F	-	TT	28.0
XT	.35	IMP	1.0	NT	3.66
THETA	.26	D	1.0	MT	.70
EL	9660	A	.7	U	.61
TP	10.8	CT	0.0	ISE	.16
TT	26.7	FHE	-	R	.471
NP	8.6	ELH	20400	CP	NA
NT	3.66	SHP	5.0	HER	NA
RP	.70	METH	2.0	P12	NA
RT	1.02	DIST	2.0	LNP	NA
G1	3.8	TOL	1e-3		
G2	4.3	SOR	1.0		

Note: The recycling coefficient, R, was not calculated.

Table E.4

NET Report #50 Case Input and Output Data

Input				Output	
Parameter	Value	Parameter	Value	Parameter	Value
QT	81.3e6	R	-	TP	11.0
LD	15.0	U	-	NP	13.4
M	2.5	F	.034	TT	64.8
XT	.35	IMP	1.0	NT	5.0
THETA	.26	D	·1.0	MT	2.3e-3
EL	9660	A	.7	U	.991
TP	7.6	CT	0.05	ISE	.21
TT	67.3	FHE	.034	R	.998
NP	14.0	ELH	20400	CP	.025
NT	5.0	SHP	4.0	HER	.99
RP	1.2	METH	2.0	P12	.30
RT	1.0	DIST	2.0	LNP	.031
G1	4.8	TOL	1e-3		
G2	3.42	SOR	1.0		

A SIMPLE ONE-DIMENSIONAL, ONE-FLUID DIVERTOR MODEL

Michael D. Baehre, O3
HQDA, MILPERCEN (DAPC-OPA-E
200 Stovall Street
Alexandria, VA 22332

FINAL REPORT: 20 May 1988

DISTRIBUTION: A

A Thesis Submitted to Rensselaer Polytechnic Institute,
Troy, New York, in Partial Fulfillment of the Requirements
for the Degree of Master of Science of Nuclear Engineering

A SIMPLE ONE-DIMENSIONAL, ONE-FLUID DIVERTOR MODEL

by

Michael D. Baehre

A Thesis Submitted to the Graduate

Faculty of Rensselaer Polytechnic Institute

in Partial Fulfillment of the

Requirements for the Degree of

MASTER OF SCIENCE

Approved:

_____

Don Steiner
Thesis Advisor

Rensselaer Polytechnic Institute
Troy, New York

May 1988

CONTENTS

LIST OF TABLES

LIST OF FIGURES

ACKNOWLEDGEMENT

ABSTRACT

Plasma exhaust and impurity control represent significant problems for the viability of fusion as an energy source. The divertor concept is an attractive solution to these problems in which fuel particles and ash are exhausted into a separate chamber, away from the plasma, where they can be impacted on a target plate, neutralized, and pumped out of the reactor. The performance of conceptual divertor designs, though, can presently only be assessed with the use of plasma edge models. This thesis examines the necessary components of these models and develops a simple, comprehensive, and accurate divertor model.

Divertor modeling is a complex process because of the strong coupling between numerous reactor systems (core plasma, first wall, divertor, pumping,...) and the nonlinearity of the fluid equations used in modeling. Some models oversimplify both the equations and processes included to obtain analytic expressions for divertor parameters. While these approaches have identified useful dependencies, they do not yield quantitatively accurate results. More sophisticated models attempt to include all the physics and solve the fluid equations in two dimensions (axially and radially) resulting in computer codes which are highly numerical and complex.

The objective in this thesis has been to develop a simple and comprehensive model of the divertor region which is highly usable and which gives quantitatively accurate results. Therefore, it includes the key processes of: neutral recycling; impurity production and radiation; remote radiative cooling; neutral pumping; particle convection; ash effects; and the effects of divertor geometry and plate material. The fluid equations are solved for the plate temperature and density, and the divertor throat temperature, using a fixed point iteration routine with Gauss-Seidel updating and successive over-relaxation. Neutral particle modeling is accomplished with a simple model of a wedge-shaped section of plasma overlying the divertor plate and a simple slab attenuation model. The results of benchmarking the model developed here against four other divertor models was very successful and validates the approach taken.

CHAPTER 1

INTRODUCTION AND HISTORICAL REVIEW

The purpose of this thesis is twofold: (1) to present an overview of the methods and approaches to modeling fusion reactor divertors; and (2) to develop a simple, yet comprehensive, model which will allow divertor performance to be examined as a function of divertor geometry, core plasma properties, and pumping capability. With such a model the sensitivity of divertor performance to key parameters can be evaluated and, thus, modifications can be identified to achieve operational requirements.

1.1 Background

Much of the current research on tokamaks centers on the problem of handling plasma exhaust and impurity control. Plasma particles will eventually diffuse outward across magnetic flux surfaces until they encounter a physical boundary, for example, the reactor vessel first wall. On striking this wall the particles deposit energy and can also physically erode the wall through sputtering. These interactions increase the cooling requirements for the first wall and decrease its service lifetime. More significantly, the influx of sputtered wall material (impurities)

1

represents an energy sink in the plasma due to atomic ionization and radiation emission by repetitive collisional excitation and bremssstralung processes. These impurities also cause a fuel depletion effect by reducing the allowable density of fuel ions in the plasma. For a given plasma electron density, an impurity ionized to a $+Z$ state will take the place of Z fuel ions $(+1)$, reducing the amount of fuel available for fusion and thereby, reducing reactor power. This fuel depletion effect also occurs by virtue of the buildup of fusion reaction by-products (helium for a D-T plasma).

The problems of heat deposition, wall erosion, fuel depletion, and plasma cooling have provided the impetus for the development of several impurity control and exhaust handling concepts. Among the most successful of these is the divertor concept.

The divertor concept involves magnetically perturbing field lines near the edge of the core plasma such that they leave the main reactor chamber and enter a separate "divertor" chamber (Figure 1.1). Plasma particles (electrons, fuel, reaction products, and impurities) diffusing out of the core plasma region are swept along these field lines until they intercept a material target or plate. In this way, particles are intentionally impacted on a specially designed target plate rather than on the vessel

Figure 1.1   Divertor Diagram

first wall. It is assumed that servicing damaged divertor plates will be less of an impact on machine availability than servicing a damaged first wall. The neutral particles coming off the divertor plate can subsequently be pumped out of the divertor chamber. Major design considerations for the divertor system include; handling the large heat fluxes (radiation and particle), coping with potentially severe material erosion problems, and providing adequate neutral pumping to satisfy impurity exhaust requirements.

1.2 Rationale for Divertor Modeling

Divertor design requires development of models for the edge plasma and divertor regions which establish plasma properties and define plasma interaction with reactor components (walls, target plate, pumps). In general these models should include transport both across and along field lines. Among the most important plasma parameters for divertor design are the plasma density and temperature in front of the divertor plate. These parameters establish the heat and particle loads which determine the cooling requirements and erosion rates at the plate. In addition, modeling of the neutral particle transport is required to estimate the fraction of neutrals (D-T and He) coming off the divertor plate that escape through the plasma fan

overlying the plate and are pumped out of the divertor chamber. The gross amount of helium-ash pumped will then determine the steady state concentration of helium in the core plasma. The total heat exhausted into the divertor determines the fraction of the fusion alpha power that will be deposited on the reactor first wall. Plasma conditions in the divertor will influence the amount of impurities produced at the plate and their probability of transport into the main plasma, poisoning it.

The above discussion implies a substantial linkage between divertor operation and ultimate fusion reactor performance. This impact has made the modeling of the plasma edge and divertor regions an important area of study and one which has received significant attention.

1.3   Models Available and Approaches

The sophistication of impurity control modeling has increased greatly over the past 5-10 years. Beginning with simple, almost heuristic models, there has been an evolution to two dimensional (2D) computer codes employing realistic geometries. In general, most of these models start with a form of the plasma fluid equations originally derived by Braginskii[1] and vary in the number of dimensions considered, atomic processes modeled, and number of fluids assumed.

One early model by Mahdavi[2] (1981) solved the fluid equations in one dimension (1D), along field lines, for the scrapeoff region by assuming the dominance of parallel electron heat conduction. This assumption allowed analytic expressions to be derived for temperature and density. The predictions of this model compare qualitatively with experimental results in reproducing a strong dependence of scrapeoff temperature and density on main plasma boundary density and a weak dependence on fusion alpha power. This model did not, however, account for the significant effects of particle recycling at the divertor plate. Another 1D, one fluid model along field lines, by Harrison, Hotston, and Harbour[3] (1982), also assumed the dominance of electron parallel heat conduction, but included neutral particle recycling, pumping, and impurity radiation. It is this neutral particle recycling which cools the plasma in front of the divertor target plate, reducing the heat load and sputtering. This model's assumption of 100% electron heat conduction has limited its application to a narrow range of plasma conditions in which such an assumption is valid.

A 1D model by Harbour and Morgan[4] (1984), ZEPHYR, uses two sets of fluid equations (electron and ion) and solves them numerically for the ion and electron temperatures and densities along field lines from a "watershed" (or symmetry) point between divertors to the divertor plate(s). The

ZEPHYR model was used for the divertor design in the International Torus (INTOR) study. Peng and Galambos[5] (1984) numerically solved a 1D, one fluid, set of equations for the temperature and density at two points (divertor throat and plate). This "two-point" model was used for scaling/parametric studies of divertor performance, and, in combination with the ZEPHYR code, was used for particle escape studies of divertors[6]. In these studies the recycling coefficient, a key parameter, was not calculated, but rather, was taken as an input from the case being benchmarked.

Other codes have been developed as 2D or quasi-2D. ODDESSA by Prinja and Conn[7] (1984) is such a quasi-2D code, in which radial solutions of the fluid equations are coupled between a watershed point and the divertor recycling region. This approach has the advantage of giving the radial variation of plasma parameters and linkage between the core plasma edge region and the divertor region without entailing the use of more complex 2D solution methods. The PLANET code[8] of the Princeton Plasma Laboratory and the code of Braams[9-10] (1983), used to model the Next European Torus (NET), are examples of 2D codes employing realistic geometries.

One difficulty encountered in solving the fluid equations is that they represent a highly nonlinear set of equations

(even in 1D) which are normally not solvable by ordinary numerical means[11]. The least cumbersome models arrive at analytic expressions only by grossly simplifying the equations. The more sophisticated 1D and 2D models are computationally cumbersome, requiring specialized numerical methods on powerful computers. Even implemented as such, it is noted that these codes are not as computationally "robust" as desired (i.e. they do not always converge)[4].

1.4 Approach and Rationale for a Simple and Comprehensive Model

The development of a divertor model involves a tradeoff between making the model readily "usable" and making it "accurate" and "applicable" to a wide range of reactor designs and divertor conditions. If one simplifies the fluid equations and neglects modeling certain key processes in the divertor, the results will be qualitatively and quantitativley suspect. If one attempts to include all the physics of the divertor in more than one dimension, the code becomes computationally complex. In many instances, this complexity makes it necessary to run the code on a mainframe and requires a large amount of pre-run preparation time to configure the code for the problem at hand and to calculate and specify various parameters (diffusion coefficients,

ionization energies ,reaction rate parameters, ect.). In this way the code becomes less interactive and less "usable".

The purpose of the research described in this thesis is to produce a simple, yet comprehensive, model of the divertor region which can be implemented on a personal computer so as to retain an interactive capability. To achieve the desired goal, the model must satisfy three requirements. First, it must remain as analytic as possible so as to reduce the variety and complexity of any numerical methods used. This requirement will limit the number of dimensions in which the fluid equations are solved. Second, it should include the following significant processes in the divertor: neutral recycling, impurity production and radiation, line radiation, neutral pumping, particle convection, and the effect of divertor geometry and plate material. Finally, the model must yield results comparable to the more sophisticated models to validate the approach used.

1.5 Outline of Thesis

Chapter 2 of this thesis presents the diverse ingredients necessary for an impurity and particle control model, and highlights the essential issues and physics involved in these models. This chapter is included to give perspective

to the final choices made for the divertor model adopted here. Chapter 3 details these choices and develops the analytic expressions and the evaluation methods used in the final model. Chapter 4 is a description and discussion of the computer code which implements the divertor model, including the numerical methods employed. Chapter 5 compares the results of this model to those obtained by some of the previously described divertor models. Finally, a summary of this work and its major conclusions are presented in Chapter 6, together with suggestions for future work and refinements .

CHAPTER 2

MODELING OF THE PLASMA EDGE REGION

Models of the plasma edge region and divertor chamber
vary widely in their approach and included processes
depending on their application. They can vary from a point
model to three dimensional (3D), and may be based on kinetic
or fluid approximations. However, as discussed below, there
are certain basic components, and fundamental processes that
must be accounted for in the development of any model.[11]

First, the model must include a set of plasma transport
equations which are tailored to a specific or schematic
geometry. To solve the equations, a set of boundary
conditions must be applied. For a divertor, these boundary
conditions generally include the sheath condition present at
the target plate. The transport equations in many instances
include particle, momentum, and energy source (or sink)
terms that must be calculated. These source terms usually
arise from the recycling of neutrals from walls or the
divertor plate, or from refueling of the plasma. Obtaining
the spatial distribution of the neutrals involves detailed
neutral transport calculations, including neutral and ion
reflection from surfaces and neutral-ion interactions.
These distribution calculations in turn enter into the
determination of (1) the helium-ash pumping efficiency of

11

the divertor, and (2) the production of impurities by charge-exchange neutrals. An estimate of impurity production (by neutrals or ions) must be included as the impurities will alter plasma energy balances via ionization and radiation losses. From a design standpoint these estimates can also provide an evaluation of the erosion by self-sputtering of reactor walls and the target plates.

A final requirement is that all these individual components and processes must be linked together in an interactive way to obtain a self-consistant solution. What follows is a more detailed discussion of each of these components and processes.

2.1 Transport Equations

Traditionally, two different sets of transport equations have been applied to the plasma edge region; kinetic, and fluid. Each is derived from the first three moments of the Boltzmann equation. The applicability, or appropriateness, of either set can be determined by estimating the collisionality of the plasma being modeled.

The effective collisionality of a plasma, ν, can be defined as the ratio of the effective mean free path for 90^0 scatter collsions of ions and electrons, λ, to a characteristic length, L, $\nu=\lambda/L$. This collisionality could

also be called the Knudsen number from molecular gas dynamics. For an axisymetric toroidal device, L is the connection length $L=\pi Rq$, where R is the plasma major radius, and q is the safety factor on edge. When $\nu<<1$, the plasma is highly collisional and the fluid approximation is appropriate. When $\nu>>1$, a kinetic treatment is warranted. Between these two limits, the fluid approach can be used, but with some caution.

The mean free path for cumulative 90^0 scatter can be written as:[11]

$$\lambda(m) \approx 5 \times 10^{16} T^2 (eV) \; n_e (m^{-3})^{-1} \qquad (2.1)$$

where T is the plasma temperature and n_e is the plasma electron density.

Equation (2.1) is plotted below in Figure 2.1 as a function of T and n_e. For typical values of L, 10-50 m, the plot implies that the fluid approximation is valid for low temperatures and high densities, but not valid for low densities and high temperatures. It should be noted that typical parameters for the plasma edge region can be densities in the range 10^{16}-10^{20} m^{-3} and temperatures in the range 1-400 ev. However, for most operating or planned devices, the edge density and temperature should be in a

Figure 2.1   The Mean Free Path for 90° Scattering
              as a Function of n and T   [reference 11]

region where the fluid approximation is applicable.

The form of the fluid equations used in most models is generally derived from the formulation of Braginskii.[1] Neglecting a few terms these equations have the form of conservation equations for particles, momentum, and energy:

$$-\nabla \cdot \vec{\Gamma} + S_n = 0$$

$$-\nabla \cdot \vec{R} + S_p = 0 \qquad\qquad (2.2)$$

$$-\nabla \cdot \vec{Q} + S_e = 0$$

where Γ, R, and Q are the particle, momentum, and energy fluxes, respectively, and S_n, S_p, S_e are the associated source terms.

Several critical assumptions are required to arrive at the above form of the fluid equations and they include: the magnetic field at any point is externally determined; steady state conditions apply (which negates any microturbulence terms); and collisions and gyromotion are sufficient to maintain a Maxwellian distribution for the particles.[12]

The fluid equations can be expanded to more detail and written in a "semi-conservative" form in which as many terms as possible are expressed as the divergence of a flux. For circular magnetic flux surfaces the equations become:[11]

Continuity

$$\frac{\partial (nv_{\parallel})}{\partial \zeta} = \frac{1}{r} \frac{\partial}{\partial r} r \left(D_{\perp} \frac{\partial n}{\partial r} - nv_r \right) + S_n \qquad (2.3)$$

Momentum

$$\frac{\partial}{\partial \zeta} \left(p_i + p_e + mnv_{\parallel}^2 + 1.28 \, \tau_i n \, T_i \frac{\partial v_{\parallel}}{\partial \zeta} \right) =$$

$$S_p + \frac{1}{r} \frac{\partial}{\partial r} \left(mv_{\parallel}(-nv_r + D_{\perp}\frac{\partial n}{\partial r}) \right) \qquad (2.4)$$

Ion Energy

$$\frac{\partial}{\partial \zeta} \left[\left(\frac{5}{2} T_i + \frac{1}{2} nm \, v_{\parallel}^2 \right) nv_{\parallel} - n\chi_{\parallel}^i \frac{\partial T_i}{\partial \zeta} \right] =$$

$$-v_{\parallel} \frac{\partial}{\partial \zeta} (nT_e) + \frac{1}{r} \frac{\partial}{\partial r} r \left[n\chi_{\perp}^i \frac{\partial T_i}{\partial r} + \left(\frac{5}{2} T_i + \frac{1}{2} mv_{\parallel}^2 \right) \cdot \right.$$

$$\left. \left(D_{\perp}\frac{\partial n}{\partial r} - nv_r \right) \right] + Q_{\Delta} + S_E^i \qquad (2.5)$$

and

Electron Energy

$$\frac{\partial}{\partial \zeta} \left(\frac{5}{2} T_e nv_{\parallel} - n\chi_{\parallel}^e \frac{\partial T_e}{\partial \zeta} \right) = v_{\parallel} \frac{\partial}{\partial \zeta} (nT_e) +$$

$$\frac{1}{r} \frac{\partial}{\partial r} r \left[\frac{5}{2} T_e \left(D_{\perp}\frac{\partial n}{\partial r} - nv_r \right) + n\chi_{\perp}^e \frac{\partial T_e}{\partial r} \right] - Q_{\Delta} + S_E^e$$

$$(2.6)$$

In these equations viscous effects have been neglected. The variable ζ is the coordinate along field lines, while r is the radial direction, the cross field direction. The velocity, $v_{\parallel}$, is the fluid velocity along field lines, v_r is the radial fluid velocity, n is the particle density, $T_{i,e}$

is the *ion, electron temperature*, m is the ion mass, τ_i is the ion collision time, $D\perp$ is a radial density diffusion coefficient, $\chi\perp,\parallel$ is a heat diffusivity (radial and parallel). The term Q_Δ is the classical ion-electron energy equipartition rate. The terms S_n, S_p, and S_e are, respectively, the density, momentum, and energy source terms from impurity and neutral atom collisions. The term $p_{i,e}$ is the ion, electron pressure (nT).

In the above equations, the requirement for plasma neutrality makes the continuity equations for the ·ions and electrons the same and the momentum balance equations for electrons and ion have been combined.

The fluid equations are four highly nonlinear, second order partial differential equations in n, $v_\parallel$, T_i, v_r, and T_e .They involve source terms which tend to be nonlinearly dependent on plasma parameters and are subject to their own modeling equations. Solution of these equations usually involves some degree of simplification (such as going to one dimension, or assuming the dominance of parallel electron conduction as the only energy transport mechanism) and an iterative process to converge on a solution because of the source terms. As a first step, though, a set of boundary conditions must be specified.

2.2   Boundary Conditions

Depending on the dimensionality of the problem, there may be as many as four boundaries to be considered in the computational mesh: the main plasma, the reaction chamber walls to which field lines are parallel, and two or more target plates. The symmetry of the problem can often be used to divide the edge plasma into two (or more) regions, each flowing to a target plate.

The boundary conditions of the main plasma can be set in several ways. The core-plasma edge density and temperatures (electron and ion) can be specified at a particular point (like the symmetry point). If the equations are only to be solved along the field lines, then these values could be used as radially representative across the entire edge region at that axial position. This would tend to overestimate the sputtering, recycling, and heat deposition on the target plate at most points since these represent peak radial values (T and n decrease radially). Another approach for a 1D solution would be to use a simple edge radial profile (exponential) in order to integrate for average values of density and temperature. This approach would tend to underestimate the heat flux to the target plate at some points (where T and n are larger than their average values) and overestimate it at others (where T and n are less than these average values). Using the same simple

radial profile, the 1D solution could be converted to a quasi-two dimensional one by solving the 1D equations stepwise across the edge region. If the full 2D equations were used, then a set of fluxes (particle, momentum, and energy) from the main plasma could be used as boundary conditions.

The boundary conditions at the wall would involve the influx of reflected charge-exchange neutrals and the impurities they produce by sputtering. These particles would represent a form of energy and momentum sinks, or particle sources. For a 2D solution the fluxes themselves could be used. For a 1D solution, the only way to include them would be as volumetric sources or sinks.

At the target plates an electrostatic potential forms. This sheath potential retards the electron flow so that ion and electron fluxes to the plate are equal, thus maintaining plasma neutrality. At the sheath the particle flow becomes collisionless, so the fluid approximation breaks down. The requirement for equal electron and ion fluxes leads to boundary conditions involving the particle and heat fluxes to the plates. From the continuity and momentum equations it can be shown that the fluid flow velocity cannot exceed the local sound speed as the plate is approached (i.e. $\bar{M} = v_{\parallel}/C_S < 1$, where $\bar{M}$ is the mach number and C_S is the sound speed). The Bohm Criterion requires that the flow velocity

at the plate be at least sonic for a stable sheath to form.[11] Therefore, the usual modeling assumption is that the fluid velocity at the plate is the local ion sound speed; i.e. $\tilde{M}=1$.

The power to the plate is usually expressed in terms of an energy transmission factor, γ , defined as the ratio of power flux to the plate to, particle flux times particle temperature. Thus,

$$\gamma_e = \frac{Q_e}{kT_e \Gamma_e} \tag{2.7}$$

$$\gamma_i = \frac{Q_i}{kT_i \Gamma_i} \tag{2.8}$$

$$\Gamma_e = \Gamma_i = n_e C_s \tag{2.9}$$

$$C_s = \left(\frac{kT_e + kT_i}{m_i} \right)^{1/2} \tag{2.10}$$

The form of the energy transmission coefficients can be expressed as:[11]

$$\gamma_e = \frac{2}{1-\nu_e} - .5 \ \ln\left[\left(2\pi \ \frac{m_e}{m_i} \right) \left(1 + \frac{T_i}{T_e} \right) \left(1 - \nu_e \right) \right] \tag{2.11}$$

$$\gamma_i = \frac{2T_i}{T_e} \tag{2.12}$$

where ν_e is the secondary electron yield per incident ion-electron pair.

Using the above energy transmission factors, the total power to the plate is:

$$Q_{plate} = \Gamma_p(kT_i\gamma_i + kT_e\gamma_e) \qquad (2.13)$$

where Γ_p is the particle flux at the plate. It should be noted that the above equation gives the energy flux that passes through the sheath to the target plate. It does not represent the actual energy deposited on the plate. This topic will be discussed in the next section along with recycling.

2.3 Neutral Particles and the Source Terms

The source terms in the fluid equations are usually derived from detailed neutral transport calculations. Neutrals can enter the plasma from several sources. The primary source of neutrals is the divertor target plate(s). Energetic hydrogen and helium ions are accelerated through the sheath and strike the divertor plate. Some of these particles are immediately backscattered as neutrals, retaining a large fraction of their original energy. The remaining particles are implanted in the target material where they come to rest as interstitial atoms. The helium atoms tend to become trapped in the material at grain

boundaries and dislocation sites. The hydrogen atoms are more mobile and can diffuse back out to the surface of the material where they recombine into molecular hydrogen and are emitted from the plate with an energy corresponding to the surface temperature of the target material. These molecules, however, are quickly dissociated and the resulting hydrogen atoms continue with an energy approximately equal to the Franck-Condon energy (3-5 ev). Because of this, the usual assumption is that the slow neutrals are emitted from the plate at the Franck-Condon energy. This flux of neutrals (fast and slow) diffuses through the plasma, undergoing excitation (emitting line radiation) and ionization by electron and ion impact. Until ionization take place, and a neutral appears as an ion with a given energy and momentum, the neutral acts as a momentum and energy sink. Thus, the spatial distribution of these neutrals and the associated excitation and ionization events serve as source/sink terms.

Once a neutral is ionized, it is swept back towards the target plate by the background plasma where it can once again impact the divertor plate. This process of repetitive neutralization at the plate and ionization near the plate is called recycling and is very dependent on plasma temperature and density since these parameters determine the reaction probabilities and rates. The recycling process is what

gives the divertor great potential for particle exhaust and impurity control. Its impact on divertor plasma parameters can be appreciated using a simple 1D recycling model, as discussed below.

Consider a plasma incident on a wall at x=a as shown in Figure 2.2. The continuity equation for the plasma is:[11]

$$\frac{\partial (nv)}{\partial x} = S = n_e \, n_o \, <\sigma v>_{ionization} \qquad (2.14)$$

where x is the direction along field lines, nv is a particle flux, n_e is the electron density, n_o is the neutral density, and $<\sigma v>$ is the electron impact ionization rate coefficient.

Integrating from the divertor entrance (x=0) to the divertor plate (x=a) yields:

$$\Gamma_a = \Gamma_o + \int_0^a n_e \, n_o \, <\sigma v> \, dx \qquad (2.15)$$

where $\Gamma_a = n_i v_a$ is the particle flux at the divertor plate (n_i is ion density), and Γ_o is the input particle flux at the divertor throat.

From the above expression it can be seen that the flux increases as the plate is approached (due to ionization of neutrals coming of the plate). A flux amplification factor

can be defined, $\mathring{A} = \Gamma_a/\Gamma_o$. Then the above equation becomes:

$$\mathring{A} = 1 + \frac{1}{\Gamma_o} \int_0^a n_e \, n_o \, <\sigma v> \, dx \; > \; 1 \qquad (2.16)$$

If the sheath boundary condition, $Q(a) = \gamma kT(a)\Gamma_a$ (where $\gamma = \gamma_i + \gamma_e$), is applied, where $Q(a)$ is the energy going to the plate at $x=a$, $kT(a)$ is the target plasma temperature (the ion and electron temperatures are assumed to be the same), and Γ_a is the target flux, and if the substitution $\Gamma_a = \Gamma_o \mathring{A}$ is made, we get:

$$kT = \frac{Q(a)}{\gamma \, \Gamma_a} = \frac{Q(a)}{\gamma \, \Gamma_o} \cdot \frac{1}{\mathring{A}} \qquad (2.17)$$

From equation (2.17) we can see that increasing $\mathring{A}$ decreases kT.

If $v_a = C_s \propto [T(a)]^{1/2}$ then:

$$Q(a) \sim \Gamma_a \, kT(a) \sim n(a) v_a kT(a)$$

$$Q(a) \sim n(a)[kT(a)]^{3/2} \quad \text{or}$$

$$n(a) \propto \frac{Q(a)}{[kT(a)]^{3/2}} \propto \mathring{A}^{3/2} \qquad (2.18)$$

Figure 2.2   Schematic Illustration of a Divertor Model

Thus, increasing the particle recycling increases n and decreases kT as noted before. Å>1 implies that each ion entering the divertor will, on average, impact the plate Å times. Therefore the energy per particle that goes to the plate is less. Another way of expressing recycling is with the recycling coefficient, R, defined by

$$R = \frac{\Gamma_a - \Gamma_o}{\Gamma_a} = \frac{\int_o^a n_e n_o \langle \sigma v \rangle_{ion} \, dx}{\Gamma_a} \qquad (2.19)$$

and representing the fraction of particles hitting the plate which are recycled particles.

The result of recycling is a cool dense plasma in front of the target plate. Besides giving each entering particle several opportunities to deposit its energy on the divertor plate, the actual amount of energy to be deposited on the plate by particle impact is reduced because each time a particle recycles it has the chance to emit line radiation by collisional excitation prior to being ionized and going back to the plate. This energy loss by line radiation in the divertor is designated as "remote radiation cooling"[13] and is another advantage to the divertor because this radiated heat flux is distributed over the entire surface

of the divertor chamber. An empirical estimate by Harrison et al[4] of the energy loss due to ionization and radiation by each ionized neutral is:

$$\chi(eV) = 17.5 + \left(5 + \frac{37.5 \ eV}{T_e}\right) \log_{10}\left(\frac{10^{21} m^{-3}}{n_e}\right) \quad (2.20)$$

Under most divertor conditions the magnitude of this energy loss is about 25 eV per ionized D-T neutral.

Post and Lackner[11] have solved the continuity equations for neutrals and ions, matching the fluxes at the plate. Using several assumptions they found two stable operating regimes for a divertor. One regime is found around $\AA \approx 1$ or $R \approx 0$ (low recycling) where neutrals stream (with little ionization) back to the main plasma or down pump ducts. For this regime the plasma temperature at the plate is high and the density low. The second stable regime is a high recycling one, where $\AA \gg 1$ or $R \approx 1$, and the divertor plasma is cooler and more dense. This is the preferred operating mode because the divertor plate heat load and sputtering is less than in the low recycling regime.

2.4 Impurities and the Source Terms

Impurities present in the plasma do not enter into the

particle source terms but at high enough densities can enter into the momentum and energy source terms by causing radiation losses via collisions. In this way impurities act as energy and momentum sinks. Low Z impurities will become fully stripped above several eV and, thereby, cease to be significant energy sinks. However, their presence in the main plasma can take the place of fuel atoms, due to plasma neutrality requirements and beta limits. The same is true for medium Z impurities which can radiate up to temperatures of around 2 keV (unlikely in a divertor). This means that until they are redeposited on a surface or pumped, they will continue to cause energy losses in the divertor plasma. Heavy impurities are capable of radiating from the core of the main plasma so they will also cause radiation losses in the divertor plasma. These heavy impurities, though, are quickly ionized so they should quickly return to the surface from which they were emitted.[11]

The primary source of impurities in the main plasma chamber (besides He) is the sputtered wall material resulting from the impact of charge-exchange neutrals on the walls. The precipitating slow neutrals could come from refueling atoms. The prime source of impurities in the divertor is obviously the divertor plates where the ions are intentionally impacted. A fraction, f , of the atoms that are sputtered off the plate will be quickly ionized and

carried back to the plate where they will redeposit and/or cause self-sputtering with a yield per impact of Y_s. Summing successive generations of self-sputtering and redeposition shows that if $fY_s < 1$ per incident ion, then the net impurity production rate, R_e, or sputtering of the plate is given by:

$$R_e = \Gamma_{H+} \; Y_{H+} \left(\frac{1}{1-fY_s}\right) \qquad (2.21)$$

where Γ_{H+} is the hydrogen ion (D or T) flux to the plate, Y_{H+} is the sputtering yield for hydrogen on the plate material, and f and Y_s are as defined above.

If $fY_s > 1$, the plate could potentially erode away very quickly due to runaway sputtering. However, at a local level, self-sputtering is a self-limiting process. An increase in sputtering will cause the plasma to cool down due to impurity radiation (described below) which will decrease the sheath potential and thereby reduce the impact energy of the D-T ions and impurity ions. This same cooling though, can allow impurities to escape into the main plasma, poisoning it. Sputtering of the divertor chamber walls can also occur as a result of charge-exchange neutrals that escape the divertor plasma.

As noted above, the major impact of impurities on the

plasma is to cool it via line radiation. Estimating the amount of impurity radiation is extremely difficult. Impurities in the divertor will radiate by: line radiation, recombination, and bremsstrahlung processes. Each of these processes is in turn dependent on the charge state of the impurity. In some cases the assumption of coronal equilibrium is made in which the rate equations for ionization and recombination to different charge states are solved based on a constant density and temperature plasma and no impurity-particle transport losses. The results of these calculations yields the following empirical expression for radiation power:[15,16]

$$P_{rad}(MW/m^3) = n_e n_{imp} \alpha(T) \, z^\beta = n_e^2 f \, L_z \qquad (2.22)$$

where $n_e(m^{-3})$ is the electron density, n_{imp} is the impurity density, $\alpha(T)$ and β are fitting constants, Z is the atomic number of the impurity, f is the fractional impurity density, and L_z is the power parameter.

These expressions are valid for Z>6 and T> 1 keV. Little data exists for the lower temperatures anticipated in the divertor. Even if such data existed, the assumption of coronal equilibrium is suspect. The timescale for the onset of coronal equilibrium in a plasma is, in the case of a

divertor, greater than the timescale for ionization and return to the target plate. Preequilibrium values for the power parameter, L_z, can be 2-10 times the equilibrium values, depending on the impurity. Additionally, there are steep temperature and density gradients near the divertor plate which would also tend to invalidate coronal power estimates. This is an area which requires further research.

It is important to note that the impurity radiation can have a beneficial effect in the divertor by cooling the plasma while depositing the radiation energy over an area substantially greater than just the divertor plate. Some divertor designs include a provision for the intentional injection of medium Z impurities (e.g. xenon) into the divertor plasma to reduce the particle heat load on the target plate.

If the divertor is to operate effectively, divertor impurities must remain in the divertor. Impurity concentrations in the core plasma of as low as .01 % can fatally poison it. There are two dominant forces on an impurity ion which tend to pull in opposite directions. The first is the frictional drag of the background plasma as it flows into the divertor. The second is a thermal force pointing in the direction of higher temperature (i.e. out of the divertor to the core plasma).

Neuhauser[14] has identified a criterion which if

satisfied, implies that highly charged impurities will tend to be entrained and drift with the background plasma back to the divertor plate. Based on a model of the above forces, the criterion for impurity entrainment is:

$$\bar{m} > \frac{\lambda_I}{\lambda_T} \qquad (2.23)$$

where $\bar{m}$ is the plasma flow mach number, λ_I is the mean free path for coulomb collisions between impurity ions and the background plasma ions, and λ_T is the axial (along field lines) scale length for changes in the ion temperature. If the criterion is met, then the divertor will accrue the advantages of plasma cooling by impurity radiation without poisoning the core plasma.

CHAPTER 3

THE TWO POINT MODEL

As noted in Chapter 1, the development of a divertor model involves a tradeoff between simplicity, ease of implementation, and completeness. One immediate simplification that can be made is to develop the model in only one dimension. The choice of dimension adopted here is the direction along field lines. Using this dimension allows for linkage back to the core plasma. An additional consideration in this selection is that radial solutions to the fluid equations tend to be very sensitive to the value of the radial diffusion and thermal diffusivity coefficients which can only be estimated.

A second simplification is to solve the model equations at only two points, rather than continuouly along field lines. The two-point method of solution of the fluid equations involves integration along field lines between the divertor throat and target plate. By limiting the solution to the densities and temperatures at only these two points, the integrals of the particle, momentum, and energy source terms can be evaluated globally, greatly simplifying their representation and method of solution.

The two-point approach to modeling the divertor will yield values for the most critical divertor-plasma

parameters without requiring an inordinate amount of numerical computing effort.

This chapter of the thesis presents the derivation of the two point analytic equations for the throat and plate temperatures and densities, and the models and methods of evaluation for key terms in these analytic expressions.

3.1 Description/Geometry

The geometry of the two-point model assumes that the edge region of the plasma can be divided into two regions: one outside the divertor, and the other inside the divertor. An idealized elemental flux tube parallel to magnetic field lines (Figure.3.1) of length L_s (outside the divertor) and L_d (inside the divertor) is "unwound" from the torus. Both L_s and L_d are dependent on the geometry and magnetic topology of the reactor. The two point model is then applied to the region inside the divertor. Appendix C presents some simple analytic expressions for estimating plasma parameters between the symmetry (watershed) point and the divertor throat. These results for throat density and temperature are used as input for the model inside the divertor.

The steady state fluid equations which will be integrated along the straightened out field lines are,[5]

Figure 3.1   Two Point Model Geometry

Continuity $\quad \dfrac{d}{dx} \quad nv = -S_n \qquad\qquad\qquad$ (3.1)

Momentum $\quad \dfrac{d}{dx}\left[\, nMv^2 + nT(1+r)\right] = S_p \qquad$ (3.2)

Energy $\quad \dfrac{d}{dx}\left\{x_o T^{2.5}\dfrac{dT}{dx} + nv\left[\dfrac{1}{2}\,Mv^2 + \dfrac{5}{2}\,T(1+r)\right]\right\} = S_e$ (3.3)

where x is the direction along field lines, S_n, S_p, and S_e are, respectively, the particle, momentum, and energy source terms, n is the particle density, v is the plasma fluid flow speed, T is the electron temperature, M is the ion mass, r is the ion to electron temperature ratio (T_i/T_e), and x_o is the electron thermal conductivity coefficient (ion conduction is neglected).

The first term inside the brackets of the momentum equation, (3.2), accounts for the momentum due to fluid flow (convection) and the second term is the temperature (internal energy) contribution to momentum. The first term inside the brackets of the energy equation, (3.3), represents the energy conducted by electrons while the second term is the energy convected by ions and electrons. The energy source term is primarily derived from the recycling of neutrals at the plate, but can be artificially increased to mimic the losses due to impurity atoms. The addditional components required in the model, as outlined

in Chapter 2, will be presented as they arise in the derivation of the modeling equations and the description of the evaluation of terms.

3.2 Integration of the Fluid Equations Along Field Lines

Integration of the energy equation yields,

$$x_o T^{2.5} \frac{dT}{dx} + nv\left[\frac{1}{2}Mv^2 + \frac{5}{2}T(1+r)\right] = \int_p^x S_e dx + C \quad (3.4)$$

If the origin, $(x=0)$, is at the plate, then the constant of integration, C, is found to be,

$$C = \left\{x_o T^{2.5}\frac{dT}{dx} + nv\left[\frac{1}{2}Mv^2 + \frac{5}{2}T(1+r)\right]\right\}\bigg|_t - \int_p^t S_e dx \quad (3.5)$$

where the first term on the right (in brackets) can be interpreted as Q_t, the energy flux that enters the throat, and the second term, as the energy loss/gain between the throat and the plate.

Integrating equation (3.4) results in

$$\left(\frac{T_t}{T_p}\right)^{7/2} - 1 = \frac{7}{2} \frac{Q_t L_d \mu}{x_o T_p^{7/2}} \qquad (3.6)$$

where T_t is the throat electron temperature, T_p is the plate electron temperature, and μ is the average fraction of energy transported in the divertor by conduction, and is given by,

$$\mu = 1 - \frac{1}{Q_t L_d} \int_p^t \left\{ \int_x^t S_e dx' + nv \left[\frac{1}{2} M v^2 + \frac{5}{2} T(1+r) \right] \right\} dx \qquad (3.7)$$

The next step in the derivation of the model equations is to eliminate the plate temperature from the right hand side of equation (3.6) using the sheath boundary condition[5],

$$Q_t - \int_p^t S_e dx = n_p v_p T_p (\gamma_e + r_p \gamma_i) \qquad (3.8)$$

where $\gamma_{e,i}$ is the sheath energy transfer factor for electrons, ions, n_p is the plate electron density, T_p is the plate electron temperature, v_p is the fluid speed at the divertor plate, and r_p is the ion to electron temperature ratio at the plate.

Solving for T_p and substituting the resulting expression

into equation (3.6) gives,

$$\left(\frac{T_t}{T_p}\right)^{7/2} - 1 = \left(\frac{n_p}{n_{\nabla T}}\right)^{7/3} \tag{3.9}$$

where $n_{\nabla T}$ is given by

$$n_{\nabla T} = \left(\frac{2x_o}{7L_D\mu}\right)^{3/7} \frac{Q_t^{4/7}\left(1 - \frac{\int_p^t S_e dx}{Q_t}\right)}{\left(\gamma_e + r_p \gamma_i\right)} \left(\frac{M}{1+r_p}\right)^{1/2} \tag{3.10}$$

and can be interpreted as a temperature gradient threshold. In reference 5 it was found that if the throat density was less than this value, heat conduction tended to overwhelm the tendancy of recycling to produce a temperature gradient near the divertor plate. This means neutral recycling becomes less effective in lowering the plate temperature if the throat density falls below this threshold value. The momentum and continuity equations are now used to eliminate T_t and T_p from the left hand side of equation (3.9) as described below.

First the momentum equation is rewritten to include the fluid mach number ($\mathbb{M} = v/C_s$),

$$-\frac{d}{dx}\left[Mn\bar{m}^2 C_s^2 + nT(1+r)\right] = S_p \qquad (3.11)$$

where C_s is the ion sound speed, and is given by

$$C_s = \left[\frac{T(1+r)}{M}\right]^{1/2} \qquad (3.12)$$

Integrating equation (3.11) and simplifying we obtain

$$nT(1+r)(1+\bar{m}^2) = \int_p^x S_p dx + C \qquad (3.13)$$

If the integral on the right is evaluated at the plate (i.e. $x=0$) then,

$$C = n_p T_p (1 + r_p)(1 + \bar{m}_p^2) = 2\, n_p T_p (1+r_p)$$

where $\bar{m}_p$ has been set equal to 1.0 as a boundary condition. Solving equation (3.13) for T we obtain

$$T = \frac{1}{n\left(1 + r\right)\left(1 + \bar{m}^2\right)}\left[\int_p^x S_p dx' + 2n_p T_p\left(1 + r_p\right)\right] \qquad (3.14)$$

Evaluating the integral of equation (3.14) out to the throat, point t, and dividing by T_p results in

$$\frac{T_t}{T_p} = \frac{1}{T_p n_t \left(1+r_t\right)\left(1+\bar{m}_t^2\right)} \left[\int_p^t S_p dx + 2n_p T_p \left(1+r_p\right) \right] \quad (3.15)$$

or rearranged as,

$$\frac{T_t}{T_p} = \frac{n_p}{n_t} \frac{1+r_p}{1+r_t} \frac{1}{1+\bar{m}_t^2} \left[2 + \frac{\int_p^t S_p dx}{n_p \left(1+r_p\right) T_p} \right] \quad (3.16)$$

The above expression can be further simplified by employing the following definitions:

R= fraction of ions hitting the plate which
   come from the ionization of neutrals
   and is equal to

$$R = \frac{\Gamma_p - \Gamma_t}{\Gamma_p} = \frac{\int_p^t S_n dx}{n_p v_p} = \frac{M^{1/2}\int_p^t S_n dx}{n_p \left[T_p\left(1+r_p\right)\right]^{1/2}} \quad (3.17)$$

where $\Gamma_{p,t}$ are, respectively, the particle fluxes at the plate and divertor throat.

$\bar{V}$ = average neutral velocity normalized to the ion speed at the plate, given by

$$\bar{V} = \frac{\frac{1}{M}\int_p^t S_p dx}{v_p \int_p^t S_n dx} = \frac{M^{-1/2}\int_p^t S_p dx}{\left[T_p\left(1+r_p\right)\right]^{1/2}\int_p^t S_n dx} \qquad (3.18)$$

Using R and $\bar{V}$ as defined above, equation (3.16) can be rewritten as

$$\frac{T_t}{T_p} = \frac{n_p}{n_t}\frac{1+r_p}{1+r_t}\frac{1}{1+\mathbb{M}^2_t}\left(2+\bar{V}R\right) \qquad (3.19)$$

Finally, this equation can be inserted into equation (3.9) to give

$$\left[\frac{n_p}{n_t}\frac{1+r_p}{1+r_t}\frac{1}{1+\mathbb{M}^2_t}\left(2+\bar{V}R\right)\right]^{7/2}-1 = \left(\frac{n_p}{n_{\nabla T}}\right)^{7/3} \qquad (3.20)$$

An expression for $\mathbb{M}_t$ can be derived from the continuity equation, the definition of R, and equation (3.19). Thus,

$$\bar{\mathbb{M}}_t = \left(\frac{a}{1-a} \right)^{1/2} \qquad (3.21)$$

where
$$a = \frac{n_p}{n_t} \left(1-R \right)^2 \left(\frac{1}{2+\bar{V}R} \right)$$

Equation (3.20) uses information from all three fluid equations in it derivation. This equation, along with equation (3.8) and a simplification of equation (3.18), can be used to solve for three of the four primary plasma parameters; T_p, n_p, T_t, and n_t. Before this can be done though, methods for evaluating the integrals of the source terms, the conduction fraction (μ), and the recycling coefficient (R) must be determined.

3.3 Evaluation of the Integrals of the Source Terms

3.3.1 Introduction

The evaluation of the integrals of the particle, momentum, and energy source terms requires a detailed understanding of divertor physics. The source terms are primarily derived from the recycling of neutrals produced at the divertor plate. Plasma ions are accelerated through the sheath, strike the divertor plate, and are neutralized. A fraction (R_n) of these particles is immediately

backscattered, retaining a large fraction (R_e) of their impact energy (see Appendix A for expressions for R_n and R_e). The remaining fraction ($1-R_n$) is implanted in the target material where the particles come to rest as interstitial atoms. The normal assumption is that at equilibrium the implanted hydrogen atoms diffuse back out to the surface of the divertor plate where they recombine into hydrogen molecules and are emitted· with an energy corresponding to the plate temperature. Dissociation by electron impact occurs quickly near the plate after emission so another assumption often used is that these neutrals are emitted from the plate as atoms (rather than molecules) with an energy equivalent to the Franck-Condon energy (3-5 eV). This flux of fast and slow neutrals then diffuses through the plasma undergoing excitation (emitting line radiation), charge exchange, and ionization (by electron impact). Each of these processes will be considered in the derivation of the integrals of the source terms.

3.3.2 Integral of the Particle Source Term

The only source of D-T particles in the divertor region is the ionization of neutrals. The value of the particle source term can be expressed as a function of the recycling coefficient defined in this chapter and Chapter 2. Thus,

$$\int_p^t S_n dx = R\Gamma_p = Rn_p \left[\frac{T_p\left(1+r_p\right)}{M} \right]^{1/2} \qquad (3.22)$$

The evaluation of the recycling coefficient is accomplished by modeling neutral transport and will be discussed in Section 3.5.

3.3.3 Integral of the Momentum Source Term

The integral of the momentum source term must account for the two energy groups of neutral particles, slow and fast. After leaving the target plate, each neutral particle can undergo charge exchange, ionization, or escape to the divertor plenum where it may return to the plasma or be pumped. Charge exchange and ionization events both contribute to the momentum source term while escape/pump events contribute nothing. Considering only these two contributing processes, F_{ion}, the fraction of neutrals coming directly from the plate which undergoes ionization rather than charge exchange, is given by,

$$F_{ion} = \frac{<\sigma v>_{ion}}{<\sigma v>_{ion} + <\sigma v>_{cx}} \tag{3.23}$$

where $<\sigma v>_{ion}$ is the reaction rate coefficient for electron impact ionization (ground state and excited state combined) and $<\sigma v>_{cx}$ is the charge exchange rate coefficient (see Appendix A for evaluation of these quantities).

Each neutral that is ionized contributes an average of $Mv_0 \sin\theta$ to the momentum source. This is derived from the assumption of perpendicular emission of the neutrals from the plate. The velocity of the neutral in this perpendicular direction is V_0, while θ is the angle of incidence of the magnetic field lines to the plate (see Figure 3.2). The neutral velocity in the field line direction is $v_0 \sin\theta$.

For the fast group the neutral velocity is given by

$$v_f = \left(\frac{2 R_e E_o}{R_n M}\right)^{1/2} = \left(\frac{2 R_e T_p \gamma_i}{R_n M}\right)^{1/2} \tag{3.24}$$

where E_o is the incident energy of the ion. For the slow group the neutral velocity would be

Figure 3.2   Momentum Source Term Geometry

$$v_s = \left(\frac{2 \, E_{fc}}{M} \right)^{1/2} \qquad (3.25)$$

where E_{fc} is the Franck-Condon energy.

The relative fraction that undergoes charge exchange is,

$$F_{cx} = 1 - F_{ion} \qquad (3.26)$$

Charge exchange represents a change in momentum because incoming ions change places with neutral particles of different speeds and directions. The calculation of this *component of the momentum source term* depends on whether neutrals are modeled with their own set of fluid equations or included in the single fluid considered here. If neutrals are accounted for separately, the contribution to the momentum source would be,

$$M(v_o \sin\theta + v_{avg}) \qquad (3.27)$$

where M is the ion mass, $v_o \sin\theta$ is the neutral velocity in the field direction, and v_{avg} is the average ion velocity between the throat and plate. The neutralization of the incoming ion causes an average loss of momentum of Mv_{avg},

where v_{avg} is calculated as,

$$v_{avg} = \frac{1}{2} \left[\left(\frac{T_t \left(1+r_t \right)}{M} \right)^{1/2} \hat{m}_t + \left(\frac{T_p \left(1+r_p \right)}{M} \right)^{1/2} \right] \quad (3.28)$$

This approach to calculating the momentum source term assumes that there is no change in direction of the initial neutral (now an ion) as a result of the charge exchange interaction. If the resulting neutral from this interaction is subsequently ionized then the momentum of the neutral (Mv_{avg}) is regained making a negative addition to the source term. If neutral particles are not accounted for separately with a set of fluid equations then the neutral contribution to the source term must be added to the ion component. This makes the charge exchange component $Mv_o \sin\theta$, the same as for ionization.

Based on the above expressions, and whether neutrals are independently modeled, the final expression(s) for the integral of the momentum source term can be written as

$$\int_p^t S_p dx = M n_p v_p R \left\{ R_n \left[F_{ion-f} v_f \sin\theta + F_{cx-f} \left(v_f \sin\theta + v_{avg} \right) \right] + \left(1 - R_n \right) \left[F_{ion-s} v_s \sin\theta + F_{cx-s} \left(v_s \sin\theta + v_{avg} \right) \right] \right\}$$

If neutral momentum pressure is included in the D-T ion equations, this expression reduces to

$$\int_p^t S_p dx = M\, n_p v_p R \left[R_n v_f \sin\theta + (1-R_n) v_s \sin\theta \right] \qquad (3.29)$$

where $n_p v_p$ represents the neutral particle flux coming off the plate at steady state and the other terms are as described previously.

Here the recycling coefficient (R) is being used as a measure of the fraction of neutral flux that undergoes interaction. Although this is a reasonable use for R, it does imply that the contribution to the momentum source term of ionized or charge exchanged neutrals coming from the divertor plenum is negligible.

Numerical evaluation of the integral of the momentum source term for a variety of divertor conditions resulted in values which are small compared to the total momentum of the D-T particles as they flow to the plate and thus, this

term has little effect on the final solution of the fluid equations. It is noted that in some models[2,3,22] this term is neglected altogether. The divertor code developed in this thesis gives the user the option of including this term or setting it to zero.

3.3.4 Integral of the Energy Source Term

The integral of the energy source term includes contributions from radiation, ionization, and charge exchange. To account for radiation and ionization losses, the average energy loss per ionization event, χ, defined previously, is used

$$\chi(eV) = 17.5 + \left(5 + \frac{37.5}{T_e(ev)}\right) \log_{10}\left(\frac{10^{21} m^{-3}}{n_e}\right) \; ev$$

For a neutral produced at the target and moving through the plasma fan in front of the divertor plate, the use of an energy loss per ionization event assigns the entire energy loss to the point of ionization. In reality it will radiate throughout its trajectory due to excitation by electron impact. Over a wide range of operating conditions, the value of χ does not vary much from a value of around 25-26 eV for hydrogen. Its value could be artificially increased to

include losses due to the radiation and ionization of impurities. This enhancement would be proportional to the amount of sputtering, impurity type, and mean free paths for impurity ionization and excitation. As noted in Chapter 2, evaluating the magnitude of this energy loss increment is difficult. Therefore, in the divertor model code this increment is treated as a multiplicative parameter, $\chi' = Imp \cdot \chi$, where Imp is a multiplicative factor, increasing D-T radiation losses to account for impurity energy losses.

Charge exchange also contributes to the energy source term. Incoming ions change places with neutrals which have different energies. The total energy of an incoming ion can be written as[5]

$$E_{ion} = 3/2 \ T + 1/2 Mv^2 \qquad (3.30)$$

where T is the plasma temperature and v is the flow speed.

If the assumption is made that the energy of the fast neutrals is approximately the same as that of the incoming ions, then the charge exchange of neutrals of this energy group contributes nothing to the energy source term. If, in addition, it is assumed that the energy of the slow neutrals is negligible compared to the energy of the incoming ions, then charge exchange represents the total loss of the

incoming ion's energy. Based on these assumptions, the integral of the energy source term can be expressed as,

$$\int_p^t S_e dx = n_p v_p \left[R\chi' + \left(1-R_n\right) F_{cx-s} \left(\frac{3}{2} T_{avg} + \frac{1}{2} M v_{avg}^2 \right) \right] \quad (3.31)$$

where T_{avg} is the average plasma temperature between the throat and plate and V_{avg} is the average flow velocity.

In equation (3.31) above, χ' is multiplied by the recycling coefficient since this represents the total fraction of neutral flux that is ionized. The second term is not multiplied by R because this term pertains only to slow neutrals. The fraction of slow neutrals that is ionized is much larger than the combined fraction of slow and fast. Therefore it is assumed that 100% of the slow neutrals undergo some sort of interaction (i.e. $R_{slow} \approx 1$).

3.4 Evaluation of the Conduction Fraction

The conduction fraction introduced in Section 3.2 (eqn 3.7) is the average fraction of energy transported in the divertor by electron conduction. Thus

$$\mu = 1 - \frac{1}{Q_t L_d} \int_p^t \left\{ \left[\int_x^t S_e dx' + nv \left[\frac{1}{2} Mv^2 + \frac{5}{2} T(1+r) \right] \right\} dx \quad (3.32)$$

Evaluation of this quantity requires a knowledge of the density, temperature, mach number, and energy source (sink) term profiles in the divertor region. The two point model does not provide this profile information so the following assumptions must be made to evaluate μ.

The first assumption is to ignore the integral of the energy source term. The major contribution to this integral comes from a narrow band near the divertor plate. While this term might be significant near the plate, it represents a small contribution to the second integral. Numerical integration of this integral has confirmed the insignificance of the source term.

The second assumption concerns the profiles of the density and ion to electron temperature ratio, (r). A previous study, using more sophisticated models[5], has shown a reasonable distribution for these two quantities has the following form, $f(x)$,

$$f(x) = f(0) + \left[f(L) - f(0) \right] \left[1 - \left(1 - \frac{x}{L} \right)^\alpha \right] \quad (3.32)$$

where α is a polynomial shape factor.

Using the continuity equation, (3.1), the mach number can be expressed in terms of n and r as

$$\tilde{m}(x) = \left(1-RR'\right)\left[\frac{n_p\left(T_p(1+r_p)\right)^{1/2}}{n\left(T\ (1+r)\right)^{1/2}}\right] \qquad (3.33)$$

where R' is the fraction of ionization up to x and is given by

$$R' = \frac{\int_p^x S_n dx'}{\int_p^t S_n dx'} \qquad (3.34)$$

Equation (3.33) can be used along with the momentum equation, (3.2), to yield the temperature profile,

$$T(x) = \left[\left(\overline{V}R\right)' + 2 - \left(1-RR'\right)^2\ \frac{n_p}{n}\ \right]\frac{n_p T_p(1+r_p)}{n\ T\ (1+r)} \qquad (3.35)$$

where $(\overline{V}R)'$ is the fraction of momentum source up to the point x and is given by

$$(\overline{V}R)' = \overline{V}R \; \frac{\int_p^x S_p \, dx'}{\int_p^t S_p \, dx'} \qquad (3.36)$$

Evaluation of R' and $(\overline{V}R)'$ requires additional assumptions about the distribution of the particle and momentum sources. One intuitively simple method is to assume an exponentially decreasing distribution for these sources. Thus

$$S_n \; \alpha \; \left[R_n EXP\left(\frac{-x}{\lambda_1}\right) + \left(1-R_n\right) EXP\left(\frac{-x}{\lambda_2}\right) \right] \qquad (3.37)$$

and

$$S_p \; \alpha \;\; R_n \left[F_{ion-f} v_f \sin\theta \, EXP\left(\frac{-x}{\lambda_1}\right) + F_{cx-f}\left(v_f \sin\theta + \right.\right.$$
$$\left.\left. v_{avg}\right) EXP\left(\frac{-x}{\lambda_3}\right) \right] + \left(1-R_n\right) \left[F_{ion-s} v_s \sin\theta \, EXP\left(\frac{-x}{\lambda_2}\right) + \right.$$
$$\left. F_{cx-s}\left(v_s \sin\theta + v_{avg}\right) EXP\left(\frac{-x}{\lambda_4}\right) \right] \qquad (3.38)$$

or in its simplified form (neutral momentum included)

$$S_p \propto R_n v_f \sin\theta \, EXP\left(\frac{-x}{\lambda_1}\right) + \left(1 - R_n\right)v_s \sin\theta \, EXP\left(\frac{-x}{\lambda_2}\right)$$

$$(3.39)$$

where λ_j is the mean free path (MFP) for; fast neutral ionization (j=1); slow neutral ionization (j=2); fast neutral charge exchange (j=3); and slow neutral charge exchange (j=4). Each mean free path is calculated as,

$$\lambda_j = \frac{v_j}{n_{av} <\sigma v>_j \sin\theta} \qquad (3.40)$$

where n_{av} is the average throat to plate density, $<\sigma v>_j$ is the appropriate reaction rate coefficient, and v_j is the particle velocity. The $\sin\theta$ term adjusts the MFP to account for the fact that the integration is being performed along field lines while the particles are assumed to come off the divertor plate perpendicularly.

Given a shape factor, α, the above set of equations can be numerically integrated to give a value for the conduction fraction, μ.

3.5 Evaluation of the Recycling Coefficient

3.5.1 Introduction

The recycling coefficient, R, was defined in Section 3.2 as the fraction of ions hitting the plate that come from the recycling of neutrals. Those neutrals that are not ionized in their first pass through the plasma, but escape to the plenum region of the divertor can eventually meet one of three fates: 1.) return to the plasma and be ionized after scattering around the divertor plenum (the probability that a neutral makes it back through the plasma to the plate , reflects, and escapes again is very small); 2.) be pumped out of the divertor plenum; or 3.) escape out the divertor throat to the core plasma where they are ionized. The contribution of this third channel is small so, to first order, what is not pumped out of the divertor chamber is eventually recycled to the divertor plate. Based on this phenomenological description the global recycling coefficient can be approximated as,

$$R = 1 - \bar{p}f \qquad (3.41)$$

where $\bar{p}$ is the average neutral escape probability (energy group and position averaged) and f is the ratio of neutrals pumped to those reaching the divertor plenum.

For the purposes of this model, the pumped fraction will be varied as a free parameter. One does have some control

over the value of this parameter based on pump speed, geometry of the pump ducts (conductance) and divertor plenum, and plenum wall materials. Calculation of the pumped fraction would be the subject of future study. Thus, the evaluation of R requires the determination of the neutral escape probability, $\bar{p}$.

3.5.2 Calculating the Neutral Escape Probability

The method used to calculate $\bar{p}$ is based on a wedge shaped section of plasma overlying the divertor plate and a simple slab attenuation approach (see Figure 3.3). First the MFP for ionization of a neutral by electron impact is calculated for slow and fast neutrals using

$$\lambda = \frac{v}{n\langle\sigma v\rangle_{ion}} \qquad (3.42)$$

where v is the fast or slow velocity, n is the electron density, and $\langle\sigma v\rangle$ is the combined ground state and excited state electron impact ionization reaction rate coefficient. The MFPs can be calculated using plate or average quantities.

The probability that a neutral of given velocity and angular direction will be ionized after being emitted from a

Figure 3.3   Geometry of Neutral Escape Probability
              Calculation

point on the divertor plate is given by

$$p(x,\phi) = EXP\left(\frac{-1(x,\phi)}{\lambda}\right) \qquad (3.44)$$

where $1(x,\phi)$ is the distance to the plasma surface (beginning of plenum) along the direction ϕ from the point x and λ is the energy/velocity dependent MFP. It should be noted that no particular allowance has been made for the effect of charge exchange events. A similar approach to calulating $\bar{p}$ (reference 3) found that this contribution to $\bar{p}$ is small so it is neglected here.

Several methods for summing these probabilities over all directions and points on the plate have been examined in this thesis. Each has been included in the final divertor model programs as options.

The first method entails calculating an average distance, $\bar{1}(x)$, to the plasma surface for each of a mesh of points on the divertor plate. At each point, 1 is expressed as a function of angle ϕ, point position (x), width of the divertor plate(x_t), and angle of incidence of the field lines to the plate (θ). This function is then integrated between $\phi=o$ and $\phi=ARC$, where ARC is the angle back to the throat of the divertor. Any neutral that is emitted in a direction greater than ARC is assumed to be ionized. This

method gives the following result

$$\bar{l}(x) = \frac{\int_0^{ARC} l(\phi)\,d\phi}{\int_0^{ARC} d\phi} = \frac{TAN\phi(x-x_t)}{ARC} \int_0^{ARC} \frac{d\phi}{ACOS\phi+BSIN\phi}$$

where A is $TAN\theta$ and B is 1.0. The explicit result is,

$$\bar{l}(x) = \frac{TAN\theta \left(x-x_t\right)}{\left(A^2 + B^2\right)^{1/2} ARC} \left\{ ln\left[TAN\tfrac{1}{2}(ARC+\theta)\right] - ln\left[TAN\left(\tfrac{\theta}{2}\right)\right] \right\}$$

$$(3.45)$$

The neutral escape probability for neutrals emitted from a point on the plate is then

$$p(x) = \frac{ARC}{\pi} \left[R_n EXP\left(\frac{-\bar{l}(x)}{\lambda_f}\right) + \left(1-R_n\right) EXP\left(\frac{-\bar{l}(x)}{\lambda_s}\right) \right] \quad (3.46)$$

where λ_f and λ_s are the fast and slow neutral ionization MFPs.

This escape probability is then calculated for a mesh of points along the divertor plate and the average, $\bar{p}$, defined as the global escape probability. The advantage to this

method lies in the fact that the integral used has an explicit solution which speeds calculation for a mesh of points. The disadvantage is that the exponential of an average escape distance is not the same as the integral of the escape probability averaged over all possible directions.

The second method involves numerically evaluating the integral of the escape probability as a function of angle. Thus,

$$p(x) = \int_0^{ARC} EXP\left(\frac{-1(\phi)}{\lambda}\right) \frac{ARC}{\pi} \ d\phi \qquad (3.47)$$

This integral is evaluated for slow and fast neutrals and the escape probability at x calculated as

$$p(x) = R_n p(x)_{fast} + \left(1-R_n\right) p(x)_{slow} \qquad (3.48)$$

Again, this evaluation must be performed for a mesh of points along the plate and the average escape probability, $\bar{p}$, calculated.

Another option included in the divertor model program is an angular probability for reflection in the integral of the second method. Some experiments have found that particle

reflection from a smooth surface was not isotropic for 90° incidence but showed a cosine distribution. Use of this option decreases the escape probability because most of the particles that escape do so by escaping from the tip of the plasma wedge. Weighting the directional escape probabilities with a cosine distribution decreases the contribution of those particles which are emitted in a direction towards this tip.

A program was written to compare the results of each of these methods against one another and against the results in reference 3. A detailed comparison of the three methods (l_{avg}, integral, and integral with a cosine distribution) can be found in Appendix D. Typical results are shown in Figure 3.4, giving the escape probalility as a function of plate position for the integral with cosine method. As seen in this figure, the escape probability increases as the thickness of the plasma overlying the plate decreases (see Figure 3.3 for geometry). Also, it is noted that the escape probability is much less for slow neutrals than for fast neutrals due to their smaller ionization MFP. Below, the results of the three methods are compared to the result of reference 3.

Figure 3.4 Neutral Escape Probability versus Plate Position

Table 3.1
Neutral Escape Probability Comparison

Approach	$\bar{p}$
l_{avg}	.067
integral	.095
integral w/cosine	.074
Ref 3	.077

For these results, plate quantities (T_p and n_p) were used. It is noted that in reference 3 a cosine distribution was employed.

3.6 Helium Effects

The steady state concentration of helium in the core plasma has a great influence on the power output of the reactor. Additionally, helium in the divertor can significantly increase the sputtering of the divertor plate and increase radiative cooling of the divertor plasma. The concentration in the core plasma and in the divertor is a function of the helium-ash removal rate from the divertor. Helium ions flow with the plasma into the divertor and impact the divertor plate where they are neutralized (some

may become permanently implanted) and return to the divertor plasma. Just as with D-T neutrals, some of the helium neutrals will be ionized and recycled to the plate while others will escape to the divertor plenum and may be pumped or return to the plasma to be ionized. Analogous to the D-T recycling coefficient, a global helium recycling coefficient can be defined as

$$R_{He} = 1 - \bar{p}_{He} f_{He} \qquad (3.49)$$

where $\bar{p}_{He}$ is the average helium neutral escape probability and f_{He} is the helium pumping probability. This pumping probability, f_{He}, may differ from the D-T pumping probability depending on pump type, plenum and duct configuration, and neutral particle (D-T or He) energy distribution. Just as with the pumping probability for D-T, f_{He} is also varied as a free parameter in the divertor model code. The escape probability for helium can be calculated using the same equations presented in section 3.5 by replacing the D-T ionization rate coefficient with the helium ionization rate coefficient.

The helium ions which originally enter the divertor are normally in the +2 charge state. The recycled helium ions, however, can be in charge state +1 or +2. This distribution of charge states will have an impact on the concentration of

helium at the plate and on the sputtering of the plate due to the sheath potential. The probability, P_{12}, that a singly charged helium ion will be ionized to the +2 state can be estimated as[3]

$$P_{12} = 1 - \text{EXP}\left(\frac{-t_{res}}{\tau_i}\right) \tag{3.50}$$

where t_{res} is the residence time of the He^+ ion in the divertor, and τ_i ($\sim 3 \times 10^{-5}$ sec) is a characteristic time for the ionization step He^+ to He^{++}.

An upper limit on this residence time can be obtained by neglecting the effects of local electric fields and expressing it as

$$t_{res} = t_t + t_{drift} \tag{3.51}$$

where t_t is a thermal equilibration time ($\sim 10^{-5}$ sec) for ion-ion collisions and t_{drift} is the ion drift time at the fluid velocity (assumed to be the plate sound speed, C_p) and is estimated as

$$t_{drift} = \frac{MFP_{ion}}{C_p} \qquad (3.52)$$

The ionization probability, P_{12}, can be used to estimate the fractional concentration of helium at the divertor plate. At steady state, the helium which enters the divertor must be equal to the helium pumped. This condition can be expressed as

$$\xi_{He}(t)\Gamma_t = \xi_{He}(p)\Gamma_p(1-R_{He}) \qquad (3.53)$$

where ξ_{He} is the fractional concentration of helium (singly and doubly charged) relative to the electron density and $\Gamma_{t,p}$ is the electron flux at the throat/plate.

The helium concentration at the throat is normally taken to be the core plasma concentration. The D-T ion flux at both locations, throat and plate, is less than the electron flux due to the presence of helium. At the throat

$$\Gamma_{t,D-T} = n_e\left(1 - 2\ \xi_{He}(t)\right)C_t \overline{m}_t \qquad (3.54)$$

and at the plate

$$\Gamma_{p,D-T} = n_e\left[1 - \left(1 + P_{12}\right)\xi_{He}(p)\right]C_p \qquad (3.55)$$

So, at the plate, part of the D-T ion flux is replaced by helium flux which will increase sputtering due to its greater mass and possible +2 charge state.

The exhaust performance of the divertor can be characterized in terms of the helium enrichment factor, ε, expressed as

$$\varepsilon = \frac{\Gamma_{He}(pump)/\ \Gamma_{D-T}(pump)}{\Gamma_{He}(t)\ /\ \Gamma_{D-T}(t)} \qquad (3.56)$$

or expressed in the quantities defined above

$$\varepsilon = \frac{\left(1-R_{He}\right)\xi_{He}(p)}{\left(1-R\right)\left[1 - \left(1 + P_{12}\right)\xi_{He}(p)\right]} \cdot \frac{\left(1 - 2\xi_{He}(t)\right)}{\xi_{He}(t)}$$

In addition to causing a fuel depletion effect and increased sputtering, the helium which is recycled in the divertor can add to the radiation energy losses, cooling the plasma. In the present calculations this radiation component has been estimated as

$$\chi_{He}(ev) = 15 + P_{12}\left(70 + \frac{3300}{T_e}\right) \qquad (3.57)$$

where χ_{He} is the energy loss per ionized helium particle and T_e is the local electron temperature. The 15 eV term corresponds to the energy loss in going from He^0 to He^+, while the remainder of the χ_{He} expression is for ionization to He^{++}. The energy loss in the divertor plasma due to helium recycling (to be added to equation (3.31)) is

$$P_{Rad-He}(eV) = n_p v_p \xi_{He}(p) \chi_{He} R_{He} \qquad (3.58)$$

Any charge exchange component to this energy loss has been neglected.

3.7 Sputtering

One of the critical concerns in designing a divertor is the sputtering rate of the target plate material. This rate will determine the service lifetime of the plate, and as noted in Chapter 2, impurity production can have a great impact on the viability of the divertor design. Once the plasma model has determined the plate temperature and density (with an estimated impurity increment), these parameters can be used to estimate the plate sputtering.

Some iterative process might be necessary to make the result self-consistent.

The sputtering rate (including self sputtering) at a point on the target plate, as expressed in Chapter 2, is

$$R_e = \Gamma_p Y \left(\frac{1}{1-fY_s} \right)$$

where Γ_p is a particle flux at a point on the plate, Y is the sputtering yield for the particular particle (incident energy and plate material dependent), Y_s is the self sputtering yield, and f is the fraction of impurities returned to the plate. The above equation is valid for $fY_s < 1$.

The sputtering yields can be determined using a sputtering model by Smith et al[21] which can be expressed as

$$Y(E_o) = \frac{C}{40} z_1^{.75} \left(z_2 - 1.8 \right)^2 \left(\frac{M_1 - .8}{M_2} \right) \frac{E_o - E_{th}}{\left(E_o - E_{th} + 50 z_1^{.75} z_2 \right)^2}$$

$$(3.59)$$

where

     C   = 2000 for incident hydrogen (^{1}H)
              = 400 for all other particles

Z_1 = atomic number of incident particle

Z_2 = atomic number of plate material

M_1 = mass number of incident particle

M_2 = mass number of plate material

E_O = incident particle energy (eV)

E_{th} = threshold energy for sputtering (eV)

The threshold energy for sputtering is given by

$$E_{th} = \frac{\left(4M_1 + M_2\right)^2}{4\, M_1 M_2}\, U_O \qquad (3.60)$$

where U_O is the binding energy of the plate material (eV). Appendix A includes a table of values for Z, M, and U_O for various plate materials.

The incident energy of particles impacting the plate can be expressed as a function of the sheath energy transmission coefficients. Thus,

$$E_O = r_p \left(E_p + ZT_p(\gamma_i - 2) \right) \qquad (3.61)$$

where E_p is the energy of the particles prior to sheath acceleration (which has a Maxwell-Boltzmann distribution at the plate), T_p is the electron temperature at the plate, and

Z is the charge of the particle.

If the temperature of the plasma is well above the sputtering threshold, then $E_p = 2T_p$ can be used,[3] and evaluating the sputtering is very straight-forward. In most instances, though, the plate temperature is less than the sputtering threshold. However, this does not imply that there is no sputtering. Particles in the high temperature tail of the Maxwell-Boltzmann distribution may still cause sputtering. Therefore, the calculation of the sputtering rate must take account of this particle distribution. Thus,

$$R_e = \Gamma_p \left(\frac{1}{1-fY_s} \right) \cdot \int_{E'}^{\infty} P(E) Y(E_o) dE \qquad (3.62)$$

where P(E) is the Maxwell-Boltzmann distribution

$$P(E) = \left(\frac{E}{T_p} \right)^{1/2} EXP \left(\frac{-E}{T_p} \right)$$

and E' is the particle energy at which $E_o = E_{th}$

$$E' = E_{th}/r_p - ZT_p(\gamma_i - 2)$$

Equation (3.62) can be numerically integrated to give the

sputtering rate.

The sputtering rate can be converted to an erosion rate (cm/yr, 100% duty) by dividing R_e by the plate material number density (cm^{-3}) and multiplying by the number of seconds in a year

$$d_e(cm/yr) = \frac{R_e}{\rho} \cdot 3.15 \times 10^7 \qquad (3.63)$$

The code for the divertor model includes a subroutine which calculates sputtering of the target plate due to deuterium, tritium, and helium (+1 and +2). An assumption necessary to implement this model is that sputtered plate material atoms return to the plate in the +1 charge state. The erosion and sputtering rates are calculated at each of 50 points across the divertor plate and the peak erosion rate outputed, along with the total impurity production rate per length of divertor.

3.8 Impacts of Radial Variations

The simplication of the fluid equations to consider only the axial direction introduces certain inaccuracies in calculating neutral escape probabilites and plate sputtering. These quantities are sensitive to the plate

density and temperaure. Use of the axial approximation makes it necessary to assume a constant plasma density and temperature across the divertor plate. To remedy this a literature search was conducted to determine how to introduce radial variation of these parameters into the divertor model.

The results of most models[9,13,17,18,19,20] show that radial density and temperature profiles are approximately exponential in both the upstream region (throat and beyond), and in the downstream region (in the divertor) and can be expressed as

$$P(r) = P_o \, EXP\left(\frac{-r}{\lambda_a}\right) \qquad (3.64)$$

where P is the parameter of interest (T or n), and λ_a is the fall-off distance for that parameter.

For density, the fall-off distance can be approximated as

$$\lambda_n = \left(D \, \tau_\|\right)^{1/2} \qquad (3.65)$$

where D is the radial diffusion coefficient (m^2/sec) (in this work experimental values have been used) and $\tau_\|$ is a characteristic transport time, approximated as

$$\tau_{\parallel} = \frac{L}{v} \qquad\qquad (3.66)$$

where L is a connection length in the region for which λ_n is being calculated, and v is an average fluid velocity in the region.

For λ_n at the target plate, L is the divertor connection length, L_d, and v is the sound speed at the plate (even though the mach number at the throat is normally small, the sound speed is large, so C_p represents a reasonable average).

The temperature fall off distance is more difficult to calculate and has been modeled many different ways. In reference 17 the ratio λ_T/λ_n was found to be an increasing function of $\chi_{\perp}/D$ and a decreasing function of the sheath energy transmission factor. Rather than attempt to calculate λ_T, the ratio λ_T/λ_n can be varied as a free parameter, A.

To test the validity of using exponential profiles for the temperature and density at the plate a separate program was written which evaluated these profiles in the pressure balance equation derived from the continuity and momentum fluid equations,

$$n_t T_t \left(1 + r_t\right)\left(1 + \tilde{m}_t{}^2\right) = 2\, n_p T_p \left(1 + r_p\right) \qquad (3.67)$$

On the basis of this investigation, it was concluded that the pressure balance equation could be satisfied radially with exponential profiles for density and temperature. In the computer model λ_n at the plate is calculated and A is an input parameter. The radial profiles for temperature and density have been added to the calculations of the recycling coefficient (including weighting each escape probability along the plate by the flux incident at that point) and sputtering rate.

CHAPTER 4

DESCRIPTION OF THE COMPUTER MODEL

To yield results, the divertor model described in Chapter 3 must be implemented on a computer using various numerical computing techniques to solve for the parameters of interest. Section 4.1 of this chapter discusses the possible solution techniques and the rationale for the selection of a fixed-point iteration approach. Section 4.2 then describes the implemented model code, DIV, in detail including; program logic and structure, data input requirements, and program output.

4.1 Discussion of Numerical Solution Techniques

Solution of the model equations given in the previous chapter involves the simultaneous solution of a system of nonlinear equations. There are several techniques that can be used to solve such a system. The first is a straight forward fixed-point iteration approach. The advantage to this method is the simplicity of implementation. While the convergence of this method is only linear to super-linear (better than linear, less than quadratic), the final solution set need not be accurate to greater than about 1% since the model is only an approximation. Given a good set

of initial guesses for the solution variables, the only concern would be the stability of the solution. The disadvantage to this method is the requirement for good initial guesses. If the initial guesses are too far from the solution values, then the results might diverge, or converge to an unstable set.

Other more sophisticated methods are based on Newton-Raphson approaches which require the evaluation or estimation (via the secant method) of the partial derivatives of the equation set . These methods involve the use of matrix operations to solve the system of equations. Such methods will normally converge more quickly than the fixed-point method (quadratic convergence) and can be written in ways to increase the chance for convergence even with poor initial guesses. However, this increase in "power" is bought at the cost of much increased complexity and computing time. Reference 5 used a software package program, HYBRID, to solve a set of model equations. Solution of this similar set required .2 seconds of Cray computer time. For the model described in this thesis, a fixed point iteration approach with some improvements has been adopted.

4.2   Computer Model DIV Description

The computer model DIV, written in IBM Fortran for an IBM-PC/AT (or compatible), uses a fixed point iteration routine to solve the model equations for the plate density and temperature, and the throat temperature using the following fixed-point equations:

$$n_p = \left[\left(\frac{n_p}{n_{\nabla T}} \right)^{7/3} + 1 \right]^{2/7} \left[\frac{n_t \left(1 + r_t \right) \left(1 + \bar{m}_t^2 \right)}{\left(2 + \bar{V}R \right) \left(1 + r_p \right)} \right] \quad (4.1)$$

derived from equation (3.20),

$$T_p = \left[\left(Q_t - \int_p^t S_e \, dx \right) \frac{M^{1/2} \left(\gamma_e + r_p \gamma_i \right)}{n_p \left(1 + r_p \right)^{1/2}} \right]^{2/3} \quad (4.2)$$

derived from equation (3.8), and

$$T_t = \frac{\left(2 + \bar{V}R \right) \left(1 + r_p \right) T_p n_p}{\left(1 + \bar{m}_t^2 \right) \left(1 + r_t \right) n_t} \quad (4.3)$$

derived from equation (3.19)

The throat density is held constant.

Input for the code (Table 4.1) requires starting values for n_p, T_p, and T_t. The user has the option of specifying the recycling coefficient, R, and/or the conduction

Table 4.1

Program DIV Input

Inputs	Definition	Units
QT	Power flux into the divertor	W/m^2
LD	Divertor connection length	m
M	D-T ion mass	amu
XT	Divertor plate width	m
THETA	Angle of incidence of magnetic field lines to the divertor plate	radians
EL	D-T reflection coefficient reduced energy	
TP	Plate electron temperature	eV
TT	Throat electron temperature	eV
NP	Plate electron density	$x10^{19}m^{-3}$
NT	Throat electron density	$x10^{19}m^{-3}$
RP	Plate ion to electron temperature ratio	
RT	Throat ion to electron temperature ratio	
G1	Electron sheath energy transmission coefficient	
G2	Ion sheath energy transmission coefficient	
R	Recycling coefficient	

Table 4.1 cont.

Input	Definition	Units
U	Conduction fraction	
F	D-T pump fraction	
IMP	Impurity increment	
D	Radial diffusion coefficient	m^2/sec
A	Temperature to density fall-off distance ratio	
CT	Fractional concentration of helium at the throat	
FHE	Helium pump fraction	
ELH	Helium reflection coefficient reduced energy	
SHP	Shape factor, α, for the conduction fraction	
METH	Method for $\bar{p}$ calculation 1=Lavg 2=integral	
DIST	Distribution for $\bar{p}$ calculation 1=none 2=cosine	
TOL	Convergence tolerance	
SOR	Over or under relaxation constant	

fraction, μ, (which will then be held constant) and of setting the momentum source term equal to zero. Otherwise these variables will be calculated. Most of the variables inputed are known quantities or can be calculated using methods presented in Appendices A and C. Others, such as the ion to electron temperature ratios and pump fractions, can be estimated from the results of other models or experiments. The only parameter for which there is no physical or calculational basis is the shape factor, α, used in calculating the conduction fraction. However, experience with the code has shown the final solution set to be insensitive to the value of α except for very low recycling cases.

After the initial data entry, the program (see flowchart of Figure 4.1) first calculates initial and intermediate quantities, such as $\dot{m}_t$, μ, R, and $\overline{V}$, based on the initial values for T_p, n_p, and T_t. The program then calculates the first of the fixed point parameters, applies successive over or under relaxation,

$$A'_{n+1} = SOR\left(A_{n+1}\right) + \left(1-SOR\right)A_n \qquad (4.4)$$

where A' is the relaxed variable and SOR is the over/under relaxation constant, and then updates the intermediate

Figure 4.1   Program DIV Flowchart

variables prior to calculating the next fixed point parameter (a la Gauss Seidel). This relaxation method was added to the fixed point routine to preclude wide oscillations (if SOR <1 is used) or to speed convergence (if SOR >1 is used) of the iterations.

The newly calculated value for the plate density is then compared to the old value using a relative error check for convergence (the user specifies the tolerance). The plate density was chosen as the convergence parameter because its equation includes information from all three fluid equations and, by practice, was found to be the most difficult parameter to get to converge. If the convergence criterion is met, then the program recalculates the intermediate parameters based on the solution set and displays this set and the intermediate parameters (Table 4.2). If the criterion is not met, then the program loops back to start another iteration. After each iteration is complete the most current values for the fixed-point parameters are displayed on the screen so the user can observe if the results are converging or diverging. After ten iterations with no convergence the user is prompted to continue or stop iterations and return to data entry. If convergence is achieved, the user is asked if sputtering should be calculated. Sputtering calculations require additional data entry (Table 4.3). The sputtering subroutine canalso be

Table 4.2

Program DIV Output

Output	Definition	Units
TP	Plate temperature	eV
NP	Plate density	$m^{-3} x 10^{-19}$
TT	Throat temperature	eV
NT	Throat density	$m^{-3} x 10^{-19}$
MT	Throat mach number	
U	Conduction fraction	
ISE	Radiation loss fraction	
R	Recycling coefficient	
CP	Fractional helium at the plate	
HER	Helium enrichment	
P12	Ionization probability of $He^{+} \rightarrow He^{++}$	
LNP	Density fall distance at the plate, λ_n	

directly accessed after the initial data entry, bypassing the divertor calculations.

An extensive number of runs with the DIV code for a variety of input data has allowed the inclusion of a number of error checks in the program to stop execution of the code if certain parameters are diverging. This has eliminated most realtime fatal errors. Appendix B includes a complete

Table 4.3

Sputtering Input Data

Input	Definition	Units
UO	Plate material binding energy	eV
Z3	Plate material atomic number	
M3	Plate material mass number	
NM	Plate material number density	$cm^{-3}x10^{-24}$
IE	Multiple of TP for upper limit to maxwell-boltzmann integration	

listing of the DIV computer code. It also has a description of each of the subroutines displayed in Figure 4.1.

CHAPTER 5

BENCHMARKING THE DIVERTOR MODEL

5.1 Introduction

As stated in Chapter 1, the goal of this research is to produce a simple, comprehensive, and accurate model of the divertor region. The requirements to limit the complexity of the model and to include all key processes have been met as described in Chapters 3 and 4. How close the model has come to satisfying the third requirement, accuracy (i.e. to yield results comparable to those of more sophisticated models), will now be discussed. In this chapter the computer code DIV is benchmarked against four other models: a model by the JAERI team[22], the Harrison et al model[3], the ZEPHYR code[4], and the Braam's code[9]. The results displayed in the comparison tables reflect only the parameters reported by each of these codes which are also calculated by DIV. Complete data input and output for each benchmark case can be found in Appendix E.

5.2 JAERI Team Model Benchmark

This model is a one fluid, 1D (axial) plasma edge model which includes remote radiative cooling, recycling, and

particle shielding at the main plasma surface. The particle, momentum, and energy source terms are evaluated by a neutral transport code. In reference 22 the code is described, and results for modeling of Doublet III compared (favorably) to experimental results. To obtain the DIV results listed in Table 5.1 the following assumptions were made: the momentum source term was set to zero, and the radiative power loss was artificially increased (by making IMP=1.45) to mimic the oxygen impurity radiation included in the JAERI calculations. Additionally, the recycling coefficient was calculated, in the absence of any divertor plate data, by assuming a plate width of .25 m and a theta of .35 radians. The pump fraction, f, was arrived at by back-calculation using the reported recycling coefficient and divertor plasma results. The remainder of the input data for DIV was the same as that used by the JAERI team for its results. The results of this comparison are listed in Table 5.1.

Table 5.1
JAERI Team Benchmark Case

Parameter	JAERI Team	DIV
T_p(eV)	4.0	3.8
n_p($\times 10^{19}$ m^{-3})	9.1	9.2
T_t(eV)	37.0	35.0
n_t($\times 10^{19}$ m^{-3})	1.8	1.8
Throat Mach Number, $\bar{M}_t$	.26	.34
Radiation fraction	.50	.51
Recycling Coefficient, R	.81	.80

The results of Table 5.1 indicate that DIV compares extremely well with the JAERI team model. The largest deviation in any fixed point parameter is less than 6%. The sensitivity of these results to changes in impurity radiation and the shape factor was also examined. A 5% increase in the impurity increment, increasing the radiation fraction by a like amount, caused about a 20% decrease in T_p and a corresponding increase in n_p. Variation of the shape factor, α, from 3 to 4, caused a 15% change in n_p and T_p. Both these sensitivities were expected. Experience with the DIV code has shown that T_p becomes more sensitive to the

impurity increment as the impurity fraction increases. In this case, the radiation fraction, is fairly large (~.5). Alternatively, it has been found that sensitivity to the shape factor decreases as the recycling coefficient increases (or as the conduction fraction increases). The recyling coefficient for this case, .81, is rather low, correlating to the sensitivity to the shape factor observed.

5.3   Harrison, et al Model Benchmark

This model is also 1D and one fluid. It includes neutral particle transport, remote radiation cooling, helium effects, and impurity radiation.   The data and results presented in reference 3 are for INTOR under "standard conditions".   One of this model's assumptions is that electron conduction is the only energy transport mechanism. The modeling assumptions for DIV in this case were that impurity radiation was zero (it was found to be negligible in reference 3) and the momentum source term was equal to zero.   Table 5.2 gives the results of this comparison.

Table 5.2
Harrison et al Model Benchmark Case

Parameter	Reference 3	DIV
T_p(eV)	25.5	23.8
n_p($\times 10^{19}$ m^{-3})	9.6	9.2
T_t(eV)	66.0	63.0
n_t($\times 10^{19}$ m^{-3})	6.97	6.97
Conduction Fraction, μ	1.00	.99
Radiation Fraction	.13	.16
Helium Enrichment, ε	3.18	2.23
Recycling Coeffient, R	.99	.99
Plate Helium Concentration	.05	.025

The DIV results compare very well with the Harrison et al results. The largest deviation of any of the parameters is for the radiation fraction (23%) and the helium enrichment (30%), but the deviation for the parameters of most interest, T_p and n_p, is less than 7%. One difference between the two models is that the Harrison model assumes that the concentration of helium at the plate is the same as the concentration in the core plasma while DIV calculates

this quantity. This difference was accounted for in the calculation of the helium enrichment but was not sufficient to account for the difference in values of the helium enrichment. Some additional runs were made to try to make the two radiation fractions equal by adjusting the impurity increment. Setting the impurity increment (IMP) equal to .85 (from an initial value of 1.0) succeeded in matching these parameters, but increased the plate temperature slightly and decreased the plate density. However, there appears to be no physical basis on which to decrement the D-T radiation value.

The results above were found to be fairly sensitive to the energy transmission factors (γ_i and γ_e). An increase in both of about 20% caused a 28% decrease in T_p and a 39% increase in n_p. The percentage changes and the directions of the changes were reversed for a 20% decrease in the energy transmission factors. The results were also found to be insensitive to the shape factor due to the large recycling coefficient and conduction fraction.

5.4 ZEPHYR Benchmark

ZEPHYR is an axial 1D, two fluid numerical divertor model developed at Culham laboratories. It includes: a simple 1D neutral model; neutral recycling; D-T radiation; particle

and energy convection; fluid viscosity; and electron/ion equipartition. It solves the fluid equations along field lines between a symmetry point and the divertor plate. The results presented in reference 4 are for an INTOR-like device. The specific results to which DIV is compared is the "Search 13A" case (one of the many results in this parametric study). The only assumption made to benchmark against this case was to set the momentum source term equal to zero. The input data values for DIV were, for the most part, all taken from the reported ZEPHYR input or ZEPHYR results (such as ion to electron temperature ratios and Q_t value). The recycling coefficient was set to the .471 value used by ZEPHYR. Benchmarking for the pump fraction value, as was done for the JAERI case, yielded a pump fraction greater than 1.0 (an impossibility). Therefore, iterative calculation of the recycling coeffcient was not possible. This benchmarking result indicates a significant difference between the neutral particle models of the two divertor models. It should be noted that the reported recycling coefficient for this case, .471, is extremely low considering the reported plate temperature (10.8 eV) and density (8.6×10^{19} m^{-3}). One final note is that helium effects were neglected. Table 5.3 displays the comparison to the ZEPHYR results.

TABLE 5.3
ZEPHYR Benchmark Case

Parameter	ZEPHYR	DIV
$T_p(eV)$	10.8	10.5
$n_p(x10^{19} \ m^{-3})$	8.6	8.68
$T_t(eV)$	26.7	28.0
$n_t(x10^{19} \ m^{-3})$	3.66	3.66
Throat Mach Number, $\bar{m}_t$	.73	.70
Radiation Fraction	.15	.16
Recycling Coefficient, R	.471	.471

The largest deviation from the ZEPHYR values was in the radiation fraction which was only 8% different. As expected, the DIV results were somewhat sensitive to the shape factor due to the low value of the conduction fraction ($\sim.14$). The results above are for $\alpha=5$. Changing this to $\alpha=6$ caused T_p/n_p to increase/decrease by about 6%. A similar sensitivity was arrived at when the shape factor was decreased to a value of 4. The results are also very sensitive to changes in the sheath energy transmission factors (though the values used for the results above were

the same as those used in reference 4). A 10% increase in the radiation fraction (by setting IMP=1.1) had only a slight effect on the temperature and density at the plate (≤6%). Because the radiation fraction is only 15% in this case, radiative cooling does not play an important role in determining the plate conditions.

5.5 Braam's Code Benchmark

This model solves the Braginskii fluid equations for electrons and ions in two dimensions (axially and radially) from a symmetry point (between divertors) to the divertor plates. The code includes particle/energy convection, viscosity, equipartition, axial variation in the radial thickness of the edge plasma (i.e. cross-sectional area), radiation, and helium effects. The results of this model, reported in the NET Report #50, reference 9, are for a NET/INTOR-like device for both the inner and outer divertor plates. In doing this benchmark case it was necessary to convert the radial results for temperature and density into average values at the plate and throat for both data input and comparison. The modeling assumptions made include: the momentum source term is zero, and the pump fractions for D-T and helium are the same. Another inherent assumption in this approach is that the average values themselves

represent a solution to the fluid equations. Some of the specific input data requirements had to be satisfied using the calculational methods of Appendix C. The pump fractions were back-calculated as described in Section 5.2, using the plate data given in the NET report. Table 5.4 reports the results of this comparison.

Table 5.4
NET Report #50 (outer target) Benchmark

Parameter	Report #50	DIV
T_p(eV)	7.6	11.0
n_p($\times 10^{19}$ m^{-3})	14.0	13.4
T_t(eV)	67.3	64.8
n_t($\times 10^{19}$ m^{-3})	5.0	5.0
Radiation Fraction	.17	.21
Recycling Coefficient,R	.998	.998
Plate Helium Concentration	.011	.025
Helium Enrichment,ε	1.0	.99

The plate temperature for this case is 45% higher than it should be and the plate concentration of helium is more than twice the Report #50 value. Additionally, the radiation

fraction is somewhat high (which makes this an unlikely candidate for lowering T_p). Numerous runs were made in an attempt to improve the results with no success. The conclusion arrived at is that the assumption, that average values represent a solution, may in fact not be valid. The disperity between the two reported helium plate concentrations may be due to the assumption the $f_{He}=f_{D-T}$ used in DIV. In some other models the pump fraction for helium is larger than that for D-T. This would tend to decrease the plate concentration bringing it closer to the Report #50 value.

The results tended to be sensitive to the sheath energy transmission factors. As expected, the results were insensitive to the shape factor (R was large) and the radiation fraction (which was low, ~21%).

5.6 Benchmarking Conclusions

In general, the divertor model DIV yields very good results when compared to other 1D axial models. Some problems arise, due to the average value assumption, when comparison is made to a 2D model. The sensitivity of the results to three input parameters, the shape factor, energy transmission factors, and radiation fraction (via the impurity increment), was examined and qualitative

dependencies identified as listed in Table 5.5 and discussed below. The most sensitive of these three parameters was the

---

Table 5.5
Parameter Sensitivities

	Sensitivity of T_p and n_p	
Parameter	Small	Large
Sheath Energy Transmission Factors, γ_i and γ_e	–	Always
Impurity Increment, IMP	If radiation fraction is small	If radiation fraction is large
Shape Factor, α	If R or μ is large	If R or μ is small

---

sheath energy transmission factors which directly control the rate at which energy can be exhausted to the divertor plate. Any increase in these factors will decrease the plate temperature, and increase the plate density. The next most sensitive parameter was the radiation fraction. This quantity could be adjusted using the impurity increment. The greatest sensitivity was found when the impurity fraction was high. This observation implies that the final plate temperature is very dependent on the total power lost by radiative processes. When the radiation fraction is low,

the sensitivity is much decreased. Finally, the sensitivity to the shape factor was found to be a function of the recycling coefficient. As R increases, the mach number at the throat decreases, decreasing the fluid flow velocity, and thereby, energy convection. This forces the conduction fraction to increase. As μ increases it becomes less sensitive to the shape factor. In general, an increase in the shape factor would independently decrease the conduction fraction, but the interplay with the other variables tends to make the net effect an increase in μ.

Several other comments are warrented as a result of the benchmarking and other program runs. The pressure at the divertor plate ($\propto n_p T_p$) is ultimately determined by the energy flux (Q_t) into the divertor. The effect of the sheath energy transmission factors and radiation fraction is only to alter the relative value of these parameters, not their product. This implies that there is only so much that can be done with the injection of impurities to reduce heat deposition and sputtering. This impurity injection approach, though, sensitizes the plate density and temperature to changes in the magnitude of the radiation fraction. Any mechanism which might cause fluctuations in the amount of radiation produced in the divertor (such as flow reversal) will cause wide variation in plate density and temperature.

Another comment concerns the inclusion of the the calculation of R in the program. The ability to allow R to vary as the program iterates has improved the convergence characteristics of the numerical techniques used and gives a more self-consistent final solution. It also appears that the low recycling regime is not accessible for some combinations of input data. In most cases, if the initial guesses for the fixed-point parameters were poor the program tended to move towards the high recycling regime. Whether this indicates a greater amount of stability for this regime, or is just a numerical quirk is not known.

Finally, a few comments about sensitivities, other than those noted in the benchmarking section, are warranted. In most cases the results of a converged run are sensitive to the throat density, n_t. As n_t increases, the plate density will increase, with a corresponding decrease in plate temperature (this is with Q_t constant). An increase in Q_t tends to increase the plate temperature. The response of the radiation energy loss mechanisms is normally not great enough to compensate for an increase in the energy flux, so the plate temperature must increase to reflect the greater amount of energy that much be exhausted to the divertor plate.

CHAPTER 6

SUMMARY, CONCLUSIONS, AND FUTURE WORK

6.1 Motivation and Objective

If fusion by magnetic confinement is ever to become a viable energy source, the problems associated with impurity production and exhaust must be solved. The divertor concept represents an attractive solution to these problems by exhausting D-T particles and helium-ash into a separate chamber, away from the core plasma, where they can be impacted on a target plate, neutralized, and pumped out of the reactor. The performance of a given divertor design, though, can presently, only be assessed with the use of plasma edge models. Expensive experimentation must eventually be performed to verify the results of these models.

The modeling itself is a complex process both because it involves a strong coupling between numerous reactor systems (core plasma, first wall, divertor, pumping, etc..) and because the fluid equations used are highly nonlinear. Some models oversimplify both the equations and processes included in order to obtain analytical expressions. While some of these simple models can identify certain dependencies, they do not yield quantitatively accurate

results. Other models attempt to include all the physics
and solve the fluid equations in two dimensions (axially and
radially) resulting in computer codes which are highly
numerical and complex. The objective of this thesis has
been to develop a simple, comprehensive, model of the
divertor region that is highly usable and gives
quantitatively accurate results.

The approach has been to solve the fluid equations in the
axial direction (along field lines) with a two point
technique in which only throat and plate quantities are of
interest. This allows the particle, momentum, and energy
source terms to be evaluated globally, simplifying their
calculation. This approach has also limited the complexity
of the numerical techniques needed to solve for the
parameters of interest. The model includes the key
processes of: neutral recycling; impurity production and
radiation; remote radiation cooling; neutral pumping;
particle convection; helium effects; and the effects of
divertor geometry and plate material. Neutral particle
modeling was accomplished using a simple model of a wedge-
shaped section of plasma overlying the divertor plate, and a
simple slab attenuation model. Additionally, a simple
exponential radial profile was introduced for the plate
temperature and density to make the calculations of neutral
recycling and sputtering more realistic. Implementation of

the model was accomplished in Fortran on a PC to make the code highly "usable" and responsive. The numerical techniques used to solve for the plate temperature and density, and the throat temperature were a fixed-point iteration routine with Gauss-Seidel updating and successive over-relaxation. Convergence with this method is fairly quick, usually requiring less than twenty iterations. The quality of the results was examined using a series of benchmarking cases, as discussed next.

6.2 Benchmarking Results

The divertor model code, DIV, was benchmarked against four other divertor models. The results of the benchmarking validated the approach taken in this research. DIV compares extremely well with the three 1D (axial) divertor models examined. The largest deviation in any of the fixed point parameters (T_p, n_p, and T_t) was less than 8%. Comparison with the results of a 2D model was less successful but not poor. One explanation for this might be that the assumption, that averages of the radial solutions of the 2D model represent an axial solution, is not valid. The sensitivity of the results to variations in a variety of parameters was examined and qualitative dependencies identified. The only input parameter which cannot be

calculated or evaluated beforehand is the shape factor used in the calculation of the conduction fraction. However, at the high recycling regimes anticipated for effective divertor operation, the results become insensitive to the value of this parameter.

6.3 Applications

The inclusion of all key processes and the interactive calculation of the recycling coefficient, helium concentration, and divertor plasma parameters, along with its PC implementation, makes DIV especially useful for conducting parametric studies of divertor designs. Once plasma results are generated, they can be input into the sputtering module to evaluate erosion rates and impurity production. Additionally, the ability to input different materials in both the divertor code and sputtering module allows for self-consistent assessments of divertor material options.

Another versatility of DIV is the variety of allowable inputs to the code which makes it possible to match other model results. Once a given model's results are matched, the effect of slight changes to the original design or input can be determined quickly.

6.4   Future Work

In conducting the research and in development of the model, certain information was found to be lacking in the literature, and certain expediencies had to be adopted. These deficiencies represent avenues for future work, as noted below.

1. Noncoronal equilibrium impurity radiation data is nonexistent. The timescale for the return of impurities to the divertor plate is smaller than that for the onset of coronal equilibrium, invalidating the coronal equilibrium assumption made by some models. There appears to be little definitive work on noncoronal equilibrium radiation. This gap has made it impossible to link the sputtering rate at the plate to the impurity radiation.

2. Some of the input data for DIV could be calculated by the program rather than calculated off-line as done now. These might include the energy flux to the divertor (Q_t) and the sheath energy transmission factors.

3.   The present model does not allow for a variation
       in the cross-sectional area of the plasma as it
       flows to the plate. This variation could have a
       significant impact on the heat deposition on the
       plate. Such an improvement would allow for a
       more realistic magnetic field line topology at
       the plate rather than the simple topology currently
       used.

4.   Models for the D-T and helium pump fractions
       (f and f_{He}) would make the final divertor
       solutions more self-consistent and increase
       accuracy in calculating the recycling
       coefficient and helium enrichment.

5.   An investigation of flow reversal and its impact
       on divertor operations would be desireable.
       Flow reversal has been identified as occuring
       when the local recycling coefficient is greater
       than 1.0.[23] The escape of divertor impurities
       into the main plasma made possible by this flow
       reversal could make operation of the divertor
       in the high recycling regime undesireable.

LITERATURE CITED

1.   S.I. Braginskii, Reviews of Plasma Physics vol. 1, ed. M.A. Leontovich, Consultants Bureau, N.Y.,205 (1965).

2.   M.A. Mahdavi et al., "A Reviewnof the Recent Expanded Boundary Divertor Experiments in the Doublet III Device," Journal of Nuclear Materials 111 & 112, 355 (1982).

3.   M.F.A. Harrison et al., "Plasma Characteristics and Gas Transport in the Single-null Poloidal Divertor of the International Tokamak Reactor," Nuclear Technology/Fusion, vol. 3, 432 (1983).

4.   P.J. Harbour et al., "Models and Codes for the Plasma Edge Region," CLM-RR/E4/3, Culham Laboratory, Oxfordshire, England, (December, 1982).

5.   J.D. Galambos and Y-K. M. Peng, " Two Point Model for Divertor Transport," ORNL/FEDC-83/14, Fusion Engineering Design Center, Oak Ridge National Laboratory, (April, 1984).

6.   J.D. Galambos ,Y-K. M. Peng, D. Heifetz, " Coupled Plasma-Neutral Transport Model for the Scrape-off Region," ORNL/FEDC-84/6, Fusion Engineering Design Center, Oak Ridge National Laboratory, (March, 1985).

7.   A.K. Prinja and R.W. Conn, " An Axially Averaged-Radial Transport Model of Tokamak Edge Plasmas," Journal of Nuclear Materials 128 & 129, 135 (1984).

8.   D.E. Post and R.F. Mattas, " Impurity Control Systems for Reactor Experiments," pp1101-1147, Physics of Plasma-wall Interactions in Controlled Fusion, Plenum Press, N.Y. (1986).

9.   M.F.A. Harrison and E.S. Hotson, " Plasma Edge Physics for NET/INTOR," NET Report #50, (December, 1985).

10. B.J. Braams, "11th European Conference on Controlled Fusion and Plasma Physics," EPS 7D, Part II, p431., Aachen,(September 1983).

11. D.E. Post and K. Lackner, " Plasma Models for Impurity Control Experiments," pp627-693, Physics of Plasma-wall Interactions in Controlled Fusion, Plenum Press, N.Y. (1986).

12. C.E. Singer, " Plasma Transport Near Material Boundaries," pp607-625, Physics of Plasma-wall Interactions in Controlled Fusion, Plenum Press, N.Y. (1986).

13. F. Wagner and K. Lackner, "Divertor Tokamak Experiments," pp931-1004, Physics of Plasma-wall Interactions in Controlled Fusion, Plenum Press, N.Y. (1986).

14. J. Neuhauser et al., " Impurity Transport in the Tokamak Scrapeoff Layer," Nuclear Fusion vol. 24 no. 1, 39 (1984).

15. D.E. Post et al., " Steady-state Radiative Cooling Rates for Low-density, High Temperature Plasmas," Atomic Data and Nuclear Data Tables, 20, 397 (1977).

16. H. Vernickel and J. Bohdansky, " A General Formula for Impurity Radiation Loss of Fusion Plasmas in Corona Equilibrium," Nuclear Fusion vol. 18 no. 10, 1467 (1978).

17. P.C. Stangeby, " The Plasma Sheath," pp41-97, Physics of Plasma-wall Interactions in Controlled Fusion, Plenum Press, N.Y. (1986).

18. M. Keilhacker et al., " The Plasma Boundary Layer in Limiter and Divertor Tokamaks," Physica Scripta T2/2, 443 (1982).

19. M.F.A. Harrison et al., " A Study of the Boundary Layer of INTOR," Journal of Nuclear Materials 93 & 94, 454 (1980).

20. M. Ulrickson and D.E. Post, " Particle and Energy Transport in the Plasma Scrape-off Zone and its Impact on Limiter Design," Journal of Vacuum Science Technology A, vol. 1 no. 2, 907 (April-June 1983).

21. D.L. Smith et al., " A Physical Sputtering Code for Fusion Applications," 9th Symposium on Engineering Problems of Fusion Research, vol. I , Chicago, Illinois, (1981).

22. M. Shimada and the JAERI team, " Modeling of Dense and Cold Divertor Plasma in D-III," Journal of Nuclear Materials 121, 184 (1984).

23. L. Spitzer, <u>Physics of Fully Ionized Gases</u>, 2nd ed., John Wiley & Sons, N.Y. 1983.

24. K.L. Bell et al., CLM-R216, Culham Laboratory, Oxfordshire, England, (1981).

25. P. Mioduszewski, " Advanced Limiters," pp.891-929, Physics of Plasma-wall Interactions in Controlled Fusion, Plenum Press, N.Y. (1986).·

APPENDIX A

INPUT DATA FOR DIVERTOR MODELING

A.1 Thermal Conduction

The Spitzer[23] electron thermal conductivity coefficient ($x = x_0 T^{2.5}$) was used in the energy equation, (3.3), and the derivatives of this equation. The value of x_0 is calculated as,

$$x_0 = \frac{31500}{<Z>\ln\Lambda} \quad W(eV)^{-7/2} m^{-1} \tag{A.1}$$

where $<Z>$ is the effective charge of the plasma (taken to be 1.25) and $\ln\Lambda$ is the coulombic logrithm (value of 13 used).

A.2 Surface Reflection

The reflection coefficients, R_n and R_e, for particles (D-T and helium) normally incident at energy E_0 on a surface were evaluated using the empirical relationships of reference 3.

For Particles

$$R_n = .19 - .237\log_{10}(E_O/EL) \qquad (A.2)$$

For Energy

$$R_e = 0.06 - .22\log_{10}(E_O/EL) \qquad (A.3)$$

where EL is a material, and particle, dependent reduced energy given by

$$EL(eV) = \frac{\left(M_1 + M_2\right)\left(Z_1 Z_2\right)\left(Z_1^{2/3} + Z_2^{2/3}\right)^{1/2}}{.03255\ M_2} \qquad (A.4)$$

where $M_{1,2}$ is the mass of the incident particle/target material, and $Z_{1,2}$ is the atomic number of the incident particle/target material.

A.3 Electron Impact Ionization Rates for Hydrogen

The equation for the rate coefficient for electron impact ionization of D-T from the ground state ($<\sigma v>_{ion}$) was taken from the divertor model, ZEPHYR[4], and is given by

$$\langle \sigma v \rangle_{ion, D-T} = EXP\left\{ \sum_{n=0}^{6} a_n \left[\ln(kT) \right]^n \right\} \qquad (A.5)$$

where kT is the electron plasma temperature in ev and a_n are fitting constants given by

$$a_0 = -45.56 \qquad\qquad a_4 = 7.43 \times 10^{-2}$$

$$a_1 = 11.44 \qquad\qquad a_5 = 4.15 \times 10^{-3}$$

$$a_2 = 3.83 \qquad\qquad a_6 = -9.49 \times 10^{-5}$$

$$a_3 = .705$$

The collisional radiative ionization rate coefficient for D-T (ionization of an excited atom) can be expressed as[3]

$$\langle \sigma v \rangle_{cr, D-T} = \langle \sigma v \rangle_{ion, D-T} \left[1 + \frac{10}{kT} \left(\frac{n}{10^{20}} \right)^{\beta} \right] \qquad (A.6)$$

where kT is the plasma temperature in eV, n is the electron plasma density in m^{-3}, and β is,

$$\beta = .5 \left[1 - 1.36 \, EXP\left(\frac{-n}{10^{19}} \right) \right]$$

A.4 Charge Exchange Rates for Hydrogen

The charge exchange rate coefficients were evaluated using the expressions given in reference 3. For a D-T plasma at average temperature T_{avg} (eV), the coefficients are:

For one particle at rest (slow neutral CX)

$$\langle \sigma v \rangle_{cx-s} = \left[\left(.4282 \ T_{avg} \right)^{.3338} \right] \times 10^{-14} \ m^3 sec^{-1} \quad (A.7)$$

For both particles at T_{avg} (fast neutral CX)

$$\langle \sigma v \rangle_{cx-f} = \left[\left(.8426 \ T_{avg} \right)^{.3369} \right] \times 10^{-14} \ m^3 sec^{-1} \quad (A.8)$$

A.5 Electron Impact Ionization Rates for Helium

The expression for the electron impact ionization rate for neutral helium was taken from reference 24 and is given by

$$\langle\sigma v\rangle_{ion,He} = EXP\left(\frac{-I}{kT}\right)\left(\frac{kT}{I}\right)^{1/2}\sum_{n=0}^{5}a_n\left[\log_{10}\left(\frac{kT}{I}\right)\right]^n m^3 sec^{-1}$$

(A.9)

where kT is the electron plasma temperature in eV, I is the ionization energy of neutral helium in eV (24.6 eV) and a_n are fitting coefficients given below:

$$a_0 = 1.5 \times 10^{-8} \qquad a_3 \simeq -3.59 \times 10^{-9}$$

$$a_1 = 5.67 \times 10^{-10} \qquad a_4 \simeq 1.55 \times 10^{-9}$$

$$a_2 = -6.08 \times 10^{-9} \qquad a_5 \simeq 1.32 \times 10^{-9}$$

The collisional radiative ionization rate coefficient for neutral helium can be expressed as[3]

$$\langle\sigma v\rangle_{cr,He} = \langle\sigma v\rangle_{ion,He}\left[1 + \left(\frac{10}{kT}\right)\left(\frac{I(He)}{I(D-T)}\right)\left(\frac{n}{10^{20}}\right)^{\beta}\right]$$

(A10)

where I is the ionization energy for helium (24.6 eV) and D-T (13.6 eV), and β is as given above.

A.6 Sputtering Data

The parameters for calculation of physical sputtering
yields used in equations (3.59) and (3.60) are listed in
Table A.1 below.[21]

Table A.1
Material Sputtering Parameters

Wall Material	Z	M	Uo(eV)
Be	4	9.0	3.4
B	5	10.8	5.7
C	6	12.0	7.4
Ti	22	47.9	4.9
V	23	50.9	5.3
Fe	26	55.9	4.3
Ni	28	58.7	4.4
Cu	29	63.5	3.5
Nb	41	92.9	7.6
Mo	42	95.9	7.8
Ta	73	180.9	10.4
W	74	183.9	11.1

Equation (2.21) presented in Chapter 2 for the

calculation of the sputtering rate due to a hydrogen ion flux can be derived based on summing the sputtering yields over a number of generations. An impacting hydrogen ion will produce Y (sputtering yield) impurity neutrals. If a fraction, f, of these plate material atoms then return to the plate, each will cause another Y_s (self sputtering yield) impurity neutrals. The total yield due to the impact of a single hydrogen ion can be represented over a number of generations by

$$\text{Total Yield} = Y + YfY_s + YfY_s\left(fY_s\right) + Y\left(fY_s\right)^3 + \ldots$$

If fY_s is < 1 then this can be rewritten as

$$\text{Total Yield} = Y\left(\frac{1}{1-fY_s}\right) \qquad (A.11)$$

So the sputtering rate due to a flux, Γ_{H+}, of hydrogen ions would be, as given by equation (2.21)

$$R_e = \Gamma_{H+}Y\left(\frac{1}{1-fY_s}\right)$$

APPENDIX B

PROGRAM DIV SUPPORT MATERIALS

This appendix contains a list of the variables in the program DIV along with a description of the subroutines in the program. Enclosed with the appendix is a printout of a sample run and the program itself.

B.1 Program Variables

Each of the significant variables used in the divertor model program DIV is described below along with its dimensions. Items with a star are data entries.

	Variable	Description
*	A	Ratio of temperature to density scale lengthes
	ARC	Angle from a point on the divertor back to the throat (Radians)
	CHE	Energy loss by radiation and ionization per recycled helium particle (eV)
	CHI	Energy loss by radiation and ionization per recycled D-T particle (eV)
	CP	Fractional plate concentration of helium

*	CT	Fractional throat concentration of helium
*	D	Particle diffusion coefficient (m^2/sec)
*	EL	Reflection coefficient reduced energy for D-T particles (eV)
*	ELM	Reflection coefficient reduced energy for helium particles (eV)
	ELOSS	Average energy loss per recycled neutral (eV)
*	DIST	Neutral reflection distribution to be used for the neutral escape probability calculation, 1=cosine, 2=none.
*	F	D-T Pump fraction, the fraction of neutrals pumped that reach the divertor plenum
*	FHE	Helium pump fraction
	FCXF	Relative probability of CX versus ionization for fast neutrals
	FCXS	Relative probability of CX versus ionization for slow neutrals
	FIF	Relative probability of ionization versus CX for fast neutrals
*	G1	Sheath energy transmission factor for electrons
*	G2	Sheath energy transmission factor for ions
	HER	Helium enrichment
*	IE	Upper integration limit as a multiple of plate temperature for sputtering calculations

*	IMP	Impurity radiation increment, a multiplicative factor
	ISE	Integral from plate to throat of the energy source term
*	LD	Divertor connection length (m)
	LCXF	Mean free path in field line direction for fast neutral CX (m)
	LCXS	MFP in field line direction for slow neutral CX (m)
	LDAF	MFP for fast neutral ionization(m)
	LDAS	MFP for slow neutral ionization(m)
	LF	MFP in field line direction for fast neutral ionization (m)
	LNP	Density scale length at the plate (m)
	LS	MFP in field line direction for slow neutral ionization (m)
*	M	D-T particle mass (amu)
*	M3	Atomic mass of plate material (amu)
*	METH	Method to be used for calculation of neutral escape probability, 1= integral, 2=lavg.
	MLT	Multiple of $<\sigma v>_{ion}$ to get total ionization rate (includes ground state and excited state rates)
	MT	Throat mach number
	NAV	Throat to plate average electron density (m^{-3})
	NDT	Temperature gradient density threshold (m^{-3})
*	NM	Plate material number density(m^{-3})

*	NP	Plate electron density (m^{-3})
*	NT	Throat electron density (m^{-3})
	P12	Ionization probability of He^{+} to He^{++}
	PBAR	Neutral escape probability
	PFT	Total fast neutral escape probability
	PH	Neutral helium escape probablity
	PST	Total slow neutral escape probability
*	QT	Energy flux entering the throat (W/m^{2})
*	R	Recycling coefficient
	RE	Energy reflection coefficient
	RHE	Helium recycling coefficient
	RN	Particle reflection coefficient
*	RP	Ion to electron temperature ratio at the plate
*	RT	Ion to electron temperature ratio at the throat
*	SHP	Shape factor for μ calculation
	SI	$<\sigma v>_{ion}$ for groundstate ionization
*	SOR	Successive under or over relaxation coefficient
	TAV	Average throat to plate electron temperature
*	THETA	Angle of incidence of field lines to divertor plate (radians)
*	TOL	Tolerance for convergence

*	TP	Plate electron temperature (eV)
*	TT	Throat electron temperature (eV)
*	U	Conduction fraction
*	UO	Binding energy for plate material (eV)
	VAVG	Average plasma flow speed (m/sec)
	VBAR	Average neutral velocity normalized to plate ion sound speed
	VF	Fast neutral speed (m/sec)
	VS	Slow neutral speed (m/sec)
	XC	Point along divertor plate (m)
*	XT	Width of divertor plate (m)
*	Z3	Atomic number of plate material

Other variables found in the program are intermediate variables. Those with a "O" suffix are original entry values retained for comparison. Any prefix with "ANS" after it is a response to a "yes" or "no" query.

B.2 Subroutine Description

This section briefly describes the subroutines included in the divertor model program DIV. The more important of these appeared on the program flow diagram, Figure 4.1.

Subroutine	Description
ICALC	Performs initial calculation

	of basic quantities used throughout the program
ESC	Calculates the neutral escape probability and recycling coefficient for D-T using ROMBERG, EVAL1 and EVAL2.
HESC	Calculates the neutral escape probability and recycling coefficient for helium using ROMBERG, EVAL1, and EVAL2.
SRVBAR	Calculates VBAR
SRMT	Calculates MT
SRNDT	Calculates ISE and NDT
MU	Calculates the conduction fraction (μ) using ROMBERG and EVAL3.
ROMBERG	Evaluates an integral using Romberg integration.
EVAL1	Function evaluation for the integral calculation of ESC and HESC for slow neutrals
EVAL2	Function evaluation for the integral calculation of ESC and HESC for fast neutrals
PROB	Function evaluation for ESC and HESC for the lavg method
EVAL3	Function evaluation for the integral of MU
SPUD	Sputtering subroutine

B.3   DIV Program Listing (attached)

PROGRAM DIV

```
C       Specifications Block

        REAL TP,TT,NP,NT,RP,RT,LD,QT,M,SHP,F,G1,
     2       G2,XT,THETA,EL,DIST,METH
        REAL MT,VBAR,PBAR,R,ISE,U,NDT,TPO,TTO,NPO,
     2       NTO,UO,RO,SOR,D,A,LNP
        REAL X(101),Y(101),Z(101),PROD,ANS,RANS,
     2       UANS,TOL,CT,CP,FHE,RH
        REAL TAV,NAV,SI,SCXS,SCXF,FIF,FCXF,FCXS,RN,
     2       RE,VF,VS,LDAS,LDAF
        REAL LCXF,LCXS,MLT,CKANS,IMP,VANS,ELH,HER,P12,TANS

C       Common Blocks- used to pass common data between
C       subroutines

        COMMON /INPUT/ TP,TT,NP,NT,RP,RT,LD,QT,M,SHP,F,G1,G2,
     2           DIST,METH,IMP,VANS,D,A,CT,FHE,ELH,THETA,EL
        COMMON /CALC/ TAV,NAV,SI,SCXS,SCXF,FIF,FCXF,FCXS,
     2           LDAS,LDAF,LCXS,LCXF,MLT,LNP,RN,RE,VF,VS
        COMMON /SR/ PBAR,R,VBAR,ISE,MT,U,NDT,RHE,CP,P12

        CHARACTER*64 FNAME

C       Format Block

100     FORMAT(' Input known parameters,QT,LD,M,XT,THETA,EL')
200     FORMAT(' Input guesses,TP,TT,NP,NT,RP,RT')
250     FORMAT(' Input plasma constants,G1,G2,R,U,F,IMP')
300     FORMAT(' Input calc parameters,SHP,METH,DIST,TOL,SOR')
400     FORMAT(' Change known parameters? 1=yes 2=no')
500     FORMAT(' Change guesses? 1=yes 2=no')
550     FORMAT(' Change plasma constants? 1=yes 2=no')
600     FORMAT(' Change shape/plasma parameters? 1=yes 2=no')
700     FORMAT(' Another calculation? 1=yes 2=no')
800     FORMAT(' 10 loops complete, continue? 1=yes 2=no')
900     FORMAT(' Store iterations? 1=yes 2=no')
1000    FORMAT(' Enter data file name')

C       Diagnostic Error Statements, all cause iterations
C       to stop

1100    FORMAT(' MT was negative')
1200    FORMAT(' NDT was Negative')
1300    FORMAT(' PROD is LT 1')
1400    FORMAT(' QT-ISE is negative')
1500    FORMAT(A)
1600    FORMAT(I4,3X,E10.4,3X,E10.4,3X,E10.4)
1700    FORMAT(' Convergence to ',E9.4,' achieved')
```

```fortran
1800  FORMAT(' TP=',E9.4,' NP=',E9.4,' TT=',E9.4,' NT=',
     2       E9.4)
1900  FORMAT(' MT=',E9.4,' U=',E9.4,' ISE=',E9.4,' R=',E9.4)
1950  FORMAT(' CP=',E9.4,'HER=',E9.4,' P12=',E9.4,'LNP=',
     2       E9.4)
2000  FORMAT(' Iteration #-',I4)
2100  FORMAT(' U is negative on TT change')
2600  FORMAT(' NP=',E10.4,' TT=',E10.4,'TP=',E10.4)
2700  FORMAT(' U is negative, TP decremented -1')
2800  FORMAT(' Do you want to calculate R? 1=yes 2=no')
2900  FORMAT(' Do you want to calculate U? 1=yes 2=no')
3000  FORMAT('ICALC')
3100  FORMAT(' SRVBAR')
3200  FORMAT(' SRMT')
3300  FORMAT(' MU=',E10.4)
3400  FORMAT(' SRNDT')
3500  FORMAT(' ESC, R=',E10.4)
3600  FORMAT(' Want to check MU? 1=yes 2=no')
3700  FORMAT(' Change input data? 1=yes 2=no')
3800  FORMAT(' Want to check R? 1=yes 2=no')
3900  FORMAT(' Change input data? 1=yes 2=no')
4000  FORMAT(' VBAR=0? 1=yes 2=no')
4100  FORMAT(' Radial/HE data,enter D,A,CT,FHE,ELH')
4200  FORMAT(' Change radial/He data? 1=yes 2=no')
4300  FORMAT(' Do you want to calculate sputtering?
     2          1=yes 2=no')
4400  FORMAT(' Jump to Sputtering? 1=yes 2=no')
4500  FORMAT(' Do you want to hold TT constant? 1=yes 2=no')
C            Prompt for Inputs

      WRITE(*,100)
      READ(*,*) QT,LD,M,XT,THETA,EL
      WRITE(*,200)
      READ(*,*) TPO,TTO,NPO,NTO,RP,RT
      WRITE(*,250)
      READ(*,*) G1,G2,RO,UO,F,IMP
      WRITE(*,4100)
      READ(*,*) D,A,CT,FHE,ELH
      WRITE(*,300)
      READ(*,*) SHP,METH,DIST,TOL,SOR

C     Initialization

70    K=1
      MT=.1
      TP=TPO
      NP=NPO
      TT=TTO
      NT=NTO
      U=UO
```

```fortran
        R=RO
        RHE=RO
        X(1)=NPO
        Y(1)=TTO
        Z(1)=TPO

C       Prompt for Jump to Sputtering Subroutine
        WRITE(*,4400)
        READ(*,*) ANS
        IF(ANS.LT.1.5) THEN
        CALL ICALC
        CP=CT
        P12=0.0
        CALL SPUD
        GOTO 65
        ENDIF

C       Prompts for calculation of VBAR, R, Mu,TT
        WRITE(*,4000)
        READ(*,*) VANS
        WRITE(*,4500)
        READ(*,*) TANS
        WRITE(*,2800)
        READ(*,*) RANS
        IF(RANS.LT.1.5) THEN
        WRITE(*,3800)
        READ(*,*) CKANS
        IF(CKANS.LT.1.5) THEN
        CALL ICALC
        CALL ESC
        WRITE(*,3500) R
        WRITE(*,3900)
        READ(*,*) CKANS
        IF(CKANS.LT.1.5) GOTO 75
        ENDIF
        ENDIF
        WRITE(*,2900)
        READ(*,*) UANS
        IF(UANS.LT.1.5) THEN
        WRITE(*,3600)
        READ(*,*) CKANS
        IF(CKANS.LT.1.5) THEN
        CALL ICALC
        CALL SRVBAR
        CALL SRMT
        CALL MU
        WRITE(*,3300) U
        WRITE(*,3700)
        READ(*,*) CKANS
        IF(CKANS.LT.1.5) GOTO 75
```

```fortran
        ENDIF
        ENDIF

C       Do loop for 10 Fixed Point iterations
20      DO 10 J=1,10
        K=K+1

80      CALL ICALC
        WRITE(*,3000)
        IF(RANS.LT.1.5) THEN
        CALL ESC
        CALL HESC
        ENDIF
        WRITE(*,3500) R
        CALL SRVBAR
        WRITE(*,3100)

        CALL SRMT
        WRITE(*,3200)
        IF(MT.LT.0.0) THEN
        WRITE(*,1100)
        GOTO 60
        ENDIF

        IF(UANS.LT.1.5) THEN
        CALL MU
        WRITE(*,3300) U
C       This decrements TP by 1 if Mu is negative
        IF(U.LT.0.0) THEN
        WRITE(*,2700)
        TP=TP-1.
        IF(TP.LT.3) GOTO 60
        GOTO 80
        ENDIF
        ENDIF

        CALL SRNDT
        WRITE(*,3400)
        IF(NDT.LT.0.0) THEN
        WRITE(*,1200)
        GOTO 60
        ENDIF

C       Use Fixed point iteration to get NP,TT,TP

        PROD=(2.+VBAR*R)*(1.+RP)/NT/(1.+RT)/(1.+MT*MT)

C       X(K) is NP
        X(K)=(((NP/NDT)**2.33333+1.)**.285714)/PROD
```

```fortran
      NP=SOR*X(K)+(1.-SOR)*X(K-1)
C     Check for Convergence on NP, if satisfied output
C     updated results

      IF(ABS((X(K)-X(K-1))/X(K)).LT.TOL) THEN

      WRITE(*,1700) TOL
      WRITE(*,1800) TP,NP,TT,NT
      HER=(1.-RHE)/(1.-R)
      WRITE(*,1900) MT,U,ISE,R
      WRITE(*,1950) CP,HER,P12,LNP*SIN(THETA)
      GOTO 60
      ENDIF

C     Now all variables are updated on most current NP
      CALL ICALC
      WRITE(*,3000)
      IF(RANS.LT.1.5) THEN
      CALL ESC
      CALL HESC
      ENDIF
      WRITE(*,3500) R
      CALL SRVBAR
      WRITE(*,3100)

      CALL SRMT
      WRITE(*,3200)
      IF(MT.LT.0.0) THEN
      WRITE(*,1100)
      GOTO 60
      ENDIF

      IF(UANS.LT.1.5) THEN
      CALL MU
      WRITE(*,3300) U
      IF(U.LT.0.0) THEN
      WRITE(*,2700)
      TP=TP-1.
      IF(TP.LT.3) GOTO 60
      GOTO 80
      ENDIF
      ENDIF

      CALL SRNDT
      WRITE(*,3400)
      IF(NDT.LT.0.0) THEN
      WRITE(*,1200)
      GOTO 60
      ENDIF
```

```
C       Y(K) is TT
        IF(TANS.LT.1.5) GOTO 35
        Y(K)=(2.+R*VBAR*(1.+RP))*NP*TP*(1.+RP)/(NT*(1.+RT)*
     2         (1.+MT*MT))
        TT=SOR*Y(K)+(1.-SOR)*Y(K-1)
C       Now all variables are updated using most current TT
        CALL ICALC
        WRITE(*,3000)
        IF(RANS.LT.1.5) THEN
        CALL ESC
        CALL HESC
        ENDIF
        WRITE(*,3500) R
        CALL SRVBAR
        WRITE(*,3100)

        CALL SRMT
        WRITE(*,3200)
        IF(MT.LT.0.0) THEN
        WRITE(*,1100)
        GOTO 60
        ENDIF

        IF(UANS.LT.1.5) THEN
        CALL MU
        WRITE(*,3300) U
        IF(U.LT.0.0) THEN
        WRITE(*,2700)
        TP=TP-1.
        IF(TP.LT.3; GOTO 60
        GOTO 80
        ENDIF
        ENDIF

        CALL SRNDT
        WRITE(*,3400)
        IF(NDT.LT.0.0) THEN
        WRITE(*,1200)
        GOTO 60
        ENDIF

        IF((QT-ISE).LT.0.0) THEN
        WRITE(*,1400)
        GOTO 60
        ENDIF

C       Z(K) is TP
35      Z(K)=(6.355E-5*(QT-ISE)/(NP*SQRT((1.+RP)/M)
     2         *(G1+RP*G2)))**.66667
        TP=SOR*Z(K)+(1.-SOR)*Z(K-1)
```

```fortran
C       Now output results of most current iteration
        WRITE(*,2000) K
        WRITE(*,2600)NP,TT,TP

10      CONTINUE

C       prompt to do ten more loops
        WRITE(*,800)
        READ(*,*) ANS
        IF(ANS.LT.1.5) GOTO 20

C       Prompt for storing iterations
60      .WRITE(*,900)
        READ(*,*) ANS
        IF(ANS.LT.1.5) THEN
        WRITE(*,1000)
        READ(*,1500) FNAME
        OPEN(2,FILE=FNAME)       .
        DO 30 I=1,K
        WRITE(2,1600) I,Z(I),Y(I),X(I)
30      CONTINUE
        CLOSE(2)
        ENDIF

C       Prompt for Sputtering calculations
        WRITE(*,4300)
        READ(*,*) ANS
        IF(ANS.LT.1.5) CALL SPUD

C       Prompts for another calculation and data changes
65      WRITE(*,700)
        READ(*,*) ANS
        IF(ANS.GT.1.5) GOTO 50
75      WRITE(*,400)
        READ(*,*) ANS
        IF(ANS.LT.1.5) THEN

        WRITE(*,100)
        READ(*,*) QT,LD,M,XT,THETA,EL
        ENDIF
        WRITE(*,500)
        READ(*,*) ANS
        IF(ANS.LT.1.5) THEN
        WRITE(*,200)
        READ(*,*) TPO,TTO,NPO,NTO,RP,RT
        ENDIF
        WRITE(*,550)
        READ(*,*) ANS
        IF(ANS.LT.1.5) THEN
```

```
      WRITE(*,250)
      READ(*,*) G1,G2,RO,UO,F,IMP
      ENDIF
      WRITE(*,4200)
      READ(*,*) ANS
      IF(ANS.LT.1.5) THEN
      WRITE(*,4100)
      READ(*,*) D,A,CT,FHE,ELH
      ENDIF
      WRITE(*,600)
      READ(*,*) ANS
      IF(ANS.LT.1.5) THEN
      WRITE(*,300)
      READ(*,*) SHP,METH,DIST,TOL,SOR
      ENDIF

      GOTO 70
50    STOP
      END



C*****************************************************************

      SUBROUTINE ICALC

C     This subroutine does initial calculations which go
C     into the CALC common block

      REAL TP,TT,NP,NT,RP,RT,LD,QT,M,SHP,F,G1,G2,
     2     XT,THETA,EL,DIST,METH
      REAL TAV,NAV,SI,SCXS,SCXF,FIF,FCXS,FCXF,
     2     RN,RE,VF,VS,LDAS,LDAF,ELH
      REAL LCXS,LCXF,MLT,Z,ZS,IMP,VANS,D,A,LNP,CT,FHE

      COMMON /INPUT/ TP,TT,NP,NT,RP,RT,LD,QT,M,SHP,
     2         F,G1,G2,XT,THETA,EL,DIST,METH,IMP,VANS,
     3         D,A,CT,FHE,ELH
      COMMON /CALC/ TAV,NAV,SI,SCXS,SCXF,FIF,FCXF,
     2         FCXS,RN,RE,VF,VS, LDAS,LDAF,LCXS,LCXF,MLT,LNP

      TAV=(TP+TT)/2.
      NAV=(NP+NT)/2.
      LNP=SQRT(D*LD/9822.27/(TP*(1.+RP)/M)**.5)/SIN(THETA)
      RN=.19-.237*ALOG10(3.*TP/EL)
      RE=.06-.22*ALOG10(3.*TP/EL)
      VF=9822.27*SQRT(6.*TP*RE/M/RN)
C       VS is based on a Franck-Condon energy of 3 ev
      VS=9822.27*SQRT(6./M)
      Z=ALOG(TAV)
      ZS=(((((-9.49e-5*Z+4.15e-3)*Z-7.43e-2)*Z
```

```fortran
2     +.705)*Z-3.83)*Z+11.44)*Z-31.74
      SI=EXP(ZS-13.82)
      MLT=2.0+(10./TAV)*(NAV/10.)**(.5*(1.-1.36*EXP(-NAV)))
      SCXS=((.4282*TAV)**.3338)*1.e-14
      SCXF=((.8426*TAV)**.3369)*1.e-14
      FIF=MLT*SI/(MLT*SI+SCXF)
      FCXF=1.-FIF
      FCXS=SCXS/(SCXS+MLT*SI)
      LDAS=VS/(NAV*1.e19*MLT*SI)/SIN(THETA)
      LDAF=VF/(NAV*1.e19*MLT*SI)/SIN(THETA)
      LCXS=VS/(NAV*1.e19*SCXS)/SIN(THETA)
      LCXF=VF/(NAV*1.e19*SCXF)/SIN(THETA)
      RETURN
      END


C********************************************************************


      SUBROUTINE SRVBAR


C     This subroutine calculates VBAR


      REAL TP,TT,NP,NT,RP,RT,LD,QT,M,SHP,F,G1,
     2     G2,XT,THETA,EL,DIST,METH
      REAL MT,VBAR,PBAR,R,ISE,U,NDT,VANS,D,A,
     2     LNP,RHE,CT,FHE,CP
      REAL TAV,NAV,SI,SCXS,SCXF,FIF,FCXF,FCXS,
     2     RN,RE,VF,VS,LDAS,LDAF
      REAL LCXF,LCXS,MLT,FVBAR,SVBAR,VAVG,IMP,ELH,P12


      COMMON /INPUT/ TP,TT,NP,NT,RP,RT,LD,QT,M,SHP,FHE,ELH,
     2         F,G1,G2,XT,THETA,EL,DIST,METH,IMP,VANS,D,A,CT
      COMMON /CALC/ TAV,NAV,SI,SCXS,SCXF,FIF,FCXF,FCXS,
     2         RN,RE,VF,VS,
LDAS,LDAF,LCXS,LCXF,MLT,LNP
      COMMON /SR/ PBAR,R,VBAR,ISE,MT,U,NDT,RHE,CP,P12


C     Calculate VBAR

      VAVG=4911.13*(MT*SQRT(TT*(1.0+RT)/M)+
     2     SQRT(TP*(1.0+RP)/M))

      FVBAR=RN*VF*SIN(THETA)
      SVBAR=(1.-RN)*VS*SIN(THETA)

      VBAR=(FVBAR+SVBAR)/(9822.27*SQRT(TP*(1.0+RP)/M))
      IF(VANS.LT.1.5) VBAR=0.0
      RETURN
      END


C********************************************************************
```

```fortran
      SUBROUTINE SRMT

C     This subroutine calculated MT, the throat mach number
      REAL TP,TT,NP,NT,RP,RT,LD,QT,M,SHP,F,G1,G2,
     2     XT,THETA,EL,DIST,METH
      REAL MT,VBAR,PBAR,R,ISE,U,NDT,MTO,A,IMP,
     2     VANS,D,AA,CT,FHE,RHE,CP
      REAL ELH,P12

      COMMON /INPUT/ TP,TT,NP,NT,RP,RT,LD,QT,M,
     2          SHP,F,G1,G2,XT,THETA,EL,
     3          DIST,METH,IMP,VANS,D,AA,CT,FHE,ELH
      COMMON /SR/ PBAR,R,VBAR,ISE,MT,U,NDT,RHE,CP,P12

C     Calculate MT

15    A=NP*(1.0-R)*(1.0-R)/(NT*(2.0+R*VBAR))
      IF(A.GT.1.0) THEN
      MT=-1.0
      RETURN
      ENDIF
      MTO=SQRT(A/(1-A))
C     This loop is to adjust VBAR using the most current MT
      IF(ABS((MTO-MT)/MTO).GT..05) THEN
      MT=MTO
      CALL SRVBAR

      GOTO 15
      ENDIF
      MT=MTO

      RETURN
      END


C***********************************************************


      SUBROUTINE SRNDT

C     This subroutine calculated NDT and most energy loss
C     related terms

      REAL TP,TT,NP,NT,RP,RT,LD,QT,M,SHP,F,G1,G2,XT,
     2     THETA,EL,DIST,METH
      REAL MT,VBAR,PBAR,R,ISE,U,NDT,VANS,D,A,LNP,CT,
     2     FHE,RHE,CP,CHE,ELH
      REAL TAV,NAV,SI,SCXS,SCXF,FIF,FCXF,FCXS,RN,
     2     RE,VF,VS,LDAS,LDAF
      REAL LCXF,LCXS,MLT,CHI,ELOSS,VAVG,IMP,TRES,P12
```

```fortran
      COMMON /INPUT/ TP,TT,NP,NT,RP,RT,LD,QT,M,SHP,
     2        F,G1,G2,XT,THETA,EL,
     3        DIST,METH,IMP,VANS,D,A,CT,FHE,ELH
      COMMON /CALC/ TAV,NAV,SI,SCXS,SCXF,FIF,FCXF,
     2        FCXS,RN,RE,VF,VS,
     3        LDAS,LDAF,LCXS,LCXF,MLT,LNP
      COMMON /SR/ PBAR,R,VBAR,ISE,MT,U,NDT,RHE,CP,P12

100   FORMAT(' ELOSS=',E10.4)

      CHI=17.5+(5.+37.5/TAV)*ALOG10(100./NAV)
      TRES=3.64*(RN*LDAF+(1.-RN)*LDAS)*SIN(THETA)/
     2      9822.27/SQRT(TP*(1+RP)/M)
      P12=1.-EXP(-(1.e-5+TRES)/3.e-5)
      CHE=15.+P12*(70+3360./TP)
      CP=CT*NT*MT*SQRT(TT*(1.+RT)/TP/(1.+RP))/(1.-RHE)/NP
      VAVG=4911.13*(MT*SQRT(TT*(1.0+RT)/M)+
     2      SQRT(TP*(1.0+RP)/M))

      ELOSS=IMP*(1.-(1.+P12)*CP)*(CHI+(1.-RN)*(1.
     2       -R)*FCXS*(1.5*TAV+
     2   5.183E-9*M*VAVG*VAVG-3.)/R)+RHE*CHE*CP/R
      WRITE(*,100) ELOSS
      ISE=R*NP*9822.27*SQRT(TP*(1.0+RP)/M)*ELOSS*1.602

      IF(ISE/QT.GT.1.0) THEN
      NDT=-1.0
      RETURN
      ENDIF
      NDT=(553.83/(U*LD))**.42857*(QT**.57143)*(1.0-ISE/QT)*
     2   SQRT(M/(1.0+RP))*6.35515E-5/(G1+RP*G2)

      RETURN
      END


C***************************************************************

      SUBROUTINE ESC

C     This subroutine calculates PBAR and R for D-T. It
C     calculates the escape probability for particles based
C     on simple exponential attentuation at 50 points across
C     the divertor plate and averages the PBAR values by
C     weighting them with the local plate particle flux

      REAL PS,PF,PST,PFT,PBAR,XC,INCR,ARC,TN,RST,
     2      R,EF1,EF2,LDS,LDF,ELH
      REAL TP,TT,NP,NT,RP,RT,LD,QT,M,SHP,F,G1,G2,
     2      XT,THETA,EL,DIST,METH
      REAL TAV,NAV,SI,SCXS,SCXF,FIF,FCXF,FCXS,RN,
```

```fortran
2       RE,VF,VS,LDAS,LDAF,CP
 REAL LCXS,LCXF,MLT,VBAR,ISE,MT,U,NDT,IMP,VANS,
2       D,A,LNP,CT,FHE,RHE
 REAL NPO,TPO,TPR,NPR,VFR,RNR,RER,MLTR,P12,FXT

 COMMON /INPUT/ TP,TT,NP,NT,RP,RT,LD,QT,M,SHP,
2          F,G1,G2,XT,THETA,
3   EL,DIST,METH,IMP,VANS,D,A,CT,FHE,ELH
 COMMON /CALC/ TAV,NAV,SI,SCXS,SCXF,FIF,FCXF,FCXS,
2          RN,RE,VF,VS,LDAS,LDAF,LCXS,LCXF,MLT,LNP
 COMMON /SR/ PBAR,R,VBAR,ISE,MT,U,NDT,RHE,CP,P12
 COMMON /SUBESC/ ARC,XC,LDF,LDS

 INTEGER JL

C    Initialize Parameters

 XC=0.0
 PST=0.0
 PFT=0.0
 PS=0.0
 PF=0.0
 EF1=1.0
 EF2=2.0
 FXT=0.0
C    Initial Calculations

 INCR=XT/50.
 TN=TAN(THETA)
 NPO=XT*NP/LNP/(1.-EXP(-XT/LNP))
 TPO=XT*TP/A/LNP/(1.-EXP(-XT/A/LNP))
C    Do Loop to Calculate Escape Probability for a mesh of
C    points

 DO 50 JL=1,49

 XC=XC+INCR
 TPR=TPO*EXP(-XC/A/LNP)
 NPR=NPO*EXP(-XC/LNP)
 RNR=.19-.237*ALOG10(3.*TPR/EL)
 RER=.06-.22*ALOG10(3.*TPR/EL)
 VFR=9822.27*SQRT(6.*TPR*RER/M/RNR)

 Z=ALOG(TPR)
 ZS=(((((-9.49e-5*Z+4.15e-3)*Z-7.43e-2)*Z
2    +.705)*Z-3.83)*Z+11.44)*Z-31.74
 SI=EXP(ZS-13.82)
 MLT=2.0+(10./TPR)*(NPR/10.)**(.5*(1.-1.36*EXP(-NPR)))
 LDS=VS/(NPR*1.e19*MLT*SI)
 LDF=VFR/(NPR*1.e19*MLT*SI)
```

```fortran
      ARC=3.1416-ACOS(XC/SQRT(XT*XT*TN*TN+XC*XC))

      IF(METH.LT.1.5) THEN
      CALL RMBG(0.0,ARC,EF1,RST)
      PS=RST/ARC
      ENDIF

      IF(METH.GT.1.5) CALL PROB(LDS,PS,THETA,XT)

      PST=PST+NPR*SQRT(TPR)*PS*(1.-RNR)

      IF(METH.LT.1.5) THEN
      CALL RMBG(0.0,ARC,EF2,RST)
      PF=RST/ARC
      ENDIF

      IF(METH.GT.1.5) CALL PROB(LDF,PF,THETA,XT)

      PFT=PFT+NPR*SQRT(TPR)*PF*RNR
      FXT=FXT+NPR*SQRT(TPR)
50    CONTINUE

C     Calculate final escape probability
      PBAR=(PFT+PST)/FXT
      R=1.-PBAR*F
      RETURN
      END


C*******************************************************************

      SUBROUTINE HESC

C     This subroutine does the same thing as ESC but for He

      REAL PS,PF,PST,PFT,PBAR,XC,INCR,ARC,TN,RST,R,
     2     EF1,EF2,LDS,LDF,ELH
      REAL TP,TT,NP,NT,RP,RT,LD,QT,M,SHP,F,G1,G2,XT,
     2     THETA,EL,DIST,METH
      REAL TAV,NAV,SI,SCXS,SCXF,FIF,FCXF,FCXS,RN,RE,
     2     VF,VS,LDAS,LDAF,CP
      REAL LCXS,LCXF,MLT,VBAR,ISE,MT,U,NDT,IMP,VANS,
     2     D,A,LNP,CT,FHE,RHE
      REAL NPO,TPO,TPR,NPR,VFR,RNR,RER,MLTR,VSH,PH,P12

      COMMON /INPUT/ TP,TT,NP,NT,RP,RT,LD,QT,M,
     2        SHP,F,G1,G2,XT,THETA,
     3        EL,DIST,METH,IMP,VANS,D,A,CT,FHE,ELH
      COMMON /CALC/ TAV,NAV,SI,SCXS,SCXF,FIF,FCXF,
     2        FCXS,RN,RE,VF,VS,
```

```
3              LDAS,LDAF,LCXS,LCXF,MLT,LNP
      COMMON /SR/ PBAR,R,VBAR,ISE,MT,U,NDT,RHE,CP,P12
      COMMON /SUBESC/ ARC,XC,LDF,LDS

      INTEGER JL

C     Initialize Parameters

      XC=0.0
      PST=0.0
      PFT=0.0
      PS=0.0
      PF=0.0
      EF1=1.0
      EF2=2.0
      FXT=0.0
C     Initial Calculations

      INCR=XT/50.
      TN=TAN(THETA)
      NPO=XT*NP/LNP/(1.-EXP(-XT/LNP))
      TPO=XT*TP/A/LNP/(1.-EXP(-XT/A/LNP))
C     Do Loop to Calculate Escape Probability for a mesh of
C     points

      DO 50 JL=1,49

      XC=XC+INCR
      TPR=TPO*EXP(-XC/A/LNP)
      NPR=NPO*EXP(-XC/LNP)
      RNR=.19-.237*ALOG10(3.*TPR/ELH)
      RER=.06-.22*ALOG10(3.*TPR/ELH)
      VFR=9822.27*SQRT(6.*TPR*RER/4./RNR)
      VSH=9822.27*SQRT(6./4.)
      Z=ALOG10(TPR/24.6)
      ZS=((((1.3207e-9*Z+1.5529e-9)*Z-3.59e-9)*Z
     2    -6.082e-9)*Z+5.666e-10)*Z+1.5e-8

      SI=EXP(-24.6/TPR)*SQRT(TPR/24.6)*ZS*1.e-6
      MLT=2.0+(18.1/TPR)*(NPR/10.)**(.5*(1.-1.36*EXP(-NPR)))
      LDS=VSH/(NPR*1.e19*MLT*SI*0.55)
      LDF=VFR/(NPR*1.e19*MLT*SI*0.55)

      ARC=3.1416-ACOS(XC/SQRT(XT*XT*TN*TN+XC*XC))

      IF(METH.LT.1.5) THEN
      CALL RMBG(0.0,ARC,EF1,RST)
      PS=RST/ARC
      ENDIF
```

```
        IF(METH.GT.1.5) CALL PROB(LDS,PS,THETA,XT)

        PST=PST+NPR*SQRT(TPR)*PS*(1.-RNR)

        IF(METH.LT.1.5) THEN
        CALL RMBG(0.0,ARC,EF2,RST)
        PF=RST/ARC
        ENDIF

        IF(METH.GT.1.5) CALL PROB(LDF,PF,THETA,XT)

        PFT=PFT+NPR*SQRT(TPR)*PF*RNR
        FXT=FXT+NPR*SQRT(TPR)
50      CONTINUE

C       Calculate final escape probability
        PH=(PFT+PST)/FXT
        RHE=1.-PH*FHE
        RETURN
        END
C*****************************************************************
C       This subroutine evaluates an integral A-B of EF using
C       Romberg integration. It is used in ESC, HESC, MU, and
C       SPUD

        SUBROUTINE RMBG(A,B,EF,RESULT)

        REAL A,B,H,V,FF,R1(12),R2(12),RA,RB,RV,EF,RESULT

        INTEGER K,J,L,M,I
C       Initial Calculations
        DO 50 I=1,12
        R1(I)=0.0
        R2(I)=0.0
50      CONTINUE

        H=B-A
C       Calculate R1,1
        IF(EF.LT.1.5) THEN
        CALL EVAL1(A,RA)
        CALL EVAL1(B,RB)
        ENDIF
        IF(EF.GT.1.5) THEN
        IF(EF.LT.2.5) THEN
        CALL EVAL2(A,RA)
        CALL EVAL2(B,RB)
        ENDIF
        ENDIF
        IF(EF.GT.2.5) THEN
        IF(EF.LT.3.5) THEN
```

```fortran
         CALL EVAL3(A,RA)
         CALL EVAL3(B,RB)
         ENDIF
         ENDIF
         IF(EF.GT.3.5) THEN
         CALL EVAL4(A,RA)
         CALL EVAL4(B,RB)
         ENDIF
         R1(1)=H*(RA+RB)/2.0
         DO 400 I=2,10
         L=2**(I-2)
         FF=0.0
         DO 100 K=1,L
         V=A+(FLOAT(K)-0.5)*H
         IF(EF.LT.1.5) THEN
         CALL EVAL1(V,RV)
         ENDIF
         IF(EF.GT.1.5) THEN
         IF (EF.LT.2.5) THEN
         CALL EVAL2(V,RV)
         ENDIF
         ENDIF
         IF(EF.GT.2.5) THEN
         IF(EF.LT.3.5) THEN
         CALL EVAL3(V,RV)
         ENDIF
         ENDIF
         IF(EF.GT.3.5) THEN
         CALL EVAL4(V,RV)
         ENDIF
         FF=FF+RV
100      CONTINUE
         R2(1)=0.5*(R1(1)+H*FF)
         DO 200 J=2,I
         R2(J)=((4.0**FLOAT(J-1)*R2(J-1))-R1(J
2          -1))/(4.0**FLOAT(J-1)-1.0)
         IF(EF.LT.3.5) THEN
         IF(ABS(R2(J)).LT.1.e-2) THEN
         R2(J)=0.0
         GOTO 500
         ENDIF
         ENDIF
         IF(ABS((R2(J)-R2(J-1))/R2(J)).LT.1.0E-3) GOTO 500
200      CONTINUE

         H=H/2.0
         DO 300 M=1,I
         R1(M)=R2(M)
300      CONTINUE
400      CONTINUE
```

```fortran
500     RESULT=R2(J)
        RETURN
        END

C****************************************************************

        SUBROUTINE EVAL1(X,RST)

C       This subroutine is function evaluation for fast
C       particle calculations of method 1 of ESC

        REAL L,ARC,XC,TN,RST,LDF,LDS,D,A,LNP,CT,FHE
        REAL TP,TT,NP,NT,RP,RT,LD,QT,M,SHP,F,G1,G2,XT,
     2       THETA,EL,DIST,METH
        REAL IMP,VANS

        COMMON /SUBESC/ ARC,XC,LDF,LDS
        COMMON /INPUT/ TP,TT,NP,NT,RP,RT,LD,QT,M,SHP,F,
     2         G1,G2,XT,THETA,EL,DIST,METH,
     3         IMP,VANS,D,A,CT,FHE,ELH

        TN=TAN(THETA)
        L=TN*(XT-XC)/(SIN(X)+TN*COS(X))
        RST=(ARC/3.1416)*EXP(-1.0*L/LDS)

        IF(DIST.LT.1.5) RST=SIN(X)*RST

        RETURN
        END

C****************************************************************

        SUBROUTINE EVAL2(X,RST)

C       This subroutine is function evaluation for slow
C       particle calculations of method 1 of ESC

        REAL L,ARC,XC,TN,RST,LDF,LDS,D,A,CT,FHE,LNP
        REAL TP,TT,NP,NT,RP,RT,LD,QT,M,SHP,F,G1,G2,
     2       XT,THETA,EL,DIST,METH
        REAL IMP,VANS

        COMMON /SUBESC/ ARC,XC,LDF,LDS
        COMMON /INPUT/ TP,TT,NP,NT,RP,RT,LD,QT,M,SHP,
     2         F,G1,G2,XT,THETA,
     3         EL,DIST,METH,IMP,VANS,D,A,CT,FHE,ELH

        TN=TAN(THETA)
        L=TN*(XT-XC)/(SIN(X)+TN*COS(X))
        RST=(ARC/3.1416)*EXP(-1.0*L/LDF)
```

```fortran
      IF(DIST.LT.1.5) RST=SIN(X)*RST

      RETURN
      END

C*************************************************************

      SUBROUTINE PROB(LDA,P,THETA,XT)

C     This subroutine is function evaluation for method 2
C     of ESC

      REAL LDA,XC,P,ARC,PT1,PT2,LAVG,TN,THETA,
     2     XT,DIST,LDF,LDS

      COMMON /SUBESC/ ARC,XC,LDF,LDS

C     Initial Calculations

      TN=TAN(THETA)

C     Calculate LAVG
      PT1=ALOG(TAN(THETA/2.0))
      PT2=ALOG(TAN((THETA+ARC)/2.0))
      LAVG=TN*(XT-XC)*(PT2-PT1)/(SQRT(1.0+TN*TN)*ARC)

C     Calculate Escape Probability
      P=(ARC/3.1416)*EXP(-1.0*LAVG/LDA)

      RETURN
      END
C*************************************************************

      SUBROUTINE MU

C     This subroutine calculates the conduction fraction

      REAL PBAR,R,VBAR,ISE,MT,U,NDT,RST,EF,IMP,VANS,
     2     D,A,RHE,CT,FHE,CP,P12
      REAL NP,TP,NT,TT,RP,RT,LD,QT,M,SHP,F,G1,G2,
     2     XT,THETA,EL,DIST,METH

      COMMON /SR/ PBAR,R,VBAR,ISE,MT,U,NDT,RHE,CP,P12
      COMMON /INPUT/ TP,TT,NP,NT,RP,RT,LD,QT,M,SHP,
     2        F,G1,G2,XT,THETA,EL,
     2   DIST,METH,IMP,VANS,D,A,CT,FHE,ELH

      CALL RMBG(0.0,LD,3.,RST)
      U=1.-RST/QT/LD
      RETURN
```

```
      END

C*************************************************************

      SUBROUTINE EVAL3(X,RST)

C     This is function evaluation for romberg integration
C     of MU

      REAL PBAR,RCY,VBAR,ISE,MT,U,NDT,RST,IMP,
     2     BOT,VANS,D,A,LNP,RHE,FHE
      REAL NP,TP,NT,TT,RP,RT,LD,QT,M,SHP,F,G1,
     2     G2,XT,THETA,EL,DIST,METH
      REAL TAV,NAV,SI,SCXS,SCXF,FIF,FCXF,FCXS,RN,
     2     RE,VF,VS,LDAS,LDAF,CP
      REAL LCXF,LCXS,MLT,FC,N,R,T,MA,RPR,TOP,
     2     VRPR,VAVG,LF,LS,P12

      COMMON /SR/ PBAR,RCY,VBAR,ISE,MT,U,NDT,RHE,CP,P12
      COMMON /INPUT/ TP,TT,NP,NT,RP,RT,LD,QT,M,SHP,F,
     2        G1,G2,XT,THETA,EL,
     3        DIST,METH,IMP,VANS,D,A,CT,FHE,ELH
      COMMON /CALC/ TAV,NAV,SI,SCXS,SCXF,FIF,
     2        FCXF,FCXS,RN,RE,VF,VS,
     3        LDAS,LDAF,LCXS,LCXF,MLT,LNP

      FC=(1.-(1.-X/LD)**SHP)
      N=NP+(NT-NP)*FC

      R=RP+(RT-RP)*FC

      LF=LDAF
      LS=LDAS

      RPR=(LF*RN*(1.-EXP(-X/LF))+(1.-RN)*LS*(1.-EXP(-X/LS)))
     2     /(LF*RN*(1.-EXP(-LD/LF))+(1.-RN)*LS*(1.-EXP(
     3     -LD/LS)))

      VAVG=4911.13*(MT*SQRT(TT*(1.+RT)/M)+
     2     SQRT(TP*(1.+RP)/M)

      TOP=RN*(FIF*SIN(THETA)*VF*(1.-EXP(-X/LF))
     2     +FCXF*(VF*SIN(THETA)+VAVG*(1.-RCY))*
     3     (1.-EXP(-X/LCXF)))+(1.-RN)*VAVG*(1.-RCY)
     4     *FCXS*(1.-EXP(-X/LCXS))

      BOT=RN*(FIF*SIN(THETA)*VF*(1.-EXP(-LD/LF))
     2     +FCXF*(VF*SIN(THETA)+VAVG*(1.-RCY))
     3     *(1.-EXP(-LD/LCXF)))+(1.-RN)*VAVG
     4     *(1.-RCY)*FCXS*(1.-EXP(-LD/LCXS))
```

```fortran
      VRPR=RCY*VBAR*TOP/BOT

      T=(VRPR+2.-(1-RCY*RPR)**2.*NP/N)*NP*TP
     2   *(1.+RP)/(N*(1.+R))

      MA=(1.-RCY*RPR)*(NP/N)*SQRT(TP*(1.+RP)/T/(1.+R))

      RST=N*MA*SQRT(T*(1.+R)/M)*(MA*MA*T*(1.+R)*.5+2.5*T*
     2   (1.+R))*1.5735E4

      RETURN
      END


C***************************************************************

      SUBROUTINE SPUD

C     This subroutine calculates sputtering on the divertor
C     plate based on an exponential profile. You can used
C     the average local temperature for each of 50 points
C     across the plate or integration of the MB distribution
C     and Yield at each.

      REAL UO,Z3,M3,NPO,TPO,X,INC,ETH1,ETH2,ETH3,
     2     TPR(51),NPR(51)
      REAL SP(51),Y1,Y2,Y3,YT,SPT,ANS,DIST,METH,
     2     IMP,VANS,D,A,CT,FHE
      REAL PBAR,RCY,VBAR,ISE,MT,U,NDT,RHE,CP,
     2     LDAS,LDAF,LCXS,LCXF,MLT
      REAL TP,TT,NP,NT,RP,RT,LD,QT,M,SHP,F,
     2     G1,G2,XT,THETA,EL,P12,LNP
      REAL TAV,NAV,SI,SCXS,SCXF,FIF,FCXF,
     2     FCXS,RN,RE,VF,VS,NM,PEAK
      REAL FLAG,SDT(51),SHE(51),EI,TPRC,IE,
     2     E1,E2,E3,RST1,RST2,RST

      COMMON /SR/ PBAR,RCY,VBAR,ISE,MT,U,NDT,RHE,CP,P12
      COMMON /INPUT/ TP,TT,NP,NT,RP,RT,LD,QT,M,SHP,
     2       F,G1,G2,XT,THETA,EL,
     3          DIST,METH,IMP,VANS,D,A,CT,FHE,ELH
      COMMON /CALC/ TAV,NAV,SI,SCXS,SCXF,FIF,
     2       FCXF,FCXS,RN,RE,VF,VS,
     3          LDAS,LDAF,LCXS,LCXF,MLT,LNP
      COMMON /MB/ TPRC,FLAG,M2,M3,UO,Z3,ETH1,ETH2

      CHARACTER*64 FNAME

C     FORMAT BLOCK
100   FORMAT(' Input plate material data,
     2          UO,Z3,M3,NM(xE24),IE ')
```

```
200     FORMAT(' Peak sputtering rate is',E10.4,' CM/YR  TP=',
       2          E9.4,' NP=',E9.4)
300    FORMAT(' Sputtering Yield per meter is',E10.4,' xE19')
400    FORMAT(' Enter sputtering data file.prn')
500    FORMAT(A)
600    FORMAT(I5,3X,E10.4,3X,E10.4,3X,E10.4,
       2          3X,E10.4,3X,E10.4)
700    FORMAT(' Do another plate material? 1=yes 2=no')
800    FORMAT(' Use average temps or integrate MB? 1=avg
       2          =integrate')
900    FORMAT(' Do you want to store data? 1=yes 2=no')
1000   FORMAT(' Impurity yield is GT 1.0 set = 0.0')
350    WRITE(*,100)
       READ(*,*) UO,Z3,M3,NM,IE
       WRITE(*,800)
       READ(*,*) ANS
       NPO=XT*NP/LNP/(1.-EXP(-XT/LNP))
       TPO=XT*TP/A/LNP/(1.-EXP(-XT/A/LNP))
       SPT=0.0
       X=0.0

       INC=XT/50.
       ETH1=UO*(4.*M+M3)*(4.*M+M3)/4./M/M3
       ETH2=UO*(16.+M3)*(16.+M3)/16./M3
       ETH3=UO*6.25

C      This block evaluates sputtering using MB integration
       IF(ANS.GT.1.5) THEN
       DO 150 I=1,50
       Y3=0.0
       SHE(I)=0.0
       SDT(I)=0.0
       TPR(I)=TPO*EXP(-X/A/LNP)
       TPRC=RP*TPR(I)
       NPR(I)=NPO*EXP(-X/LNP)
       E3=(G2-2.)*RP*TPR(I)
       IF(E3.GT.ETH3) THEN
       Y3=YLD(UO,400.,Z3,Z3,M3,M3,E3,ETH3)
       IF(Y3.GT.1.0) THEN
       WRITE(*,1000)
       Y3=0.0
       ENDIF
       ENDIF
       EI=.5*(ETH1-(G2-2.)*RP*TPR(I))
       IF(EI.LT.0.0) EI=0.0
       IF(EI.LT.IE*TPRC) THEN
       FLAG=1.

       IF(EI.LT.1.5*TPRC) THEN
       CALL RMBG(EI,1.5*TPRC,4.,RST1)
```

```fortran
      CALL RMBG(1.5*TPRC,IE*TPRC,4.,RST2)
      ENDIF
      IF(EI.GT.1.5*TPRC) THEN
      CALL RMBG(EI,IE*TPRC,4.,RST1)
      ENDIF
      RST=RST1+RST2
      RST1=0.0
      RST2=0.0
      SDT(I)=(1.-(1.+P12)*CP)*RST*NPR(I)*SQRT(TPR(I)*
     2       (1.+RP)/M)*11083.6/(1.-Y3)
      ENDIF
      EI=.5*(ETH2-2.*(G2-2.)*RP*TPR(I))
      IF(EI.LT.0.0) EI=0.0
      IF(CP.LT.0.001) GOTO 550

      IF(EI.LT.IE*TPRC) THEN
      FLAG=2.
      IF(EI.LT.1.5*TPRC) THEN
      CALL RMBG(EI,1.5*TPRC,4.,RST1)
      CALL RMBG(1.5*TPRC,IE*TPRC,4.,RST2)
      ENDIF
      IF(EI.GT.1.5*TPRC) THEN
      CALL RMBG(EI,IE*TPRC,4.,RST1)
      ENDIF
      RST=RST1+RST2
      RST1=0.0
      RST2=0.0
      SHE(I)=P12*CP*RST*NPR(I)*SQRT(TPR(I)*(1.+RP)/M)
     2       *11083.5/(1.-Y3)
      ENDIF
      EI=.5*(ETH2-1.*(G2-2.)*RP*TPR(I))
      IF(EI.LT.0.0) EI=0.0
      IF(CP.LT.0.001) GOTO 550

      IF(EI.LT.IE*TPRC) THEN
      FLAG=3.
      IF(EI.LT.1.5*TPRC) THEN
      CALL RMBG(EI,1.5*TPRC,4.,RST1)
      CALL RMBG(1.5*TPRC,IE*TPRC,4.,RST2)
      ENDIF
      IF(EI.GT.1.5*TPRC) THEN
      CALL RMBG(EI,IE*TPRC,4.,RST1)
      ENDIF
      RST=RST1+RST2
      RST1=0.0
      RST2=0.0
      SHE(I)=SHE(I)+(1.-P12)*CP*RST*NPR(I)*
     2       SQRT(TPR(I)*(1.+RP)/M)*11083.5/(1.-Y3)
      ENDIF
550   SP(I)=SDT(I)+SHE(I)
```

```fortran
        SPT=SPT+0.02*XT*SP(I)
        X=X+INC

150     CONTINUE
        ENDIF

C       This block evaluates sputtering using average local
C       temp
        IF(ANS.LT.1.5) THEN
        DO 450 I=1,50
        Y1=0.0
        Y2=0.0
        Y3=0.0
        SDT(I)=0.0
        SHE(I)=0.0
        TPR(I)=TPO*EXP(-X/A/LNP)
        TPRC=TPR(I)
        NPR(I)=NPO*EXP(-X/LNP)
        E1=TPR(I)*G2*RP
        E2=TPR(I)*2.*RP*(G2-1.)
        E3=TPR(I)*RP*(G2-1.)
        IF(E3.GT.ETH3) THEN
        Y3=YLD(UO,400.,Z3,Z3,M3,M3,E3,ETH3)
        IF(Y3.GT.1.0) THEN
        WRITE(*,1000)
        Y3=0.0
        ENDIF
        ENDIF
        IF(E1.GT.ETH1) THEN
        Y1=YLD(UO,400.,1.,Z3,M,M3,E1,ETH1)
        ENDIF
        IF(E2.GT.ETH2) THEN
        Y2=YLD(UO,400.,2.,Z3,4.,M3,E2,ETH2)
        ENDIF
        SDT(I)=9822.27*NPR(I)*SQRT(TPR(I)*(1.+RP)/M)*Y1*(1.
     2       -(1.+P12)*CP)/(1.-Y3)
        SHE(I)=9822.27*NPR(I)*SQRT(TPR(I)*(1.+RP)/M)*
     2       Y2*CP/(1.-Y3)
        SP(I)=SDT(I)+SHE(I)
        SPT=SPT+.02*XT*SP(I)
        X=X+INC
450     CONTINUE
        ENDIF

C       On screen Output of results
        PEAK= SP(1)*.0315/NM
        WRITE(*,200) PEAK,RP*TPR(1),NPR(1)
        WRITE(*,300) SPT

C       Prompt for storage of  sputtering rates for each of 50
```

```fortran
C       points
        WRITE(*,900)
        READ(*,*) ANS
        IF(ANS.LT.1.5) THEN
        WRITE(*,400)
        READ(*,500) FNAME
        OPEN(3,FILE=FNAME)
        DO 250 J=1,50
        WRITE(3,600) J,SP(J),SDT(J),SHE(J),TPR(J),NPR(J)

250     CONTINUE
        CLOSE(3)
        ENDIF
C       Prompt for another calculation
75      WRITE(*,700)
        READ(*,*) ANS
        IF(ANS.LT.1.5) GOTO 350
        RETURN

        END
```

```
C*************************************************************

        REAL FUNCTION YLD(UO,C,Z1,Z2,M1,M2,EO,ETH)

C       This is sputtering yield function evaluation based on
C       D.L. Smith's model

        REAL UO,C,Z1,Z2,M1,M2,EO,ETH

        YLD=C*Z1**.75*(Z2-1.8)*(Z2-1.8)*((M1-.8)/M2)
     2     **1.5*(EO-ETH)/UO/(EO-ETH+50.*Z2*Z1**.75)**2.
        RETURN

        END

C*************************************************************

        SUBROUTINE EVAL4(E,RST)

C       This is function evaluation for MB integration of
C       SPUD
        REAL TP,TT,NP,NT,RP,RT,LD,QT,M,SHP,F,G1,
     2       G2,XT,THETA,EL,DIST,METH
        REAL IMP,VANS,D,A,CT,FHE,ELH,TPRC,FLAG,
     2       M2,M3,UO,Z3,ETH1,ETH2,EO
        REAL RST,E

        COMMON /INPUT/ TP,TT,NP,NT,RP,RT,LD,QT,M,SHP,F,
     2          G1,G2,XT,THETA,EL,
```

```
3          DIST,METH,IMP,VANS,D,A,CT,FHE,ELH
   COMMON /MB/ TPRC,FLAG,M2,M3,UO,Z3,ETH1,ETH2

   IF(FLAG.LT.1.5) THEN

   EO=2.0*E+TPRC*(G2-2.)

   RST=SQRT(E/TPRC)*EXP(-E/TPRC)*
2      YLD(UO,400.,1.,Z3,M,M3,EO,ETH1)/TPRC
   ENDIF
   IF(FLAG.GT.1.5) THEN
   IF(FLAG.LT.2.5) THEN
   EO=2.*E+2.*TPRC*(G2-2.)
   RST=SQRT(E/TPRC)*EXP(-E/TPRC)*
2      YLD(UO,400.,2.,Z3,4.,M3,EO,ETH2)/TPRC
   ENDIF
   ENDIF
   IF(FLAG.GT.2.5) THEN
   EO=2.*E+1.*TPRC*(G2-2.)
   RST=SQRT(E/TPRC)*EXP(-E/TPRC)*
2      YLD(UO,400.,2.,Z3,4.,M3,EO,ETH2)/TPRC
   ENDIF
   RETURN
   END
```

APPENDIX C

GENERIC DIVERTOR MODELING

The best approach in modeling a divertor is to use as many known data values as possible. However, in the absence of knowledge about the value of a particular parameter some sort of estimate must be made in order to continue modeling. The purpose of this appendix is to present calculational methods for the estimation of some DIV input parameters and reasonable ranges for others.

C.1 Power Flux into the Divertor, Q_t

The power flux into the divertor can be estimated using the equation

$$Q_t \ (W/m^2) = \frac{P}{N \ A_{\parallel,d}} \qquad (C.1)$$

where P (W) is the total power to be exhausted, N is the number of divertor plates (a reactor may have more than one divertor, each with more than one plate), and $A_{\parallel,d}(m^2)$ is the cross-sectional area of the plasma as it flows into the divertor.

The power to be exhausted and the number of divertor plates are usually known, so determining Q_t depends on finding the plasma cross sectional area. For a Tokamak, this area can be estimated as[3]

$$A_{\parallel,d}(m^2) = \frac{F_e 2\pi\ a\ \Delta_s}{q} \qquad (C.2)$$

where a(m) is the plasma minor radius, Δ_s(m) is the scapeoff thickness (normally several heat flux scale lengthes, λ_Q), q is the safety factor on edge, and F_e is a flux expansion factor at the throat to account for the normal expansion of magnetic field lines as they enter the divertor. Reference 3 gives a value for F_e of about 1.4. The heat flux scale length, λ_Q(m), is often a given parameter. If it is not given, it can be estimated using[25]

$$\lambda_Q = \frac{\lambda_n \lambda_T}{\frac{3}{2}\lambda_n + \lambda_T} = \frac{A\lambda_n}{\left(\frac{3}{2} + A\right)} \qquad (C.3)$$

where A is the ratio of temperature to density scale lengthes. The density scale length, λ_n, would be calculated as given in Section 3.8 using some estimate of the fluid velocity ($\sim$.3-.5 of the sound speed).

C.2 The Divertor Connection Length, L_D

This connection length is the distance along field lines between the divertor throat and the target plate. It is a function of the magnetic field line topology and sensitive to the plate position being considered. If its value is unknown, some fraction (.2-.3) of the outside connection length can be used. The outside connection length, L_s, is

$$L_s(m) = \frac{2\pi \, Rq}{N} \qquad (C.4)$$

where $R(m)$ is the plasma major radius and N is the number of divertors. Thus

$$L_D(m) \approx .25 \, L_s \qquad (C.5)$$

C.3 The Throat Electron Plasma Temperature, T_t

If the symmetry point electron temperature, T_s, is specified, this value can be extrapolated forward to the divertor throat using an equation based on 100% electron thermal conduction[3]

$$T_T^{7/2}(eV) = T_S^{7/2}(eV) - \frac{7P\ L_S}{4A_{\parallel,S}N\ x_o} \qquad (C.5)$$

where P and L_S are as previously defined, N is the number of divertor plates, $A_{\parallel,S}(m^2)$ is the cross-sectional area of the plasma outside the divertor (i.e. no flux expansion factor), and x_o is the Spitzer electron thermal conductivity coefficient ($\sim 2000\ W(eV)^{-7/2}m^{-1}$).

C.4 The Throat Electron Density, n_t

The pressure balance equation can be used to estimate the throat electron density, once the throat temperature has been calculated. Thus,

$$n_t(m^{-3}) = \frac{n_s\ T_s}{T_t} \qquad (C.6)$$

where $n_s(m^{-3})$ is the symmetry point electron density. The mach numbers squared ($\tilde{m}^2$) at both locations are assumed to be small and can be neglected. If after a computer run the mach number at the throat is found not to be small, then this value could be used to adjust the throat density (divide by $1 + \tilde{m}_t^2$).

C.5 Estimates for the Plate Electron Temperature and Density, T_p and n_p

Another equation based on the assumption of 100% electron thermal conduction can be used to get an initial estimate of T_p.[3] Thus,

$$T_p^{7/2}(eV) = T_t^{7/2}(eV) - \frac{7Q_t L_D}{2 \, x_o} \qquad (C.7)$$

and the plate electron density estimated using the pressure balance equation,

$$n_p(m^{-3}) = \frac{n_t \, T_t \left(1 + r_t\right)}{2T_p\left(1 + r_p\right)} \qquad (C.8)$$

where the mach number at the throat has been assumed to be zero and the mach number at the plate set equal to 1.0. If a sample run shows the mach number at the throat not to be small, then the plate density can be adjusted by multiplying by $(1 + \mathbb{M}_t^2)$.

C.6   Reasonable Ranges for Other Input Parameters

Based on a review of the literature and experience with the DIV code, Table C.1 below displays reasonable ranges for other input parameters for which no calculation or estimate has been given in the body of this thesis or this appendix.

Table C.1
Parameter Ranges

Parameter	Units	Range
Pump Fractions f and f_{He}	-	0-.5
Diffusion Coefficient, D	m^2/sec	.8-1.5
Scale Length Ratio, A	-	.7-1.1
Shape Factor, α	-	3-8
Field Line Angle of Incidence, θ	Radians	.09-.79 ($5^{\circ}-45^{\circ}$)

A few additional comments regarding other parameter values are warranted. The mass the the D-T ions is usually taken to be 2.5 amu. If you are going to calculate R and μ in the DIV program, then these input values do not matter.

APPENDIX D

DISCUSSION OF NEUTRAL ESCAPE PROBABILITY

As stated in Chapter 3, the recycling coefficient, R, can be approximated as $1-\bar{p}f$, where f is the pumped fraction, and $\bar{p}$ is the average neutral escape probability. Section 3.5 outlined the various calculational approaches to determining $\bar{p}$. This appendix presents a discussion of the effects of variations in certain parameters on the neutral escape probability and a comparison of the three calculational methods.

D.1 Effects of Varying Parameters

The parameters required to calculate the neutral escape probability are:

X_t - the width of the divertor plate (M)

θ - the angle of incidence of the field lines to the divertor plate (radians)

T   - the temperature of the plasma in front of the plate (eV). This could be the plate temperature or an average of the throat and plate tempertures.

n   - the electron density in front of the plate. (m^{-3}) Again, this could be the plate or an average quantity.

EL   - the material and particle dependent reduced energy for the calculation of the reflection

coefficients (eV).

I   - Number of mesh points along the divertor plate

Each of these parameters was varied to examine its effect on the neutral escape probability. In each case, the effect on $\bar{p}$ was qualitatively predictable. These effects are discussed below.

X_t - As X_t increased the escape probability decreased. This was due to the fractional decrease in the tip area of the plasma wedge. Most of the particles that escape do so out of the tip of the plasma wedge. Increasing the width of the divertor plate just increases the area from which particles do not escape.

θ - As θ increased the escape probability decreased. This makes sense, since increasing θ increases the effective thickness of the plasma.

T   - As T increased, the escape probability decreased. The temperature is used in the calculation of particle ionization MFP, appearing in both the numerator (velocity term), and the denominator (in the reaction rate coefficient). This result implies that the $<\sigma v>_{ion}$ term is more sensitive to temperature than the velocity term.

n   - As the density increased $\bar{p}$ decreased. This is because the MFP for ionization scales as $1/n$ for density. Increasing n decreases the MFP and thereby the escape probability.

EL   - As EL increases so does $\bar{p}$. For a larger reduced energy the fraction of particles in the fast group is greater. Particles from this group make up most of those that escape, so increasing their fraction increases the escape probability.

I   - Past an I of 50 (especially for larger escape probabilities) the difference between calculated escape probabilities is less than 5%. Based on

this an I of 50 was used for the escape
probability subroutine in the divertor model
program DIV.

D.2 Comparison of Methods

As described in Section 3.5, there are three different
methods that can be used in the divertor model program to
calculate $\bar{p}$. The "l_{avg}" method calculates an average escape
distance (distance to the plenum) for each mesh point. The
escape probability for a particle emitted from a point is
then, $p=\exp[-\bar{l}(x)/\lambda]$, where λ is the appropriate energy
group ionization MFP. The second method, "integral",
integrates the escape probability, $p=\exp[-l(x,\phi)/\lambda]$,
directly to arrive at $\bar{p}$. The third method, "Integral
w/cosine distribution", is the same as the second but adds a
cosine angular distribution probability for the reflected
particles.

Figure D.1 presents the results of calculating $\bar{p}$ using
each of the three methods for a range of electron densities
from 5×10^{18} to 5×10^{20} m^{-3}. At high escape probabilities
(corresponding to low recycling) the l_{avg} and Integral
methods yield very similar values for $\bar{p}$ while the Integral
w/cosine method is 50-60% lower. The l_{avg} and Integral
methods continue to be close in value down to values of .5
for $\bar{p}$. Beyond this point the methods are not far apart in

absolute value but as fractions of each other the difference increases to about 30% at small values of $\bar{p}$. The Integral w/cosine method produces a value for $\bar{p}$ lower than the other two methods except for $\bar{p} < .1$. In this region the l_{avg} method is a reasonable approximation for the Integral w/cosine method (assumed to be the most realistic predictor of the actual escape probability because it takes angular probability into account) and takes much less computational time. All three methods are available in the DIV program.

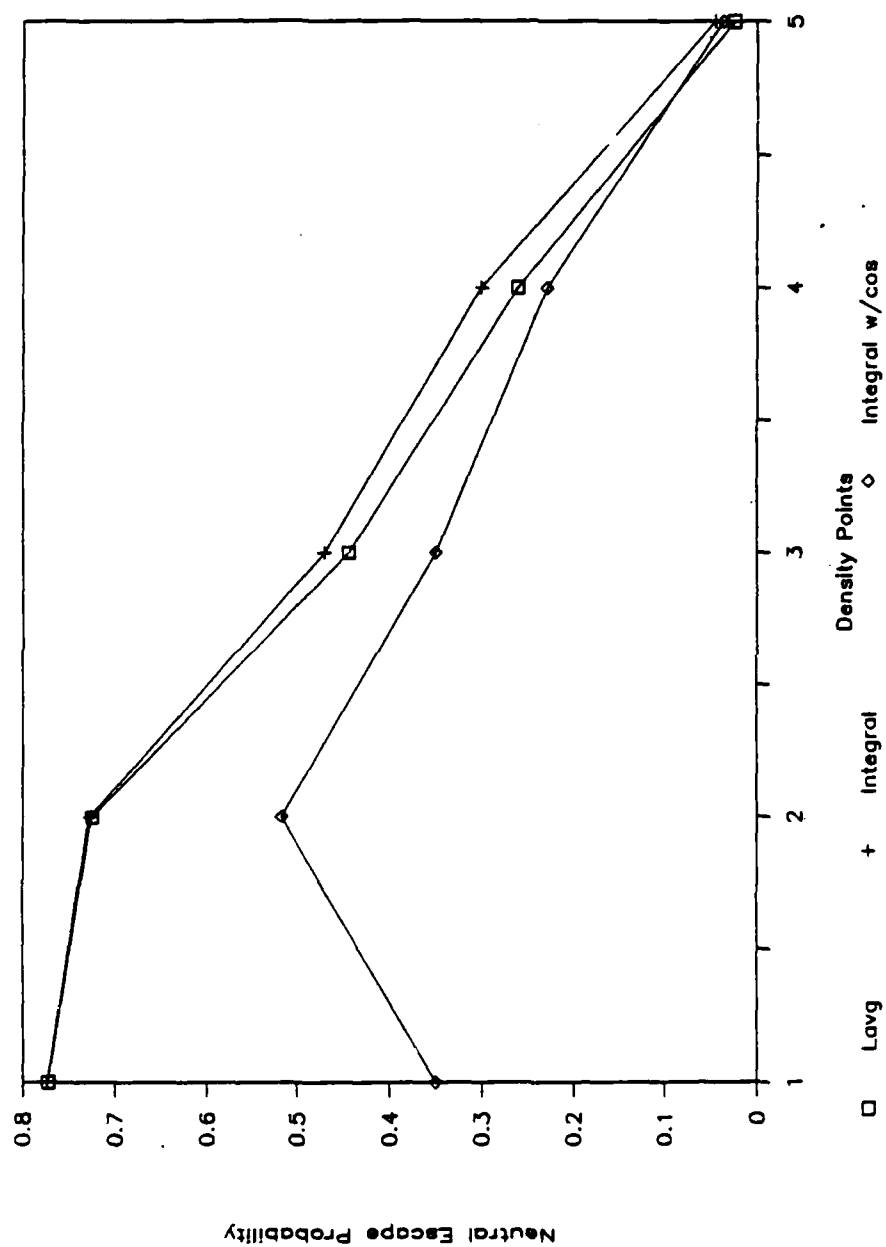Figure D.1   Neutral Escape Probability Calculation
Method Comparison

APPENDIX E

BENCHMARKING INPUT AND OUTPUT DATA

This appendix tabulates the DIV input data used in the benchmarking cases presented in Chapter 5, along with the output from the divertor model code. The symbols used in the tables that follow are the same DIV program variables presented in Tables 4.1 and 4.2 of Chapter 4.

Table E.1

JAERI Case Input and Output Data

Input				Output	
Parameter	Value	Parameter	Value	Parameter	Value
QT	17e6	R	.81	TP	3.8
LD	13.33	U	-	NP	9.1
M	2.0	F	1.14	TT	35.0
XT	.29	IMP	1.45	NT	1.8
THETA	.35	D	1.0	MT	.34
EL	9660	A	.7	U	.61
TP	4.0	CT	0.0	ISE	.51
TT	37.0	FHE	1.14	R	.8
NP	9.1	ELH	20400	CP	NA
NT	1.8	SHP	3.0	HER	NA
RP	1.0	METH	2.0	P12	NA
RT	1.0	DIST	2.0	LNP	NA
G1	3.9	TOL	1e-3		
G2	3.9	SOR	1.0		

Note: NA means "Not Applicable"

Table E.2

Harrison et al Case Input and Output Data

Input				Output	
Parameter	Value	Parameter	Value	Parameter	Value
QT	107e6	R	.99	TP	23.8
LD	10.0	U	–	NP	9.2
M	2.5	F	.028	TT	63.0
XT	.27	IMP	1.0	NT	6.97
THETA	.26	D	1.0	MT	8.1e-4
EL	9660	A	.7	U	.99
TP	25.5	CT	.05	ISE	.16
TT	66.0	FHE	.031	R	.99
NP	9.24	ELH	20400	CP	.025
NT	6.97	SHP	4.0	HER	2.23
RP	1.0	METH	2.0	P12	.30
RT	1.0	DIST	2.0	LNP	.021
G1	3.0	TOL	1e-3		
G2	3.0	SOR	1.0		

Table E.3

ZEHPYR Case Input and Output Data

Input				Output	
Parameter	Value	Parameter	Value	Parameter	Value
QT	31e6	R	.471	TP	10.5
LD	15.0	U	-	NP	8.68
M	2.5	F	-	TT	28.0
XT	.35	IMP	1.0	NT	3.66
THETA	.26	D	1.0	MT	.70
EL	9660	A	.7	U	.61
TP	10.8	CT	0.0	ISE	.16
TT	26.7	FHE	-	R	.471
NP	8.6	ELH	20400	CP	NA
NT	3.66	SHP	5.0	HER	NA
RP	.70	METH	2.0	P12	NA
RT	1.02	DIST	2.0	LNP	NA
G1	3.8	TOL	1e-3		
G2	4.3	SOR	1.0		

Note: The recycling coefficient, R, was not calculated.

Table E.4

NET Report #50 Case Input and Output Data

Input				Output	
Parameter	Value	Parameter	Value	Parameter	Value
QT	81.3e6	R	–	TP	11.0
LD	15.0	U	–	NP	13.4
M	2.5	F	.034	TT	64.8
XT	.35	IMP	1.0	NT	5.0
THETA	.26	D	1.0	MT	2.3e-3
EL	9660	A	.7	U	.991
TP	7.6	CT	0.05	ISE	.21
TT	67.3	FHE	.034	R	.998
NP	14.0	ELH	20400	CP	.025
NT	5.0	SHP	4.0	HER	.99
RP	1.2	METH	2.0	P12	.30
RT	1.0	DIST	2.0	LNP	.031
G1	4.8	TOL	1e-3		
G2	3.42	SOR	1.0		

MICROCOPY RESOLUTION TEST CHART

NATIONAL BUREAU OF STANDARDS-1963-A